Role of Patched homologs in development and cellular physiology in *Caenorhabditis elegans*

Inauguraldissertation

zur

Erlangung der Würde eines Doktors der Philosophie

vorgelegt der

Philosophisch-Naturwissenschaftlichen Fakultät

der Universität Basel

von

Carla Elizabeth Cadena del Castillo

aus

Mexico Stadt, Mexico

Basel, 2020

Genehmigt von der Philosophisch-Naturwissenschaftlichen Fakultät
auf Antrag von

Prof. Dr. Anne Spang
Prof. Dr. Michel Labouesse

Basel, den 18 Februar 2020.

Prof. Dr. Martin Spiess
Dekan der Philosophisch-Naturwissenschaftliche Fakultät

“El mundo era tan reciente, que muchas cosas carecían de nombre, y para mencionarlas había que señalarlas con el dedo.”

“The world was so recent that many things lacked names, and in order to indicate them it was necessary to point.”

Excerpt from Cien años de soledad, Gabriel García Márquez

To my mom and grandma
To Carlos

Acknowledgements

This work was performed in the group of Prof. Dr. Anne Spang at the Biozentrum of the University of Basel (Switzerland). I would like to express my gratitude to the following people:

My Ph.D. supervisor Anne Spang for giving me the opportunity to conduct my Ph.D. in her lab.

My Ph.D. committee members, Michel Labouesse and Rafal Ciosk, for all the support and good input.

The technical and administrative staff of the 5th floor and the Spang lab, Brigitte Olufsen, Maja Güntensperger, Dora Stetak, Cedrin Kueng, Diego Stohrer, Jonas Fürst, Elisabete, and Fatima Reis.

All present and past members of the Spang Lab, Julia Stevens, Jachen Solinger, Kiril Tishinov, Harun-Or Rashid, Maria Podinovskaya, Emmanouil Kyriakakis, Artan Ademi, Irene Arcones, Pascal Ankli, Claudia Stohrer, Martina Huranova, Thomas Gross, Congwei Wang, Ludovic Enkler, Sheuli Begun and Danie Ott.

All the 5th-floor members, specially Mitsugu Shimobayashi, for the advice and experimental help and Asier González Seviné, Valentina Millarte, and Mirjam Pennauer for all the support and good moments.

Attila Stetak from the Division of Molecular Neuroscience for all the advice that helped to complete the present work.

Iskra Katic from the FMI, Basel, for the good advice and all her work to set a platform where the worm community in Basel can have fruitful discussions.

The IMCF-Biozentrum for their support and advice with image acquisition and analysis.

The Microscopy center from the UZH, especially to Andres Kaech, for his hard work with the EM analysis and the productive discussion of the results.

Kathrin Brændgaard, Jonathan Brewer, Vita Solovyeva, and Nils Færgeman from the USD for their support during the CARS experiments.

Yanik Hauser for giving us the hint of the oscillation of PTC-3 and PTR.4.

Carlos Eduardo Flores Tinoco for all the help and advice with data analysis, endless discussions, and suggestions. Overall, thanks for always been there, every day, every minute, every moment. Without you, nothing would be possible.

Last but not least, thanks to my family and friends for all the support and love.

Preface

A millenary journey to understand development

"*Even the scientists were on this side of the question. The English naturalist Ross announced learnedly that: "To question that beetles and wasps were generated in cow dung is to question reason, sense, and experience.*" [1]

From our current perspective, it is evident how a new organism is created; however, this discussion has fascinated and challenged people since ancient times. Nowadays, we know that multicellular organisms are not created as wholly made beings. Instead, we arise by the process of gradual progressive transformation known as development. In most cases, the development of a multicellular organism begins with a single cell: the fertilized egg, which divides and differentiates to produce all the cells of the body [2]. However, achieving this basic biological concept has neither been easy nor straightforward, and throughout millennia scientists developed numerous theories to explain how an organism arises.

Remarkably, already 300 BC, Aristotle wondered about the development of organisms. He opened an egg and observed the daily changes in the developing chick. Then, he formulated the idea of sequential growth of the embryo's parts by the development of latent fragments that already exist in the seed. In part, Aristotle postulated two concepts that remained dormant for many years. On one hand, epigenesis, which is the *de novo* generation of each individual and on the other hand, preformation, where all the organs are initially present in a miniature form inside the egg. Outstandingly, humanity had to wait 2000 years to formally scrutinize these concepts again. First, we learned from Francesco Redi, Lazzaro Spallanzani, and Louis Pasteur that all organisms come from another organism. In the case of animals, thanks to the work from William Harvey, we know that all of us come from a single entity, the egg [3]. However, the nature and the content of such an egg remained elusive for many more years.

The invention of the microscope by Leeuwenhoek enabled scientists, like Marcello Malpighi, to continue Aristotle's studies on the developing chick, albeit at a microscopic resolution. Malpighi wished to know whether inside an egg before the hen's incubation, a miniaturized chick was already present. Unfortunately, he misinterpreted his findings; he thought he was observing a non-incubated egg and supported preformation theories (some theories suggest that his mistake may come from the Italian summer temperatures which resembled an incubation which could have triggered the chick development). Therefore, the work of Malpighi started maybe the hugest dispute in embryology, the debate, or, more

precisely, the battle over epigenesis versus preformation [4]. It will take humanity 150 years and plenty of resources to puzzle out the incognita. It was not until the 1820s that the preformationism era came to an end with the work of Christian Pander. He discovered that the embryo originates from undifferentiated layers (germ layers) that develop into the rest of the organs [5]. However, one of the most amazing disclosures in biology was still to occur. Karl Reinhold Ernst von Baer made this discovery. Back in 1828, von Baer reported, "*I have two small embryos preserved in alcohol, that I forgot to label. At present, I am unable to determine the genus to which they belong. They may be lizards, small birds, or even mammals.*" [4]. At that time, von Baer did not realize the power of his observations, which set the basis of the relationship between development and evolution. In other words, he discovered that across the animal kingdom, we all share the same developmental mechanisms [3]. Nowadays, such a relationship allows us to make use of the similarities between animal species to better understand the succession of changes that must take place in an organism to ultimately give rise to an adult [3].

The fact that animals evolved from a common ancestor in which critical developmental genes were already present entitles us to extrapolate underlying developmental mechanisms from worms (e.g., nematodes) to mammals. Vertebrates diverged approximately 600 million years ago, and still in humans, around 50% of the genes show common ancestry with the nematodes [3]. It is fascinating that throughout these 600 million years, all these developmental mechanisms have stayed almost unchanged, and even more remarkable is that they work in such a perfect way that animals managed to colonize the whole Earth. However, from time to time, there are "mistakes" during development, often, as a consequence of a mutation, organisms that differ from the "normal" specimens arise [5]. Such deviant specimens amazed humanity since ancient times, and maybe they are even responsible for creating myths. For sure, already in the 1660s, the existence of an abominable one-eyed horse resembling the mythical Cyclops was formally documented for the first time [6]. However, it was just in 1968 that it became clear that the condition of being a one-eyed creature (cyclopia) could be induced by "monster-former" compounds (teratogens) derived from the plant *Veratrum californicum* [7]. Moreover, thanks to developmental studies in the fruit fly, the molecular mechanisms behind cyclopia were revealed. These studies pointed to the existence of a signaling pathway known as the Hedgehog (Hh) pathway, which is responsible for the establishment of the developmental plan of animals, including the formation of both eyes, and adulthood processes[8]. Consequently, proving von Baer's observations and showing the striking developmental similarities between evolutionarily distant organisms, in this case, flies and humans. As a result of the exceptional work on describing the Hedgehog pathway and the contribution

regarding the genetic control of early embryonic development, Christiane Nüsslein-Volhard and Eric F. Wieschaus received the Nobel prize in 1995.

The Hh pathway is one of the central regulators of animal development; it has a role in several developmental processes, and it has become a paradigm for classical signaling [9]. Furthermore, the significance of the study of Hh signaling broadens from evolutionary developmental biology to regenerative medicine and cancer research. Consequently, the list of processes requiring Hh signaling expands continuously, as expected, such expansion grows along with the number of publications inquiring Hh roles and means of action. Regardless of the existence of thousands of studies concerning Hh signaling, there are still many open questions regarding the contribution of Hh signaling in development and animal physiology. For instance, while the receptor of the Hh pathway is conserved throughout the animal kingdom, key components presumably essential for signal transduction are not found in some animals like nematodes. A fact that makes this pathway especially enigmatic [9], why would worms keep a truncated signaling pathway? To generally enlarge our knowledge of the conserved but non-canonical roles of Hh signaling, in this work, we focused on the study of one of the evolutionarily conserved components of the pathway in the nematodes. Our findings will help us to better understand in more detail some of the most enigmatic and elusive features of the pathway.

Table of contents

Summary

The Hedgehog (Hh) signaling pathway is essential for animal development and health maintenance. In the canonical Hh pathway, the signaling molecule Hh binds to the membrane cholesterol transporter PTCH, thereby relieving the inhibition of Smoothened (SMO), which in turn activates a signaling cascade required for proper development. Nonetheless, increasing evidence points to the existence of SMO-independent Hh pathways. However, the co-existence with the canonical pathway has undermined the efforts to characterize these novel pathways. *C. elegans* is an excellent model to study SMO-independent Hh pathways. However, even if this worm lacks SMO, the PTCH homologs are essential for worm development, therefore, indicating that the Hh pathway still operates in worms. Thus, we studied the role of two PTCH proteins in the *C. elegans'* SMO-independent context to elucidate their function in an essential non-canonical Hh pathway.

Here, we demonstrate that the loss of PTC-3 leads to the accumulation of cholesterol at the plasma membrane *in vivo*. Further analysis of the lipid metabolism revealed a reduction in acyl-chain length and desaturation, which suggested membrane structure defects. Indeed, we discovered defects in ER structure and lipid droplets. Even more, we show evidence that cholesterol accumulation modulates the function of nuclear hormone receptors such as the PPARα homologs NHR-49 and NHR-181. Finally, reduction of dietary cholesterol rescued all described phenotypes, consequently improving development and survival. Therefore, our data uncover a novel SMO-independent pathway which is necessary for lipid homeostasis and fat storage.

Concomitant with the evolution of PTCH homologs, Patched-related proteins (PTR), another group of proteins derived from the ancestral PTCH evolved. However, the roles PTRs play in the cell and whether they share functions with other PTCH proteins remains to be determined. Our work indicates that cholesterol regulation is a conserved function of the PTR protein PTR-4. However, we showed that PTC-3 and PTR-4 have different and specific roles in *C. elegans* development. Interestingly, the analysis of PTR-4 expression pattern revealed that protein levels and localization are dynamic throughout larval growth, suggesting dynamic cholesterol levels during development. Finally, a phenotypical characterization of animals lacking PTR-4 protein or a hypomorph allele of PTR-4 revealed a role of the protein in cuticle stability, which has an impact on locomotion.

In summary, through the use of the nematode as a model organism, we have shown how PTCH proteins have a conserved role in cholesterol modulation. Furthermore, we demonstrated that they have essential SMO-independent roles.

1. Introduction

Studies in metazoans have revealed that while the final result of a developing organism looks quite different, there is remarkable preservation in the developmental mechanisms among animals. For instance, if we compare flies and humans, we can appreciate that we own the same developmental signaling pathways, and our cells share the same cell-to-cell communication processes. Moreover, some critical cellular mechanisms during animal development have even been first described in a small worm, *C. elegans*. This nematode was the first multicellular organism to be sequenced. Furthermore, it was a critical model for breakthrough discoveries deserving Nobel prizes, such as the genetic control of programmed cell death [10] and gene silencing by interference RNA (RNAi) [11]. *C. elegans* is a free-living nematode that grows in the wild on rotting fruits and stems. This nematode provides several advantages as a model organism. It is one of the most convenient laboratory animals to handle, thanks to its small size (~1 mm length), rapid life cycle (~48 hrs. from egg to sexually mature animal), hermaphrodite condition (capable of self-fertilization), and large brood size (~ 300 fertilized eggs per hermaphrodite). In the lab, it is cultivated on agar plates seeded with *Escherichia coli* as a food source [12–14]. Even more convenient, there is a broad molecular toolkit to study gene expression and protein localization in the worm. It includes the insertion of genes into the worm (either extrachromosomal and integrated arrays, or single gene integration), followed by germ-line transmission of the gene and further analysis of the resulting phenotype in the progeny [15,16]. As well, RNAi, a specific post-transcriptional gene silencing process that can be triggered by double-stranded RNA (dsRNA), is extensively used in *C. elegans* [11]. dsRNA can be delivered into life worms by four means, injection of dsRNA into the animal, soaking the worm in dsRNA, *in vivo* production of dsRNA from transgenic promoters, and the easiest of all, feeding with bacteria producing dsRNA [17].

C. elegans larval development occurs outside the eggshell (Fig.1.1). Worm's development comprises four larval stages and a facultative diapause stage. These characteristics make *C. elegans* an excellent organism to study and manipulate essential genes *in vivo* during development after critical developmental stages. Therefore, in combination with RNAi, we can affect protein expression in precise moments [18].

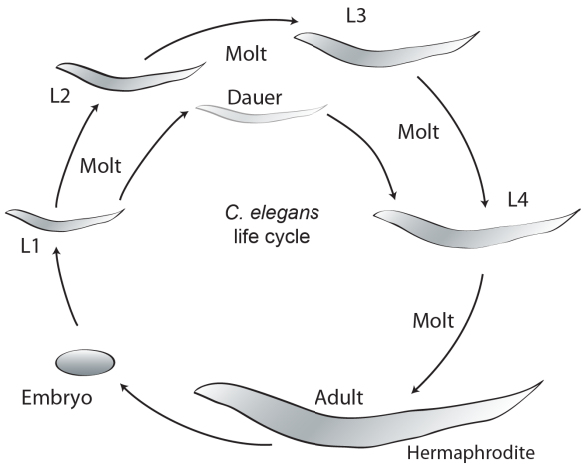

Figure 1.1. *C. elegans* life cycle. *C. elegans* development starts inside the egg, and its life cycle comprises four larval stages. After hatching, the embryo enters the first larval stage known as L1. If the larva encounters an environment with an adequate nutrition source, it progresses from the L1 stage to the subsequent larval stages by the process of molting to the L2, L3, and L4 until adulthood. However, if in the L1 and L2 stages, the larva faces limited nutrients, overcrowding, or high temperature, the nematodes arrest their development and enter the alternative developmental stage, called dauer. Dauer larvae can survive several months without any food waiting for suitable environmental conditions to resume development [19].

1.1 Importance of the Hedgehog pathway

Developmental analyses of the last hundred years have shown numerous examples of cell-to-cell communication mechanisms implicated in the regulation of metazoan development. Interestingly, most of the signaling molecules reported are part of a reduced group of families of secreted factors: PDGF, FGF, TGF-β, ephrin, Wnt, or the Hedgehog (Hh) family. Since the discovery of the Hedgehog pathway, it is recognized as a key mediator of numerous central processes in development, and its activity is crucial for most vertebrates and invertebrates [20].

Hh was discovered as a gene involved in the development of the fruit fly embryo. It is responsible for establishing *Drosophila* embryonic segment polarity [21,22]. Later, it became clear that in many animals, Hh signaling plays a crucial function in directing patterning events during embryonic development [22]. Specifically, the Hh pathway is implicated in the regulation of central nervous system polarity and neural patterning in chicks and mammals [23,24]. Thus, the impaired Hh signaling pathway has been associated with congenital defects [25]. As a morphogen, Hh controls gene expression in a concentration-dependent manner [26]. Additionally, the Hh pathway is regulating the differentiation, proliferation, and maintenance of the stem cell population in both embryos and adults [9,27].

Importantly, the Hh pathway has also a role in cancer-related processes and healthy adulthood maintenance. Accordingly, it is not surprising that recent advancements in

developmental biology and cancer biology revealed many similarities between early development and tumorigenesis [28]. For instance, in the adult gut epithelium, the up-regulation of Hh is associated with the differentiation of gastric glands and gastric metaplasia [29]. These outcomes correlate with the postulated functions of Hh in differentiated digestive tissues as a mediator of gut stem cell maintenance [30].

Mutations in central components of the pathway are responsible for Gorlin syndrome [31,32], and the deregulation of the Hh pathway is connected to numerous types of cancer [33], for instance, basal cell carcinoma [34], leukemia [35,36], skin[31], lung [37], brain [38], and gastrointestinal [39] cancers. In 2012 a competitive antagonist of the pathway was approved by the FDA to treat basal cell carcinoma and Gorlin syndrome[40]. Unfortunately, new clinical trials of further Hh signaling inhibitors in other types of cancer as pancreatic, colon, and ovarian cancers have failed, indicating an existent need for broadening our understanding of Hh signaling [40–43].

1.2 The Hedgehog pathway

The Hh pathway is a mean of intercellular communication. The signal-sending cell of the Hh pathway produces Hh as a precursor. Then, Hh is activated by its cleavage into two fragments. It is noteworthy to mention that the active fragment (N-terminus) requires further modification before secretion. Two modifications are added to the active polypeptide, cholesterol to its C-terminus and palmitate to the N-terminus [44]. In animals (e.g., mammals), these modifications are likely required to allow Hh to interact with lipoprotein particles, thereby allowing it to travel to the target cells [45–47]. Once the modified Hh molecule reaches the target cell, Hh binds the receptor PTCH repressing its function. In the absence of Hh, the receptor PTCH inhibits the G-protein-coupled receptor Smoothened (SMO) without physically interacting with it. After PTCH inhibition of SMO is released, SMO activity promotes the transcription of developmental genes by inhibiting the repressive action of Fused (Fu), Suppressor of fused (SuFu), and Costal 2 (Cos2) on the transcription factor Cubitus interruptus (Ci)[48–51] (Fig. 1.2).

Due to the importance of the Hh pathway in development and health maintenance, various regulatory feedback loops ensure proper levels of Hh signaling. For example, PTCH is a transcriptional target of the Hh pathway. Since Hh signaling promotes PTCH transcription, it creates negative feedback by restoring SMO inhibition if no more Hh is present [40]. Likewise, in mammals, the Ci homolog GLI promotes its own transcription, and the newly synthesized GLI creates a positive regulatory loop promoting gene transcription in response to Hh activation [27]. Consequently, any alteration in these regulatory feedback loops could give rise to abnormal signaling by either too high or too low activation of the

pathway, resulting in developmental defects and possibly carcinogenesis. Still, the fact that blocking SMO is not efficient as a general cancer treatment has postulated that Hh may act in part independently of SMO. Even more, new data is emerging that points to the existence of Hh pathways independent of the well-characterized canonical Hh pathway (SMO-GLI dependent axis).

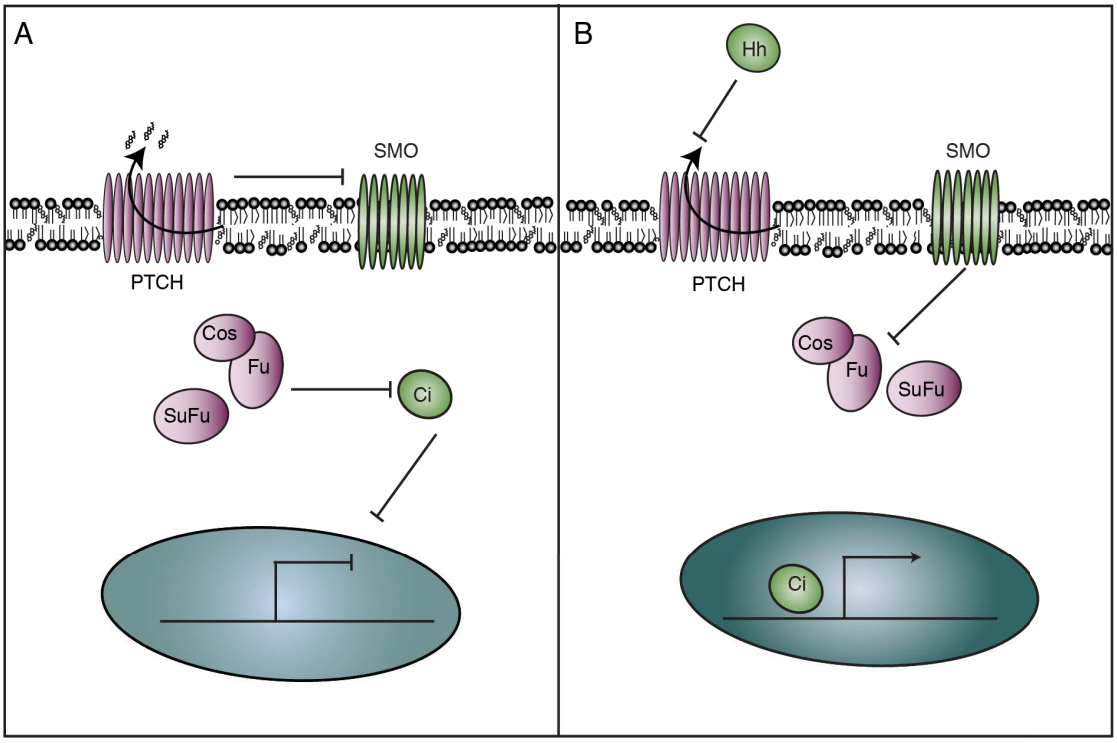

Figure 1.2. Canonical Hedgehog pathway. (**A**) In the absence of a mature Hh ligand, PTCH1 inhibits SMO letting the processing complex containing SuFu, Fu, and Cos2 to repress the transcription factors Ci. (**B**) Mature Hh ligand binds to PTCH, causing the de-repression of SMO, which then stops the inhibition of Ci that promotes transcriptional activation of target genes.

There are at least two different non-canonical pathways, the ones where SMO gets activated, but GLI does not (SMO-dependent) and the pathways in which SMO does not participate (SMO-independent). While the canonical Hh pathway has been studied for many years in numerous different tissues and organisms, alternative non-canonical pathways are currently poorly characterized. Moreover, the little knowledge we have about non-canonical pathways is related to the SMO-dependent pathway. However, there is a great need for the understanding of non-canonical SMO-independent pathways due to its potential importance in health and development [41,52–54].

PTCH1 has been suggested to be one of the most commonly mutated tumor suppressors. Therefore, there is a notable need to understand better the roles of PTCH proteins [41]. Even more, besides the canonical pathway, PTCH1 plays a crucial role in non-canonical pathways. Besides Hh molecules, the only protein that has been found so far to bind PTCH is Cyclin B1 [55,56], which in some cases could explain SMO-independent effects. Still, the lack of additional PTCH physical interactors suggests that PTCH functions

independently of SMO are due to a long-range activity. Recently, it was shown that in colon cancer-derived stem cells, the non-canonical Hh signaling positively regulates the WNT pathway [57]. Importantly, this new pathway is dependent on the interaction between SHH and PTCH1 but independent of the action of SMO [57]. These results strongly suggest that besides the primary role of PTCH1 targeting SMO, and the previously mentioned Cyclin B interaction, the protein may have other targets. However, the plausible non-existing interaction between PTCH and its targets limits the study of the non-canonical Hh pathway. As an alternative, some studies have proposed that an evolutionary evaluation can pinpoint the origin of Hh signaling and provide light into the PTCH mechanism [58].

1.3 The evolution of the Hedgehog pathway

The Hh pathway went through several changes and expansions during evolution, but still, the central mechanism and functions of the Hh pathway remain virtually unchanged from arthropods to mammals. Specifically, in mammals three hedgehog ligands exist, Sonic hedgehog (SHH), Indian hedgehog (IHH) and Desert hedgehog (DHH) [27]. PTCH receptors include the two homologs PTCH1 and PTCH2. Hence, both the receptors and ligands could play redundant functions in signaling [59,60]. Furthermore, in mammals, Ci evolved into three members GLI1, GLI2, and GLI3. Interestingly, while GLI1 and GLI2 are activators of the pathway whose expression increases in response to Hh ligands, GLI3 is a negative regulator of the pathway [61,62].

Despite the identified redundancies and gene amplification, the primary Hh pathway is highly conserved during evolution, except for nematodes, where PTCH proteins (PTC) and Hh are present, but SMO is absent (Fig. 1.3A-C). As a result, it is of singular interest to analyze the pathway in nematodes as a way to study essential PTCH dependent but SMO-independent pathways. A phylogenetic analysis of PTC showed that PTC-1 and PTC-3 are clear homologs of PTCH. On the other hand, in worms, another group of proteins, PTCH related proteins (PTRs), evolved, they share a common ancestor with PTCH but diverge in evolution together with mammalian PTCH domain-containing proteins (PTCHD) (Fig. 1.3D). While PTCHD proteins do not seem to be involved in Hh signaling [58,63–65], the role of PTRs in Hh signaling is unknown [49,66,67].

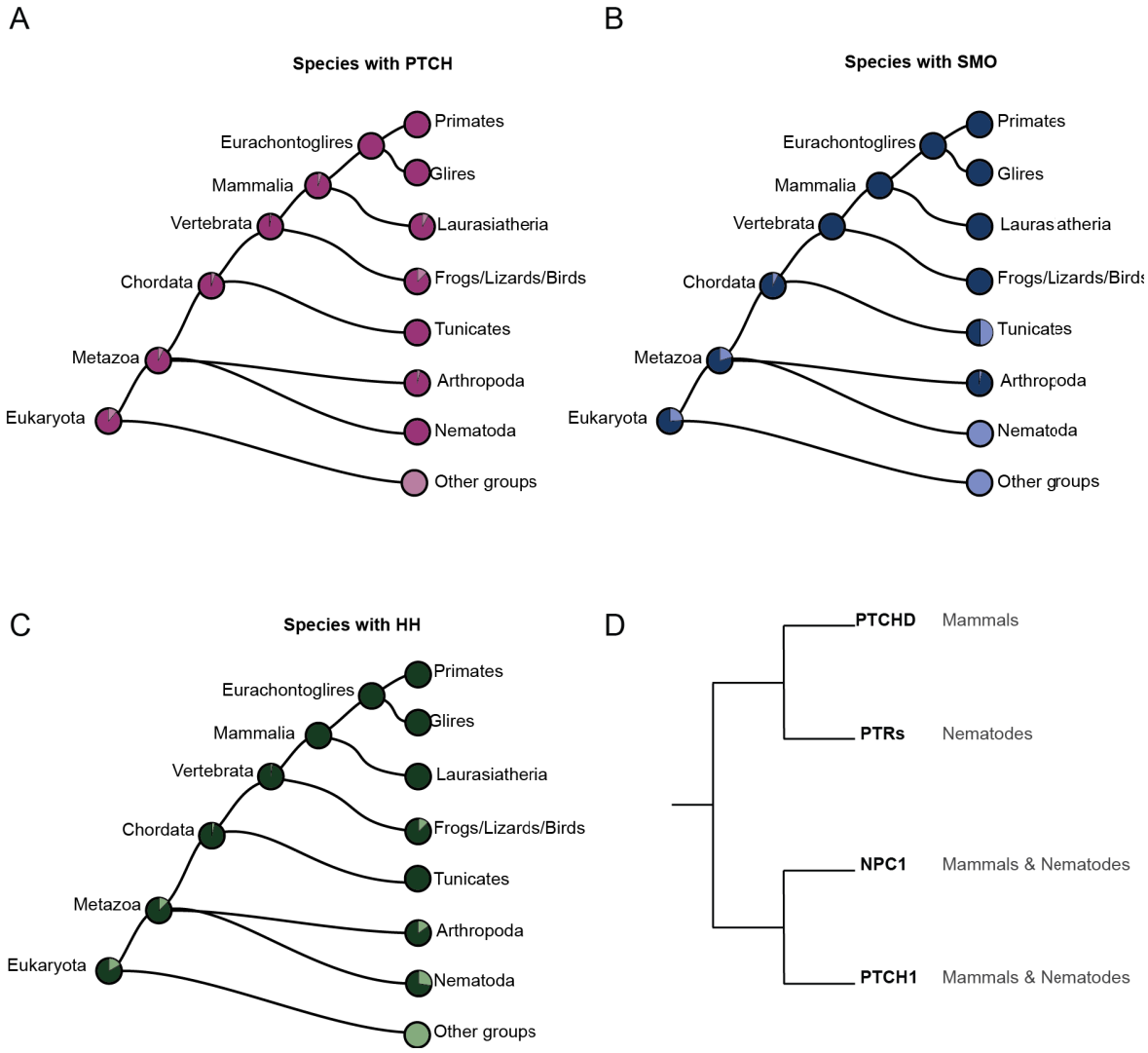

Figure 1.3. Conservation of PTCH and SMO in Eukaryotes. Gene trees of PTCH (**A**) SMO (**B**) or Hh (**C**) depicting their presence in different eukaryotes. Dark color represents the protein present in the labeled species, and light color indicates the proportion of group members missing the protein. While PTCH and Hh are present in most metazoans, SMO is absent in the *Nematoda* phylum. Adapted from Treefam [68,69]. (**D**) Phylogenetic comparison of PTCH, NPC, PTCHD and PTRs. The phylogenetic analysis was done using PhylomeDB V4[66,70]

A more detailed study of the pathway components existing in nematodes postulated that even though the 61 proteins with sequence similarity to Hh evolved from an ancestral Hh, they do not share the same structural features [71]. These Hh-like molecules are divided into four families Warthog (WRT), Groundhog (GRD), Groundhog-like (GRL), and Quahog (QUA)[72,73]. WRT and GRD are related to Hedgehog (Hh) through the carboxy-terminal auto-processing domain known as HOG. Interestingly, the active signaling part of the *Drosophila* and mammalian Hh is the N-terminal region and not the C-terminal. Therefore, it is likely that the nematode Hh can signal only in *C. elegans* and will not be recognized by the mammalian PTCH [58]. From the ten genes that have HOG modules, five are associated with a Wart domain and three with multiple copies of the Ground domain. Wart and Ground domains also occur in genes with no HOG domains; these genes are the GRL, WRT, GRD,

and GRL arose from each other, and some studies suggest that together with Hh genes are derived from a common ancestral gene [74]. The Hh related genes in worms have a predicted signal peptide for secretion, and then, it is likely that they are secreted. Therefore, they could interact with the PTCH homologs (PTC-1 and PTC-3) similarly to Hedgehog with PTCH in other organisms [58].

Another component of the pathway, TRA-1, the homolog of the transcription factor GLI, is involved in sex determination and gonad development in males and hermaphrodites, however, whether PTC proteins regulate its activity is still debated [49,71,75]. In addition, several other key players of the Hedgehog pathway, such as SuFu and Cos homologs, have been lost during evolution in nematodes. Furthermore, as mentioned previously, no SMO homolog is encoded in the worm genome (Fig.1.3 C). Consequently, nematodes seem to have retained an incomplete Hh signaling pathway in which some components are missing while other components as PTCH exist (Fig.1.4).

Proteins from the PTCH family are predicted to contain 12 transmembrane domains, and a sterol-sensing domain (SSD). PTCH proteins are members of a protein superfamily that contains bacterial and archaeal resistance-nodulation division (RND) transporters. PTCH and RND transporters are proton antiporters that catalyze active transmembrane efflux of substrates by the use of a physiological proton gradient [76,77]. It has been postulated that throughout the transition to multicellular organisms, a pre-existing sterol homeostasis system mediated by a PTCH ancestral protein acquired new functions in signaling [58]. Initially, the primordial sterol transporter diversified into a primitive PTCH, which could sense sterol concentration and modulate its levels in specific cellular membranes. Secondly, one of the descendants of the PTCH ancestor became transcriptionally controlled by a primitive SMO-GPCR that sensed the same sterol. Finally, the incidental addition of cholesterol to the Hh protein moiety originally conveyed the system under the control of gene expression. On that account, an adjacent cell could secrete the Hh bound to cholesterol and block the transporter, providing how the Hh secreting cell would now able to change the perceived state of the receiving cell. This way, a cell–cell communication system was established [58]. Hence, the fact that nematodes express PTCH homologs, that in the case of *C. elegans* are essential for development and survival [72,73] makes tempting to speculate that PTCH could have additional targets besides SMO (Fig.1.4). Those targets are likely part of a SMO-independent pathway that higher metazoans might have conserved. More importantly, in *C. elegans*, those targets are expected to be essential for survival; altogether, this makes worms a new exciting system to study the role of the evolutionarily conserved elements of the Hh pathway.

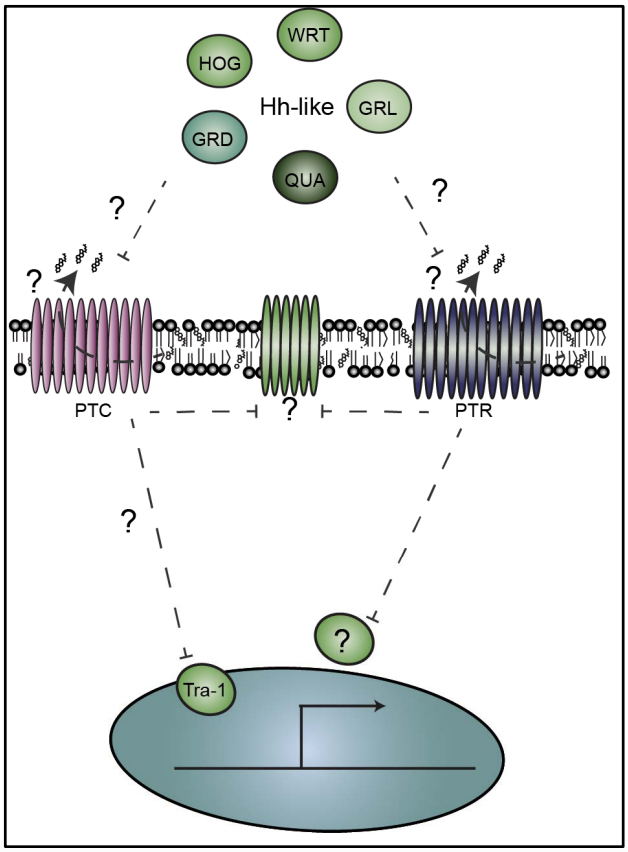

Figure 1.4. The Hh pathway in *C. elegans*. There is no canonical Hh signaling in nematodes. The worm genome encodes two PTCH homologs, PTC-1 and PTC-3, and 24 Patched related proteins (PTRs). It is not known if nematode PTC and PTR proteins can export cholesterol and whether they are regulated by one of the 61 HH like molecules (GRL, WRT, HOG, QUA, GRD). The link between PTC and PTRs and the Ci homolog, TRA-1, or other effectors remains unknown [72,73].

As just mentioned, although there is no *bona fide* Hh signaling pathway in nematodes, their genome still encodes two PTCH homologs, the essential proteins PTC-1 and PTC-3 [72,73]. In nematodes, it is unknown if a Hh-like molecule can bind PTCH proteins. Even more intriguingly, there is a group of PTCH homologs known as Patched related proteins (PTR), which have sequence similarities to PTCH. Additionally, they play an essential role in worm development, and in some cases, are crucial for the animal survival [72,73]. For PTR-24, it has been proposed that a Hh-like protein (in this case, GRL-21) can regulate it [78]. Similarly, GRL-7 has been suggested to interact and function with PTR-18 (personal communication Dr. Masamitsu Fukuyama). However, the functions and the biological consequences of the binding of GRLs to the PTRs remain currently unknown.

In *C. elegans*, we do not know the mechanism of action of the PTC and PTR proteins, even though some of them (PTC-1, PTC-3, PTR-2 and, PTR-4) are essential for worm development and survival [72]. Remarkably, most worm PTC proteins own highly conserved regions in the transporter-like region comprising the transmembrane domain 4 and 10 suggesting a conserved function with PTCH1 [18,72]. The reported expression pattern of the PTC and PTR indicates that PTC-3 and most PTRs oscillate during larval development [79]. Intriguingly, the oscillation pattern is different for each PTC/PTR (Fig. 1.5A).

The rhythmic mRNA expression suggests that most of these proteins are involved in the regulation of development. In terms of tissue expression patterns, it is interesting to notice that most PTC and PTRs are primarily expressed in the hypodermis (worm's epidermis[80]), but PTC-1 and PTC-3 expression levels are higher in comparison to PTR proteins [81] (Fig. 1.5B). Even so, it is intriguing that worms require more than 20 PTC and PTRs with very tight regulation of the mRNA levels during larval development.

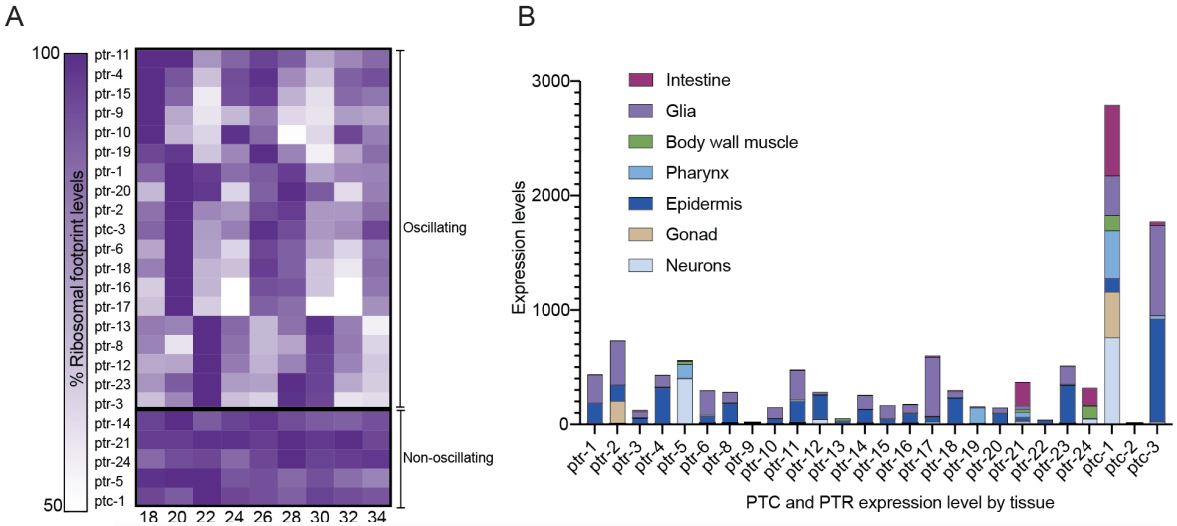

Figure 1.5. Comparison of PTC and PTR expression pattern. (**A**) The ribosomal footprints of PTC and PTR proteins during *C. elegans* larval development, revealed a change in ribosomal footprint levels during time. The oscillations are not synchronized among the different PTCH homologs. Data was obtained from the published data set of [79]. (**B**) Tissue-specific expression levels of PTC and PTR proteins in L2 nematodes, data were obtained from a published data set [81].

Previous studies have shown that PTC-1 is acting in the germline and its progenitors. Proper germ cell cytokinesis requires the action of PTC-1, but in contrast to the vertebrate homologs, it has no role in body patterning or proliferation [82]. PTR-4, PTR-18, and PTR-23 are suggested to be involved in endocytosis of yolk during oocyte maturation [72]. Additionally, PTR-23 is known to have a function in osmoregulation [83]. On the other hand, PTR-24 appears to regulate mitochondrial fragmentation and lipid accumulation [78].

PTC-3 null mutant embryos exhibited normal morphogenesis and muscle activity before hatching. However, hatched larva died with a fluid-filled appearance, which suggested a defect in osmoregulation [18]. Furthermore, *ptc-3(RNAi)* feeding experiments showed that PTC-3 is essential during larval development, and RNAi treated animals do not reach adulthood [18]. Similarly, loss of PTC-3 resulted in molting defects and decreased body size, supporting the notion of the requirement of PTC-3 activity throughout larval development [18,72]. Notably, for these functions, PTC-3 requires an intact and functional permease domain[18]. However, the PTC-3 mechanism of action remains mostly elusive, and the molecule transported by its permease domain has not yet been identified. Moreover, the role of the SSD in the PTC-3 function is currently unknown. Structurally, PTC-3 is

predicted to share similarities in the cytoplasmic N- and C-termini with the mammalian PTCH1 protein [84]. When PTCH1 structure is compared with the predicted structure of PTC-3 it can be noticed that both of them are very alike (Fig 1.6A B), in a superposition of both structures few differences can be detected (Fig. 1.6C) this supports the idea that both may have a conserved function.

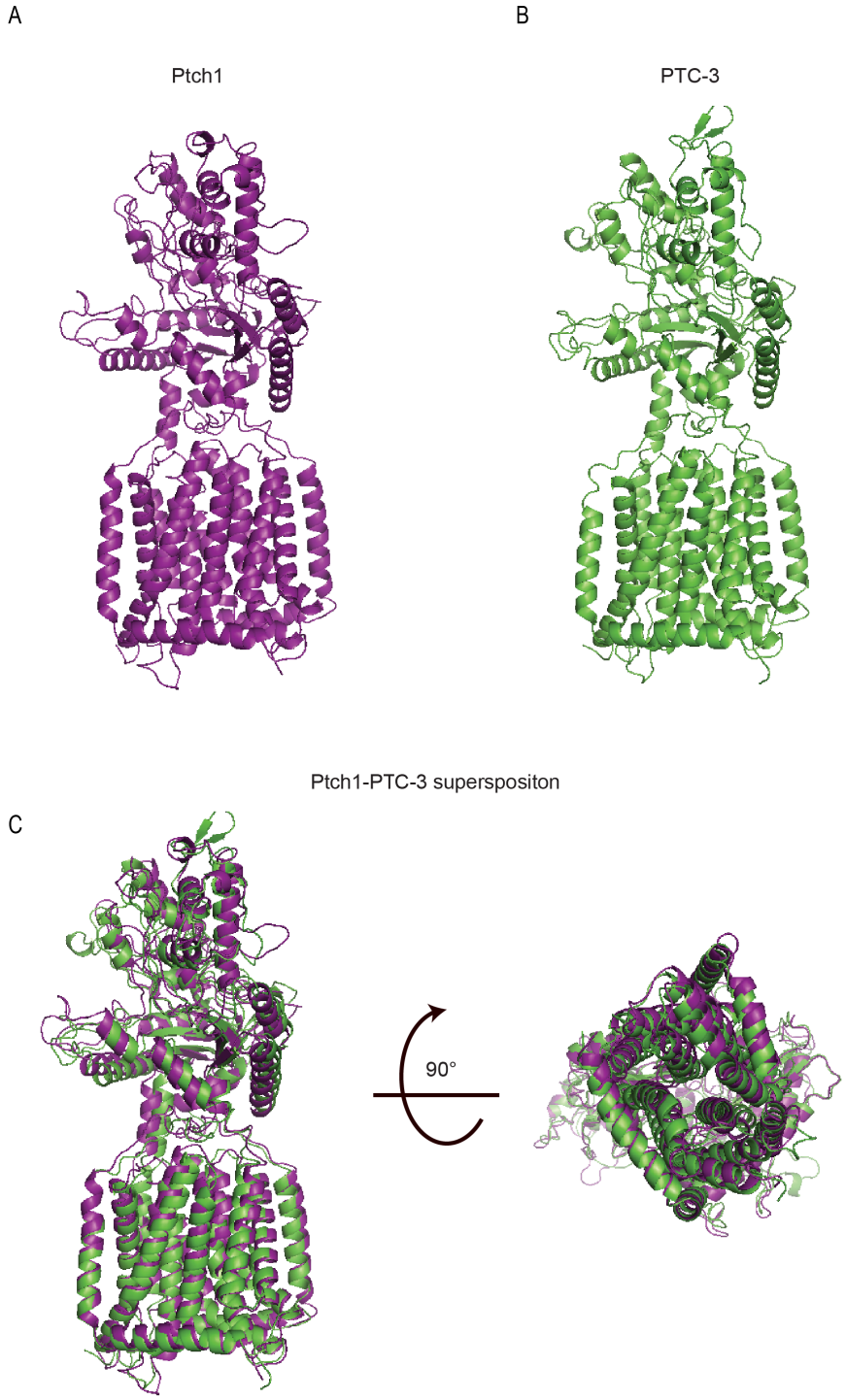

Figure 1.6. PTCH1 and PTC-3 are predicted to share structural similarities. (**A**) PTCH1 structure resolved by CryoEM [85]. (**B**) PTC-3 structure based on Phyre2 prediction [84] (**C**) Superposition of PTCH1 and PTC-3 protein structures. Protein structures were visualized with PyMol [86].

Even though PTC proteins have been shown to have multiple roles in regulating *C. elegans* physiology and development, the molecular mechanisms underlying the function of the different PTC and PTRs in nematodes remain mostly unknown. Therefore, they are a possible approach to study PTCH-dependent but SMO-independent Hh signaling. Consequently, there is a need to characterize their functions and effects in cellular physiology.

1.4 Cholesterol levels as decisive mediators of PTCH function

The structural analysis of PTCH1 provided strong evidence that PTCH1 functions as a cholesterol permease [85,87–90]. More precisely, PTCH1 structure revealed a hydrophobic conduit with sterol-like contents[90], two additional steroid-shaped densities were resolved, one in the extracellular domain and a second one in the membrane-embedded cavity of PTCH1's SSD. Furthermore, structural changes upon Hh binding suggest that Hh inhibits the permease function, and as a consequence, plasma membrane cholesterol levels would increase. Altogether, demonstrating *in vitro* that PTCH1 mediates the export of inner leaflet cholesterol, export that can be regulated by Hh[89] (Fig.1.7).

The dimerization of PTCH1 has been suggested as a critical feature to initiate Hh signaling[87]. Interestingly, the structural analysis showed an asymmetric arrangement of two PTCH1 molecules[87]. The binding of SHH to a tunnel in the PTCH1 structure explains PTCH1's dimerization. This tunnel can be blocked by mutations in the extracellular domain of PTCH1, mimicking a palmitate insertion. These mutations abolish the Hh pathway repression by PTCH1. Similarly, a structure-guided mutational analysis revealed that interaction between SHH and PTCH1 is steroid-related [85,90]. As a result, both modifications (palmitate and cholesterol) on SHH may function to join two PTCH1 receptors (Fig. 1.7).

Although SMO can bind different sterols, cholesterol acts as an endogenous SMO activator, driving its conformational change, which enables further signaling[91]. Therefore, it is very likely that the inhibition exerted by PTCH on SMO is cholesterol-dependent. Advocating that SMO might sense the increase of membrane cholesterol levels upon Hh binding to PTCH1 through its sterol sensing domain, such sensing thereby activates the GPCR [77,92]. Further evidence was provided by the shared essentiality of the hydrophobic pore in PTCH1. The pore is not just necessary for cholesterol export but also for SMO suppression[90]. This cholesterol-dependent mechanism would then explain the non-stoichiometric inhibition of PTCH1 over SMO [93].

Figure 1.7. PTCH1 controls cholesterol levels in the plasma membrane. (**A**) PTCH1 transports cholesterol out of the inner leaflet of the plasma membrane. (**B**) Upon Hh binding (green), PTCH1 dimerizes, and cholesterol transport is inhibited. Images of protein structures were visualized with PyMol [85–87].

Moreover, the intracellular localization of PTCH1 and SMO supports the hypothesis of cholesterol-mediated PTCH1 regulation of SMO. An inherent feature of the SHH signaling is its activity dependence on PTCH1 and SMO localization. Active PTCH1 has been described to localize to cilia, a microtubule-based organelle that protrudes from the membrane. Secreted SHH binds to PTCH1 in cilia reducing its diffusion and as a consequence getting it removed from cilia [94]. Likewise, depletion of cellular cholesterol mimics PTCH1 reduced diffusion. This reduced motion suggests that the change of PTCH1 localization upon SHH addition could be due to PTCH1 membrane microenvironment modification. Such modification might be related to PTCH role in cholesterol transport [95]. Likewise, once PTCH1 inhibition over SMO is released, SMO accumulates in the cilia [95]. SMO relocation strongly advocates that the observed effects on protein localization upon SHH binding may be related to the repression of PTCH cholesterol efflux ability and further accumulation of membrane cholesterol.

Whether cholesterol regulation is a common feature of all PTCH proteins is not known. It remains to be addressed the potential conservation of the cholesterol transporter function in the nematode and PTR proteins. Interestingly, PTR-2 is upregulated after cholesterol treatment [96]. Furthermore, a mutation in PTR-6 has been described to induce changes in membrane permeability that can be counteracted by the depletion of PTR-23, PTR-15, or the worm homolog of sterol O-acyltransferase 1, which catalyzes the formation of cholesterol esters[97]. Altogether, these results suggest a link between PTC homologs and cholesterol.

1.5 Modulation of cell signaling by cholesterol

Cholesterol is the most abundant steroid in animals; it is a fundamental component of cell membranes and lipoproteins. Cholesterol can be found in two states in the cells,

esterified in lipid droplets and unesterified in cellular membranes. More than 80% of all sterols in *C. elegans* are unesterified sterols, mainly 7-dehydrocholesterol (40.5%) and cholesterol (52.3%)[98]. Cholesterol has unique chemical properties. It has very low water solubility, however, due to its hydrophilic C3-hydroxyl group it is an amphipathic molecule (Fig.1.8 A). It can localize to polar-nonpolar interfaces like cell membranes, where its hydroxyl group faces the cytosolic, luminal, and extracellular surfaces and the hydrocarbon rings are embedded into the hydrophobic layer composed by the fatty acid (FA) acyl chains [99](Fig. 1.8 B and C).

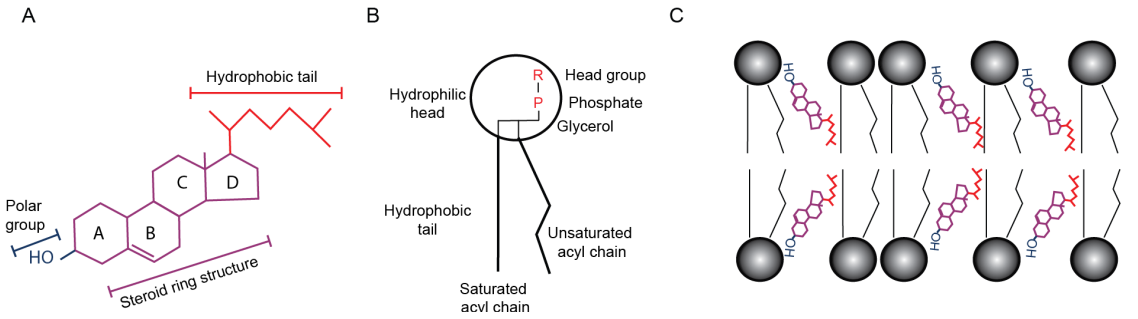

Figure 1.8. Cholesterol properties. (**A**) Model of the cholesterol structure. Cholesterol contains 27 carbon atoms that form 4 ring structures, marked with letters from A to D, a carbon tail, and a hydroxyl group. (**B**) Phospholipid structure consisting of a glycerol molecule, two fatty acids, and a modified phosphate group bound to a polar head group. **(C)** Cholesterol's hydroxyl group aligns with the phospholipid phosphate heads while the hydrophobic portion lays into the hydrophobic layer.

Mammals can produce cholesterol in the liver from acetyl- CoA or take it up from the diet [100]. The mammalian cells take up cholesterol bound to low-density lipoproteins (LDL) by endocytosis. Then, LDL-cholesterol is translocated to late endosomes from where it reaches the lysosomes. In lysosomes, cholesterol is transferred from LDL into the membranes by the proteins Niemann-Pick type C 1 and 2 (Npc1 and Npc2). Npc1 evolved from a common PTCH ancestral transporter [101].

In membranes, cholesterol affects the overall membrane structure. In the presence of monounsaturated fatty acids (MUFAs), cholesterol induces condensation and rigidification of the membrane, affecting stiffness, permeability, and protein distribution (Fig. 1.9) [102]. Cholesterol can regulate protein activity through different mechanisms. On the one hand, cholesterol can act as a ligand interacting with specific amino acid sequences (e.g., SSD domains in SMO [77,85,92]), on the other hand, it can be covalently bound through post-translational modifications to other proteins (e.g., Hh molecules[75]). The cholesterol binding to proteins can induce conformational changes and promote protein activation (e.g., SMO [92]). Additionally, it can alter the diffusive properties of other proteins (e.g., Hh). Direct interaction with cholesterol can likewise affect protein localization (e.g., ciliar localization of PTCH [77,85,91,92,95]). Furthermore, cholesterol can help recruiting proteins into cholesterol-rich membrane microdomains, called lipid rafts, which represent signaling platforms (Fig. 1.9).

The rafts concentrate specific proteins, promoting the local accumulation of membrane sensors, receptors, and transporters. That accumulation enhances protein activity by contributing to their colocalization with binding partners [103,104]. Consequently, membrane cholesterol deregulation may play a crucial role in pathogenic processes such as cancer. Indeed, increased cholesterol efflux contributes to cell reprogramming and tumor-promoting functions[105]. Due to its integral role in regulating membrane fluidity, cells must preserve an optimal amount of cholesterol at different cellular membranes. Surprisingly, the mechanisms of how the cells regulate optimal cholesterol levels in different membranes are not yet well understood.

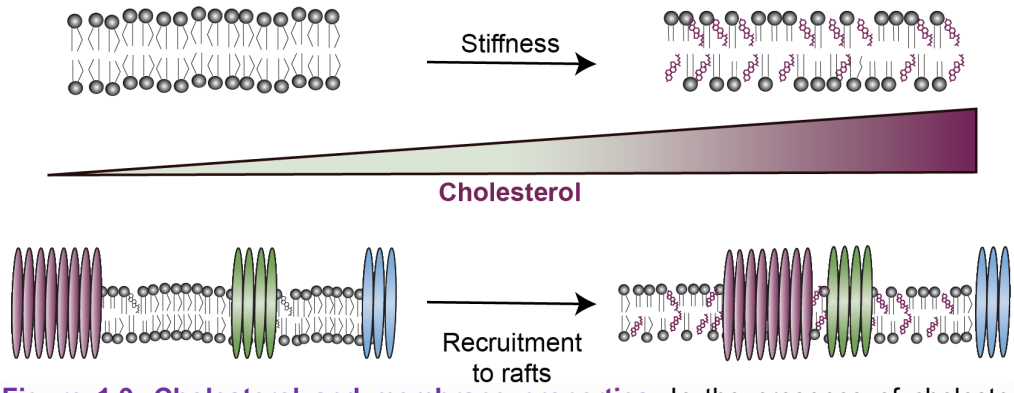

Figure 1.9. Cholesterol and membrane properties. In the presence of cholesterol, membrane fluidity is affected, and membrane microdomains with high concentrations of sphingolipids and cholesterol form. They serve as platforms to concentrate certain proteins at the plasma membrane.

Importantly, the cholesterol transport function of PTCH opens the possibility of additional un-explored interaction of the Hh pathway with other signaling pathways. In addition to SMO, receptors of other signaling pathways could be re-localized, and its activation could be affected due to changing cholesterol levels in the membranes as a consequence of PTCH function. It is relevant to keep in mind that throughout development, parallel to the Hh gradient other signaling molecules such as WNT, FGF and retinoic acid also establish gradients and the combined action of all these gradients is required to ensure correct developmental patterning [40]. Hence, changes in cholesterol levels may affect multiple developmentally critical signaling pathways. Indeed, membrane cholesterol levels seem to affect the WNT pathway [106]. However, it is not yet known whether Hh and WNT pathways are coregulated by cholesterol in specific tissues or developmental stages.

In addition to the influence of membrane properties, as well, sterols can regulate the transcription of a variety of genes[107–111]. For example, in mammals, the sterol regulatory element-binding proteins (SREBPs) respond to nutrient levels regulating lipid metabolism [108,112]. The action of the two SREBP isoforms differs in mammals [113]. The isoform SREBP2 controls the expression of cholesterogenic genes and stays under a cholesterol-mediated negative feedback regulation. Initially, cells produce the SREBP2 protein as an inactive

precursor located at the ER. Cholesterol depletion promotes transit of SREBP2 to the Golgi where it is cleaved, allowing the active fragment to stimulate gene expression. In contrast to SREBP2, SREBP1 regulates fatty acid, phospholipid, and triacylglycerol biosynthesis. As expected, SREBP1 is not controlled by cholesterol but rather by feeding cues like phosphatidylcholine depletion[113]. Remarkably, *C. elegans* has only one single ortholog of SREBP, SBP-1, which regulates lipid storage, similar to SREBP1 [114]. SBP-1 prompts transcription of stearoyl-CoA desaturase genes. As well, SBP-1 responds to low levels of S-adenosylmethionine and phosphatidylcholine to activate lipogenesis[115]. A response similar to SREBP2 has not been found in *C. elegans*, contributing to the lack of knowledge of the precise mechanism of cholesterol regulation in the nematode.

Sterol signaling during *C. elegans* development

It is important to note that in contrast to mammals, *C. elegans* is a cholesterol auxotroph that relies on dietary sterol ingestion for normal growth[116]. The lack of cholesterol during worm development reduces adult life expectancy by 40%. Furthermore, sterol deprived animals lose motility and muscle mass [117]. For normal growth and development in the wild, nematodes can directly utilize cholesterol or convert plant sterols such as sitosterol and stigmasterol into 7-dehydrocholesterol and cholesterol [118,119]. In the laboratory, worms are grown in the presence of 5 mg/l of cholesterol[120]. A study using the cholesterol analog DHE showed in adults cholesterol accumulation in the oocytes and sperm, while in developing larvae, cholesterol is enriched in the pharynx, nerve ring, and intestine [121].

Contrary to mammals in *C. elegans*, the majority of sterols are not esterified and stored in lipid droplets. Consequently, the immediate use of them either as structural or signaling components is expected. However, it is unknown how *C. elegans* is using and regulating sterols across its development and lifetime. This process is expected to be crucial, provided the worm's inability to store large amounts of cholesterol.

Sterol signaling has an essential role during worm development. In the wild, larvae need to sense the environment and decide between developing into adults or entering dauer diapause and wait for proper conditions to develop into adults (Fig. 1.4). In the decision making of entrance into dauer stage or continuous development, steroid hormones are essential [122,123]. Accordingly, worms require cholesterol available at the right time and place in order to synthesize dafachronic acid (DA), the hormone required to achieve reproductive growth [124]. When larvae encounter a favorable environment, the insulin and TGFβ pathways are active, and growing larvae produce Δ4- and Δ7-dafachronic acid. To generate DA, worms convert cholesterol into 7-dehydrocholesterol (7-DHC) by the Rieske oxygenase DAF-36, followed by the action of the short-chain dehydrogenase DHS-16 and the cytochrome P450 known as DAF-9 or the hydroxysteroid dehydrogenase HSD-1 [125,126]. DA

binds and activates the transcription factor DAF-12, preventing the entry into the dauer stage[123]. If the environment is not advantageous for development, worms do not produce DA, and therefore DAF-12 does not become active [127].

There is growing evidence showing that in the nematode, cholesterol has a role in DA-independent processes [111]. Consequently, specific levels of steroid hormones may prompt different signals [124]. Unfortunately, due to the lack of precise analytical methods to convincingly uncover the relationship between steroids and physiological outcomes, these interactions remain elusive.

Alternative targets of sterol signaling in *C. elegans* are nuclear hormone receptors (NHRs). NHRs are a family of transcription factors regulated by lipophilic molecules like steroids, retinoids, bile, and fatty acids. Interestingly, in the worm, NHRs suffered a vast expansion, there are 284 receptors, compared to 21 in flies and 48 in humans [128]. NHRs can form heterodimers harboring distinct functions [129–131]. Regardless of the great importance of NHR regulation, the physiological ligands of most NHRs are scantily characterized due to a lack of suitable techniques. More importantly, the role that the massive NHR expansion plays during nematode life and development is unknown. Interestingly, NHRs are also known to affect molting, which is dependent on sterol regulation[111].

Molting is the process of removing the old larval cuticle with a new bigger cuticle. The cuticle is the worm exoskeleton that safeguards the worm from the environment. The cuticle attaches to worm muscles. Consequently, locomotion requires an integral and functional cuticle [132]. Cuticle and molting defects can be a consequence of mutations in genes encoding structural components of the cuticle. As previously mentioned, additionally to defects in the structural components of the cuticle, alterations in other signaling molecules can induce cuticle defects, for instance, impaired sterol signaling, and alterations in genes related to hormonal control (e.g., NHRs) promote cuticle defects [72,122,133–135]. Furthermore, another group of genes linked to molting defects are PTC and PTR proteins.

Altogether, the observed phenotypes in PTC mutant worms and the molecular function of PTC proteins suggest a connection between them and the regulation of cholesterol signaling [77,87–89]. Under this premise of a conserved cholesterol transport function, the oscillating levels of PTC, PTRs, and Hh-like proteins, we hypothesized that PTC and PTRs give the worm the possibility to finely time cholesterol levels locally and temporally throughout development, potentially to control sterol signaling.

2. Aim of the thesis

This thesis aimed to elucidate the molecular mechanism of a non-canonical Hh pathway using the *C. elegans* as model system. Even though there is extensive evidence highlighting the relevance of the non-canonical Hh pathways, the study of SMO-independent effects is limited. This hampered examination is due to the potential functional overlap of PTCH in the canonical and non-canonical pathways. As canonical Hh signaling is absent in *C. elegans*, the nematode represents a perfect model to study non-canonical signaling. Here we focused on the function of the essential PTCH homolog PTC-3.

Specifically, we set the following objectives:

•Determine the conservation of PTCH1 function in the *C. elegans* PTCH homolog PTC-3.

•Elucidate the role of PTC-3 *in vivo*.

•Investigate the particular effects of PTC-3 lost in cellular functioning.

•Examine the role of PTC-3 regulating signaling in *C. elegans*.

Besides PTCH, there is a big group of related proteins known as PTR proteins which in *C. elegans* some PTRs are also essential. As the second aim of this thesis we aimed to characterize the function of one essential PTR, PTR-4. The particular objectives of this part of the thesis were:

• Characterize the cellular consequences of the lack of PTR-4, an essential PTCHD homolog in *C. elegans*.

• Address the potential overlapping functions of PTC-3 and PTR-4 in cellular physiology.

3. Results

3.1 *C. elegans* PTCH regulates lipid homeostasis by controlling cellular cholesterol levels.

The following manuscript was submitted for publication at the time of the submission of this thesis. The figures and text have been adapted to match the present work. The submitted manuscript can be found in https://www.biorxiv.org/content/10.1101/816256v1. bioRxiv 816256; doi: https://doi.org/10.1101/816256

Patched regulates lipid homeostasis by controlling cellular cholesterol levels

Carla E. Cadena del Castillo[1], J. Thomas Hannich[2], Andres Kaech[3], Hirohisa Chiyoda[4], Masamitsu Fukuyama[4], Nils J. Færgeman[5], Howard Riezman[2] and Anne Spang[1]

[1]Biozentrum, University of Basel, Switzerland [2] Department of Biochemistry and NCCR Chemical Biology, University of Geneva, Switzerland, [3]Center for Microscopy and Image Analysis, University of Zürich, Switzerland, [4]Laboratory of Physiological Chemistry, Graduate School of Pharmaceutical Sciences, University of Tokyo, Tokyo, Japan, [5]Department of Biochemistry and Molecular Biology, Villum Center for Bioanalytical Sciences, University of Southern Denmark, Odense, Denmark.

Corresponding Author:
Anne Spang
Biozentrum
University of Basel
Klingelbergstrasse 70
CH-4056 Basel
Switzerland

Email: anne.spang@unibas.ch
Phone: +41 61 207 2380

Author contributions

AS and CECC wrote the manuscript and designed the experiments. CECC performed the majority of the experiments. TH and HR performed the Lipidomic analysis. AK generated the TEM and FIB-SEM data. MF and HC generated the PTC-3-GFP *C. elegans* strain. NF supervised the CARS experiments. AS, CECC, TH, HR and AK analyzed the data. All authors commented on the manuscript.

3.1.1 Abstract

Hedgehog (Hh) signaling is essential during development and in organ physiology. In the canonical pathway, Hh binding to Patched (PTCH) relieves the inhibition of Smoothened (SMO). Yet, PTCH may also perform SMO-independent functions. While the PTCH homolog PTC-3 is essential in *C. elegans*, worms lack SMO, providing an excellent model to probe non-canonical PTCH function. Here, we show that PTC-3 is a cholesterol transporter. *ptc-3(RNAi)* leads to accumulation of intracellular cholesterol and defects in ER structure and lipid droplet formation. These phenotypes were accompanied by a reduction in acyl chain (FA) length and desaturation. *ptc-3(RNAi)*-induced lethality, fat storage, and ER morphology defects were rescued by reducing dietary cholesterol. We provide evidence that cholesterol accumulation modulates the function of nuclear hormone receptors such as of the PPARα homolog NHR-49 and NHR-181, and affects FA composition. Our data uncover a novel role for PTCH in organelle structure maintenance and fat metabolism.

3.1.2 Introduction

The Hedgehog (Hh) signaling pathway is crucial during animal development and has also demonstrated roles independent of development stages. The Hh receptor PTCH is among the most mutated tumor suppressors [90], and more specifically, PTCH1 mutations are the cause of the Gorlin Syndrome [32]. In the classical Hh signaling pathway, PTCH inhibits the plasma membrane G-protein coupled receptor (GPCR) smoothened (SMO). Upon Hh binding to PTCH, this inhibition is relieved, and SMO can activate a downstream signaling cascade. The mechanism by which PTCH inhibits SMO was enigmatic for a long time because PTCH represses SMO without direct contact [59]. PTCH1 was shown to be able to transport cholesterol [77,89,95] which in turn will directly activate SMO[91], a finding that was supported by recent structural analyses [85,87,88,90]. The structures suggest that Hh inhibits PTCH transporter function, and hence plasma membrane cholesterol levels could increase. Such an increase of cholesterol might be sensed through the sterol sensing domain in SMO and thereby activate the GPCR. As PTCH may mainly function as a cholesterol transporter, it might also affect other signaling pathways. In fact, in recent years, SMO-independent PTCH signaling has been reported [52,53,56,57]. However, the mechanistic understanding of these non-canonical Hh signaling pathways remains largely unknown.

Caenorhabditis elegans expresses two PTCH homologs, PTC-1 and PTC-3, which are essential for development and survival [49,72,136]. While PTC-1 function appears to be mostly restricted to the germline, PTC-3 is expressed in somatic tissues [18,81,82]. No clear SMO homolog is encoded in the genome. In addition, some of the other downstream targets of the canonical Hh signaling pathway are also missing. In fact, it was proposed that SMO and those components were specifically lost during evolution in nematodes [49,71,74,75]. For example, SUFU is not conserved, and the homolog of the transcription factor Gli, TRA-1, is involved in sex determination and gonad development in males and hermaphrodites [137]. For that reason, *C. elegans* provides an excellent model to study non-canonical, SMO-independent Hh signaling pathways, in particular in somatic tissues. To dissect SMO-independent PTCH functions, we concentrated on PTC-3, which is expressed in somatic tissues, in particular in the epidermis, glia, and gut [81]. We found that reduction of PTC-3 levels causes the accumulation of intracellular cholesterol and a reduction in poly unsaturated fatty acids (PUFAs). Moreover, the endoplasmic reticulum lost most of its reticulate tubular form and developed elaborate sheet structures in the intestine. This effect, in turn, strongly impaired lipid droplet biogenesis, resulting in the inability of the animal to store fat. Reduction of dietary cholesterol rescued fat storage defects, the ER morphology defects, and improved development and survival in *ptc-3(RNAi)* animals. Cholesterol levels influence nuclear hormone receptor activity, such as of the PPARα homolog NHR-49, which is involved in the regulation of FA synthesis. Thus, our data demonstrate that PTCH also

controls intracellular cholesterol levels in *C. elegans*. Moreover, we show that PTCH thereby impinges on FA metabolism, organellar structure and fat storage capacity.

3.1.3 Results

3.1.3.1 PTC-3 has cell autonomous and non-autonomous functions and is required for lipid storage in the intestine.

In order to understand the function of PTCH proteins in *C. elegans*, we decided first to revisit the phenotypes caused by the depletion of the somatically expressed PTC-3. Like its mammalian homolog, *ptc-3* is essential for development. Consistently, it has been reported that *ptc-3(RNAi)* results in growth, molting, and vulva morphogenesis defects [18,72]. Given the essential role of PTCH in development, we started the knockdown by *RNAi* only at the L2 stage of development, allowing the worms to progress further in development and even some to reach adulthood. In addition to the previously reported phenotypes, we noticed that the *ptc-3(RNAi)* animals were much paler than their mock-treated counterparts (Fig. 3.1.1A). Pale worms are an indication of defects in fat storage. *C. elegans* has a much simpler body plan than humans, and hence some *C. elegans* organs take over more functions. For example, the worm intestine has paracrine functions and also serves as the fat storage organ [138]. Thus, in a simplified view, the *C. elegans* intestine represents the functional equivalent of the human intestine, adipose tissue, and liver. To test whether PTC-3 was expressed in the gut as indicated by genome-wide expression analyses [81], we raised antibodies against PTC-3 (Fig. 3.1.S1A). Those antibodies decorated the apical membrane of gut epithelial cells, while no plasma membrane signal was detected in oocytes, consistent with the notion that PTC-3 is present only in somatic tissues (Fig. 3.1.1B). This localization was confirmed with a GFP-tagged PTC-3 (Fig. 3.1.S1B).

To determine which phenotype is dependent on intestinal PTC-3, we performed a gut-specific knockdown of PTC-3 [139]. *ptc-3(RNAi^{gut})* animals were still paler and thinner than mock-treated animals (Fig. 3.1.1C). Moreover, vulva morphogenesis defects were also observed upon the *ptc-3(RNAi^{gut})* regime, indicating that PTC-3 has cell-autonomous and non-autonomous functions.

As outlined above, pale phenotypes are often associated with lipid storage defects in worms [138,140]. Nile Red staining indeed showed a reduction in lipid content in *ptc-3(RNAi)* animals (Fig. 3.1.1D and E). Of note, this reduction was observed in the intestine, but not in the germline, in accordance with the absence of PTC-3 expression in oocytes. A drawback of Nile Red staining is that autofluorescence in the intestine caused by lysosome-related organelles (LROs) is also potentially measured at the same time, which may confound the results. Therefore, we turned to Coherent anti-Stokes Raman Scattering Microscopy (CARS), a dye-free method recognized for accurate *in vivo* lipid detection in worms [141]. This analysis confirmed the Nile Red staining, and we observed an about 50% reduction in lipid content (Fig. 3.1.1F and G), indicating that we can use Nile Red for further

analysis. The CARS signal did not overlap with the autofluorescence of LROs (Fig. S1C). We conclude that loss of *PTC-3* causes a reduction in fat storage in the intestine.

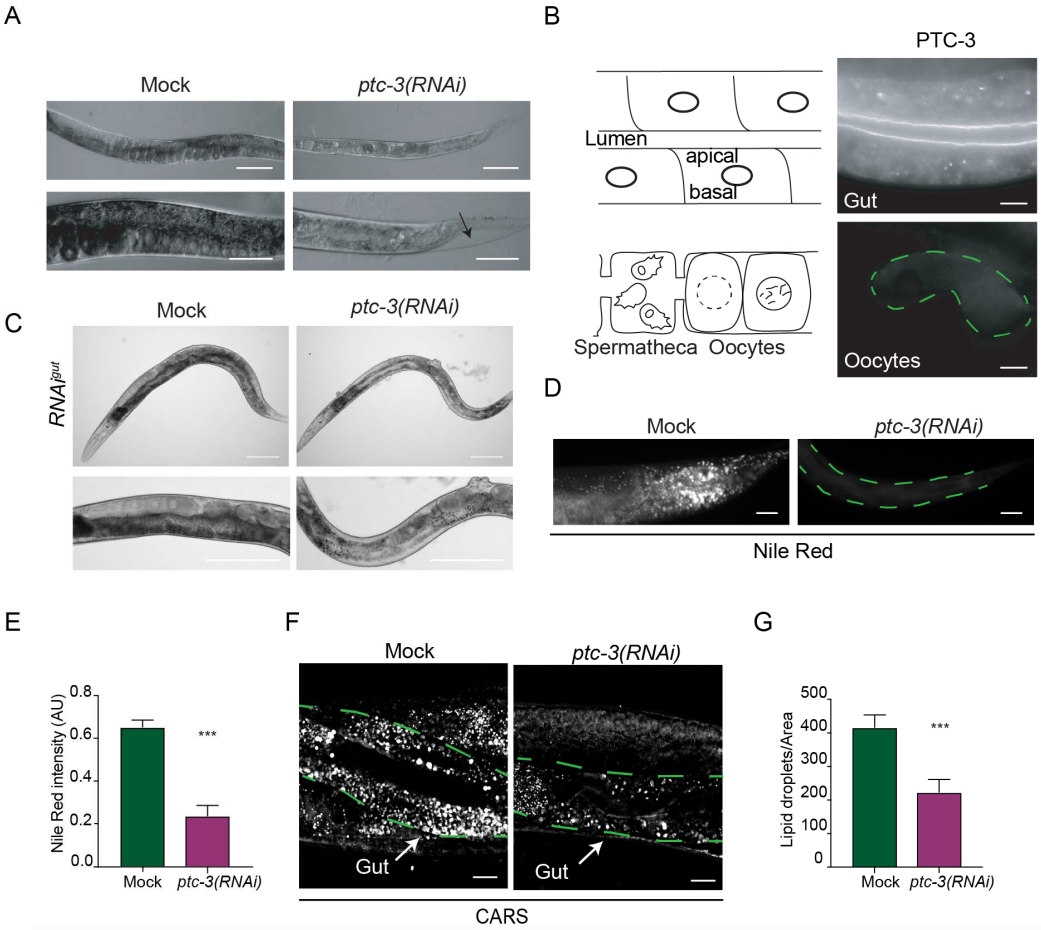

Figure 3.1.1. Loss of PTC-3 causes developmental and fat storage defects. (**A**) Light microscopy images of adult N2 worms grown from L2 larva on mock or *ptc-3(RNAi)* bacteria. *ptc-3(RNAi)* animals are smaller, paler and show cuticle defects. The arrow points to a cuticular defect. Scale bars upper panel 20 µm, lower panels 100 µm. (**B**) Immunofluorescence of isolated intestine and gonad from wild-type worms. Schematic representation of the intestine and the proximal gonad. PTC-3 is present at the intestinal apical membrane. Scale bar 10 µm. (**C**) PTC-3 has cell autonomous and non-cell autonomous functions. Light microscopy images of adult gut specific RNAi worms *(RNAi^{gut})* grown from L1 larva on mock or *ptc-3(RNAi)* bacteria. *ptc-3(RNAi^{gut})* animals show intestinal and vulval defects. Scale bars 100 µm. (**D**) Lipid content is reduced in *ptc-3(RNAi)* animals. Nile Red staining of mock and *ptc-3(RNAi)* treated worms. Scale bars 20 µm. (**E**) Quantification of Nile Red staining shown in (D). Error bars are SEM. *** p<0.0001. (**F**) CARS microscopy reveals reduction of lipid levels in live *ptc-3(RNAi)* animals. Scale bars 10 µm. The intestine is outlined by green dashed lines. Arrows point to the intestine. (**G**) Quantification of CARS signal. Error bars are SEM. *** p<0.0001.

3.1.3.2 PTC-3 is a cholesterol transporter

Recent data suggested that mammalian PTCH1 acts as a cholesterol transporter [77,85,87–90]. To investigate whether PTC-3 shares the function of PTCH1 as cholesterol transporter, we first expressed PTC-3 in *Saccharomyces cerevisiae*, which does not contain any cholesterol [142] and measured cholesterol efflux from cells using TopFluor cholesterol in a pulse-chase experiment (Fig. 3.1.2A). PTC-3 expressing yeast cells exported cholesterol significantly faster out of the cell than control cells, similar to what has been observed for

mammalian PTCH1[89]. This efflux capacity was dependent on an active permease domain, since a mutation in the permease domain [18], *ptc-3*^{D697A}, strongly reduced the cholesterol efflux. The *ptc-3*^{D697A} mutation has been reported to cause larval lethality in worms [18], establishing that cholesterol efflux is the essential function of PTCH. Next, we repeated the pulse-chase experiment in worms. While in mock-treated worms, TopFluor cholesterol was present mostly in the gut lumen, it was still strongly accumulated in the intestine in *ptc-3(RNAi)* worms after the washout, further demonstrating the role as cholesterol transporter (Fig. 3.1.2B). Finally, we measured sterol levels by mass spectrometry. Cholesterol levels were increased in *ptc-3(RNAi)* worms, while 7-dihydrocholesterol (7-DHC) and lophenol levels were decreased (Fig. 3.1.2C). 7-DHC and lophenol are downstream products of

cholesterol in worms, indicating that cholesterol metabolism might also be affected by *ptc-3(RNAi)*. Taken together our data strongly suggest that PTC-3, like PTCH1, is a cholesterol transporter at the plasma membrane.

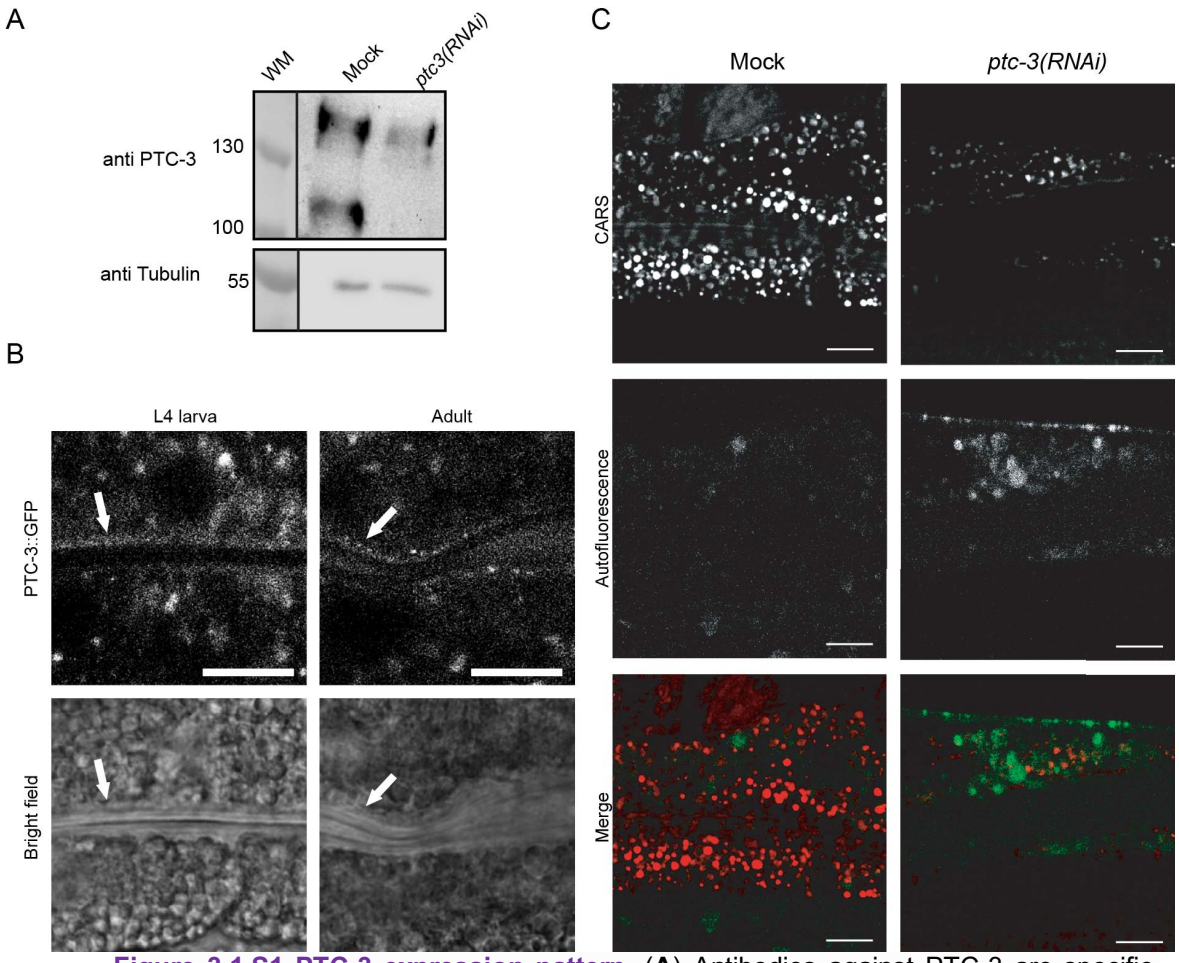

Figure 3.1.S1 PTC-3 expression pattern. (**A**) Antibodies against PTC-3 are specific. Immunoblot of lysates of mock or *ptc-3 (RNAi)* treated worms. (**B**) PTC-3 gut localization was confirmed with a GFP-tagged PTC-3. Arrows point to the apical intestinal membrane. Scale bars 10 µm (**C**) Mock and *ptc-3(RNAi)* treated animals were imaged with CARS microscopy. The signal did not overlap with the autofluorescence of LROs, validating the proper spectral separation of the filters, and that we can detect specifically lipid droplets. Scale bars 10 µm.

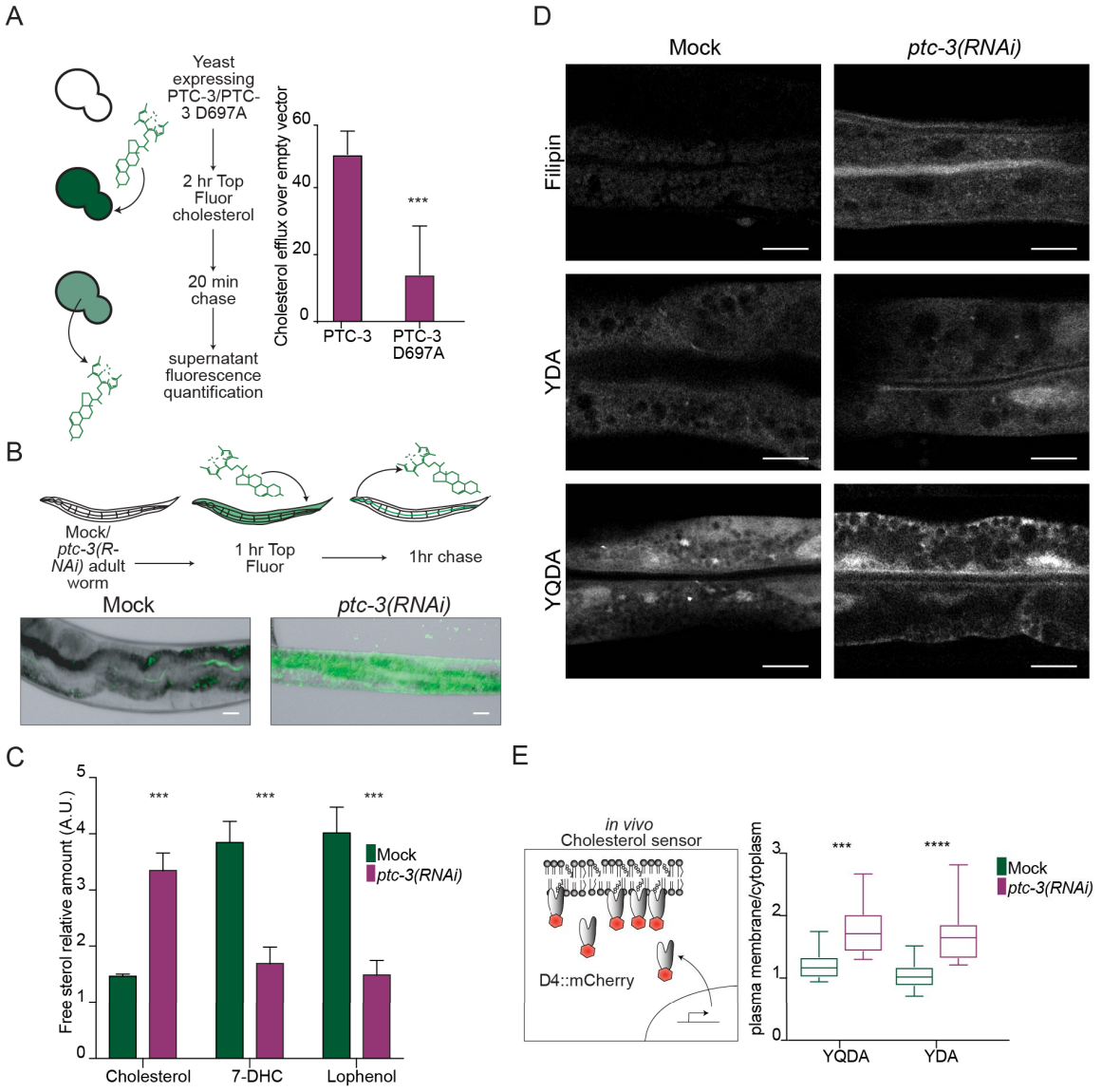

Figure 3.1.2. PTC-3 is a cholesterol transporter. (**A**) *S. cerevisiae* expressing PTC-3 or PTC-3^{D697A} were incubated for 2 hr with 2.5 mM TopFluor® Cholesterol, washed, re-suspended in cholesterol free buffer, and after 20 min, fluorescence intensity of the supernatant was measured. PTC-3 expression induced cholesterol efflux from yeast, which was abolished by the D697A mutation. Error bars are SD. *** p <0.0001 (**B**) N2 worms fed with mock or *ptc-3(RNAi)* were incubated with 2.5 mM TopFluor® Cholesterol for 1 hr. After 1 hr chase, animals were imaged. Scale bar 10 µm. (**C**) Cholesterol accumulates in *ptc-3(RNAi)* animals. Quantification of sterols by MS. Error bars are SEM. *** p<0.0001. (**D**) Cholesterol identification by Filipin or mutagenized YDA or YQDA D4::mCherry cholesterol sensor in the worm gut in mock or *ptc-3(RNAi)* treated animals. *ptc-3 (RNAi)* induces membrane cholesterol accumulation in the intestinal apical membrane. Scale bars 10 µm. (**E**) Quantification of apical membrane enrichment over cytoplasm of the cholesterol sensors YDA or YQDA D4::mCherry. *** p<0.0001.

3.1.3.3 Cholesterol accumulates predominantly in the apical membrane in the intestine of *ptc-3(RNAi)* animals

Cholesterol accumulates in *ptc-3(RNAi)* worms because it cannot be pumped out of the cells. In addition, cholesterol is not efficiently metabolized into 7-DHC and lophenol under those conditions. We speculated where the excess of cholesterol would reside in the cell. First, we used filipin, which binds specifically to cholesterol. While we could barely detect any filipin staining in mock-treated animals, *ptc-3(RNAi)* worms showed a strong fluorescent signal in the apical membrane in the intestine and also some appreciable increase in intracellular fluorescence (Fig. 3.1.2D). To corroborate this finding, we next employed two versions of the domain 4 of perfringolysin fused to mCherry probe (D4-mCherry), YDA and YQDA, which have different sensitivities in the detection of cholesterol [143–145]. We expressed the probes constitutively in the *C. elegans* intestine and analyzed their cellular distribution. Similar to the filipin staining, the mCherry signal increased in the plasma membrane for both probes *in ptc-3(RNAi)* animals compared to mock-treated controls. (Fig. 3.1.2D and E). Thus, the strongest cholesterol accumulation is observed in the apical membrane in the intestine of *ptc-3(RNAi)* animals. We envisage that cholesterol levels are also increased, albeit to a lesser extent, in intracellular membranes.

3.1.3.4 Low dietary cholesterol rescues *ptc-3(RNAi)* phenotypes

It is plausible that the cholesterol accumulation is the cause for the observed phenotypes in *ptc-3(RNAi)* animals. *C. elegans* is unable to synthesize cholesterol and must ingest it through the diet [116]. In the lab, cholesterol is provided in the growth medium. Strikingly, when we omitted cholesterol from the growth medium, *ptc-3(RNAi)* worms developed much better, with 89% reaching adulthood (Fig. 3.1.3A and B). Moreover, the pale phenotype was strongly reduced, and lipid storage was improved (Fig. 3.1.3C and D). Thus, reducing cholesterol accumulation rescued developmental as well as fat storage defects in *ptc-3(RNAi)* worms. Since cholesterol conversion into 7-DHC was also impaired, we asked whether increasing the levels of 7-DHC would likewise rescue the *ptc-3(RNAi)* phenotypes. However, addition of 7-DHC did not alleviate the *ptc-3(RNAi)* phenotype (Fig. 3.1.S2). We conclude that most of the *ptc-3(RNAi)* phenotypes are linked to the regulation of intracellular cholesterol levels. Moreover, the accumulation of cholesterol, and not the inability of the *ptc-3(RNAi)* animals to process cholesterol efficiently, appears to be detrimental for the organism.

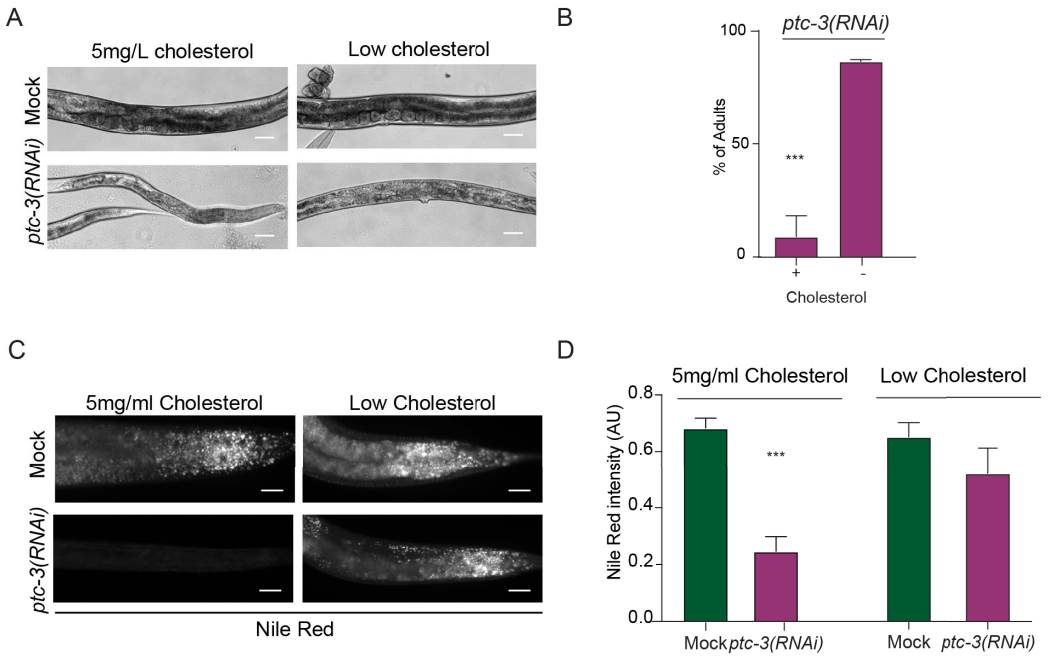

Figure 3.1.3. Low dietary cholesterol rescues ptc-3(RNAi) induced phenotypes. Worms feed from L1 larva under standard cholesterol conditions (5 mg/l) or low cholesterol conditions (no added cholesterol) for 3 days. (**A**) Representative light microscopy images of mock- or *ptc-3(RNAi)*-treated worms on low cholesterol plates Scale bars 20 µm. (**B**) Quantification of number of *ptc-3(RNAi)*-treated worms that reached adulthood in the absence of cholesterol in the growth medium. Error bars are SEM. *** p<0.0001. (**C**) Nile Red staining of lipid droplets in *C. elegans* mock- and *ptc-3(RNAi)*-treated animals on normal or low cholesterol conditions. In low cholesterol conditions, lipid droplet levels are restored in *ptc-3(RNAi)* animals. Scale bars 20 µm. (**D**) Quantification of Nile Red staining of data shown in (C). The normal cholesterol data are the same as depicted in Fig. 3.1.1E.

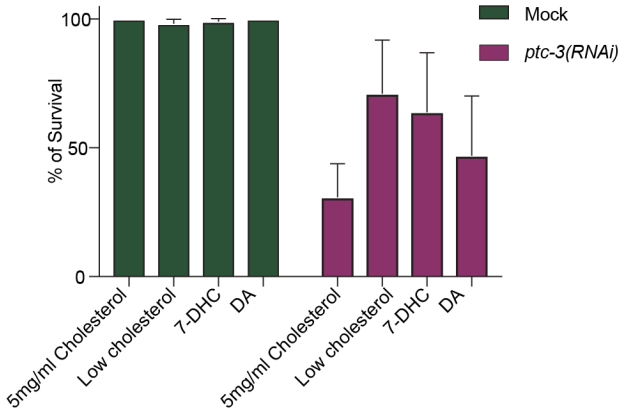

Figure 3.1.S2. Neither 7-DHC nor DA rescued the ptc-3(RNAi) phenotype. Quantification of number of *ptc-3(RNAi)* treated worms that reached adulthood when fed from L1 larva under standard cholesterol conditions (5 mg/l), without cholesterol or if 7-DHC or DA was added for 3 days. Addition of 7-DHC or DA did not alleviate the *ptc-3(RNAi)* arrested phenotype over the no cholesterol control. Error bars are SEM.

3.1.3.5 Lipid droplets biogenesis and ER morphology are impaired upon *ptc-3(RNAi)*

Cellular fat is mostly stored in lipid droplets, which originate from the endoplasmic reticulum (ER). In *ptc-3(RNAi)* animals, we observed defects in fat storage dependent on the intracellular cholesterol levels. Thus, we investigated whether the ER was affected by loss of PTC-3 function using intestinally expressed TRAM-GFP. We observed morphological alterations in the ER in *ptc-3(RNAi)* animals, which were, however, hard to interpret (Fig. 3.1.S3).

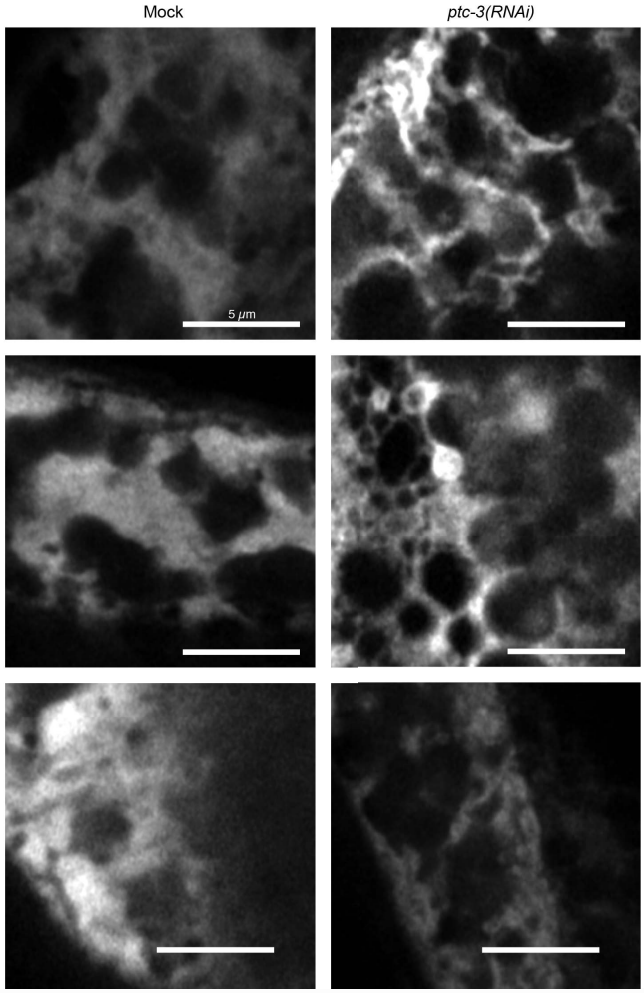

Figure 3.1.S3. ER morphology appears to be altered upon ptc-3(RNAi). Light microscopy images of intestinally expressed TRAM-GFP. Images suggest morphological alterations in the ER in *ptc-3(RNAi)* animals. Scale bar 5 µm.

To gain a better understanding of the phenotype, we performed electron microscopy. Not unexpectedly, given the fat storage defect, lipid droplets were essentially absent in *ptc-3(RNAi)* intestines (Fig 3.1.4A). Even more strikingly, the ER had lost most of its reticulate structures and formed long lines. Such long lines in 2D are indicative of ER sheets in 3D [146]. We used focused ion beam scanning electron microscopy (FIB-SEM) and machine learning algorithms to obtain information on the ER structure in 3D. Indeed, the

reticulate, tubular structure of the ER was dramatically reduced in *ptc-3(RNAi)* when compared to mock; instead, enormous ER-sheets and clusters were formed (Fig. 3.1.4B, Fig. 3.1.S4). Taken together, our data so far suggest that the cholesterol accumulation, due to the absence of PTC-3, impairs ER structure and thereby lipid droplet formation. If the cellular cholesterol levels were indeed the critical factor, then reducing dietary cholesterol in *ptc-3(RNAi)* animals should alleviate the ER phenotype. Indeed, *ptc-3(RNAi)* animals raised on a low cholesterol diet displayed reticulated ER and lipid droplets (Fig. 3.1.4A).

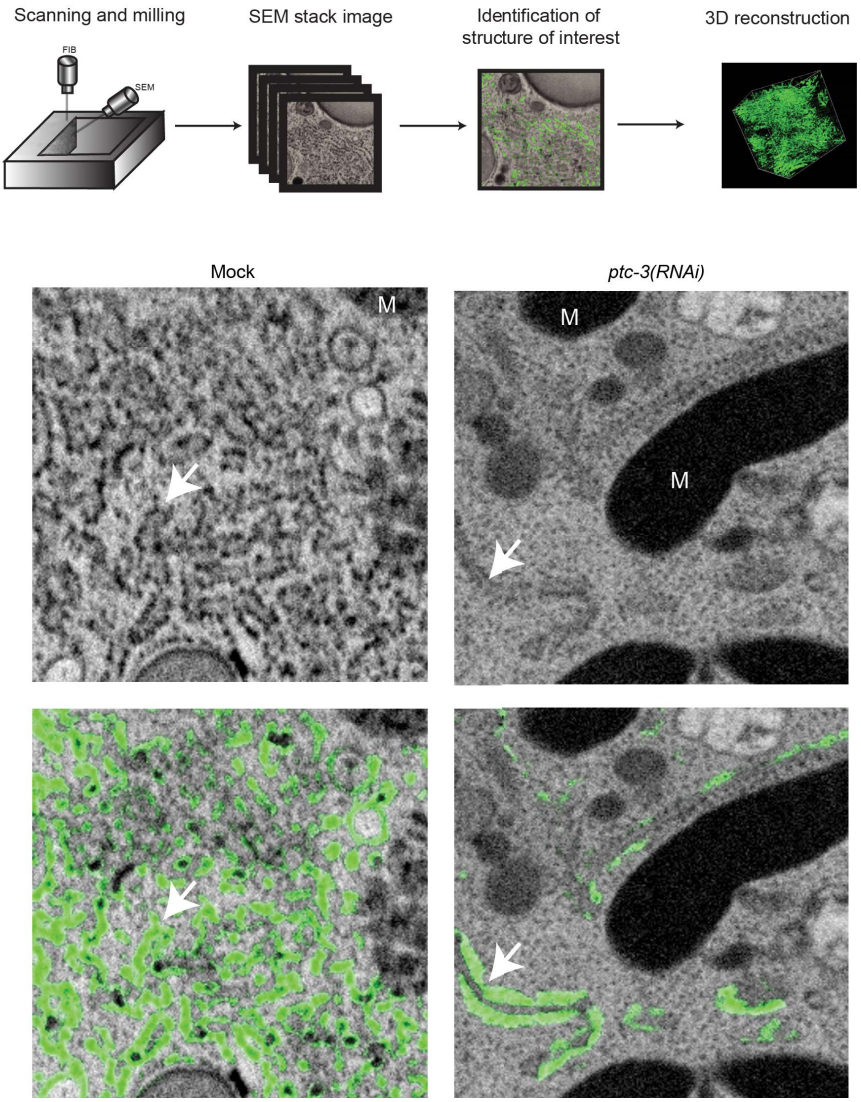

Figure 3.1.S4. FIB-SEM analysis of intestinal cell reveal sheet-like ER in *ptc-3(RNAi)* animals. (**A**) Workflow of FIB-SEM analysis. After TEM analysis a region of interest was chosen, SEM images were acquire followed by milling steps. A SEM Z-stack was generated, and identification of the ER was done by iLastik training. (**B**) Representative images showing automatic ER identification in green by iLastik after machine learning training sessions. Scale bars 200 nm.

Thus, cellular cholesterol levels strongly influence ER morphology and function. At this point, we were unable to determine whether this effect is direct or indirect. Even though

most of the cholesterol accumulated in the apical plasma membrane in *ptc-3(RNAi)* animals, we cannot exclude that there is also an accumulation of cholesterol in the ER. Unfortunately, filipin bleaches very fast, and the D4-mCherry sensors are present throughout the cell so that we were only able to detect very strong local accumulations. Still, the inability of the ER membrane to form lipid droplets and the sheet structure might be linked to the increased membrane bending rigidity.

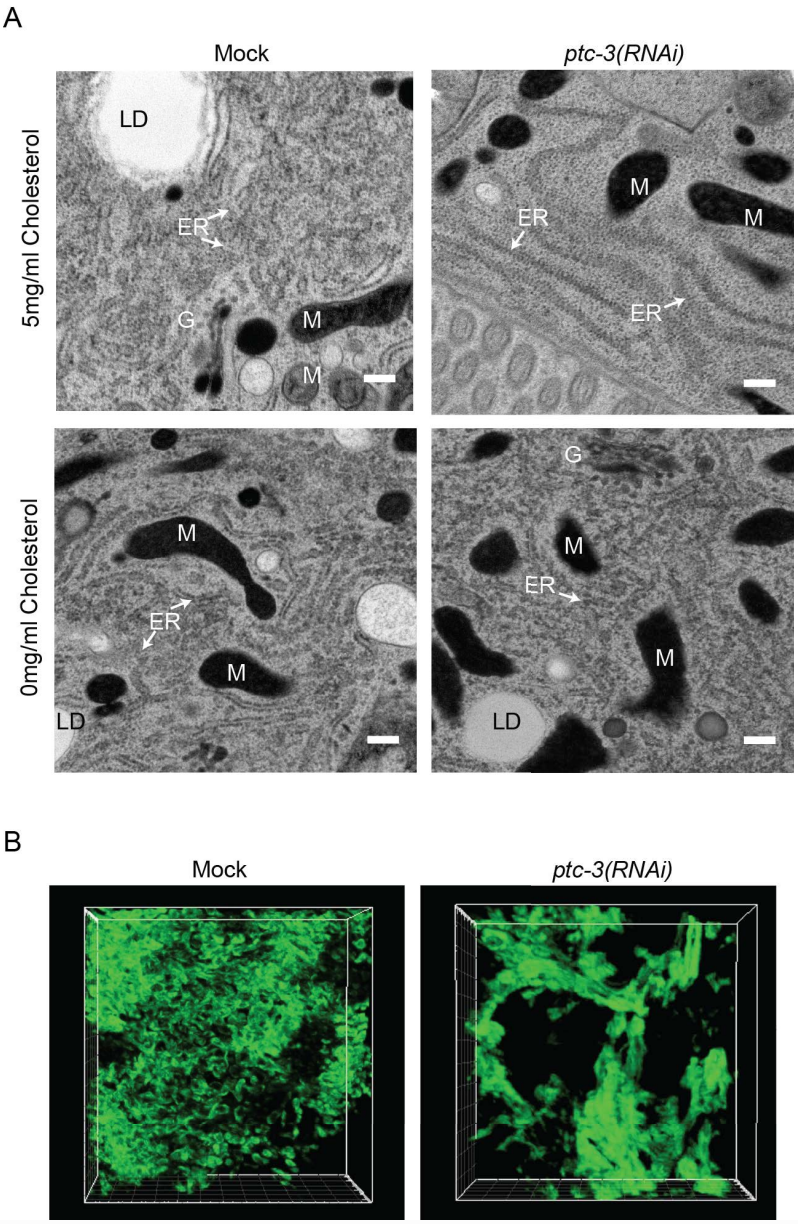

Figure 3.1.4. ptc-3(RNAi) reduces LD in the gut and induces changes in the ER structure. (**A**) Transmission electron microscopy (TEM) of mock and *ptc-3(RNAi)* treated animals reveal a reduction of reticulate ER structures and LD in *ptc-3(RNAi)* animals. This phenotype is rescued by omission of cholesterol in the medium. ER: Endoplasmic reticulum, LD: lipid droplet, M: mitochondria, G: Golgi. Scale bars 200 nm. (**B**) Reconstitution of ER membranes from FIB-SEM images of mock and *ptc-3(RNAi)* treated animals using machine learning. *ptc-3(RNAi)* induces sheet-like ER structures.

3.1.3.6 Fatty acid acyl chain length and desaturation is reduced in *ptc-3(RNAi)* animals

To test this hypothesis, we first performed a simple experiment in which we modulated the growth temperature. Membrane fluidity increases as a function of temperature, while membrane bending rigidity decreases. Consistent with our hypothesis, the development and viability of *ptc-3(RNAi)* animals were improved at an elevated temperature (Fig. 3.1.5A and B).

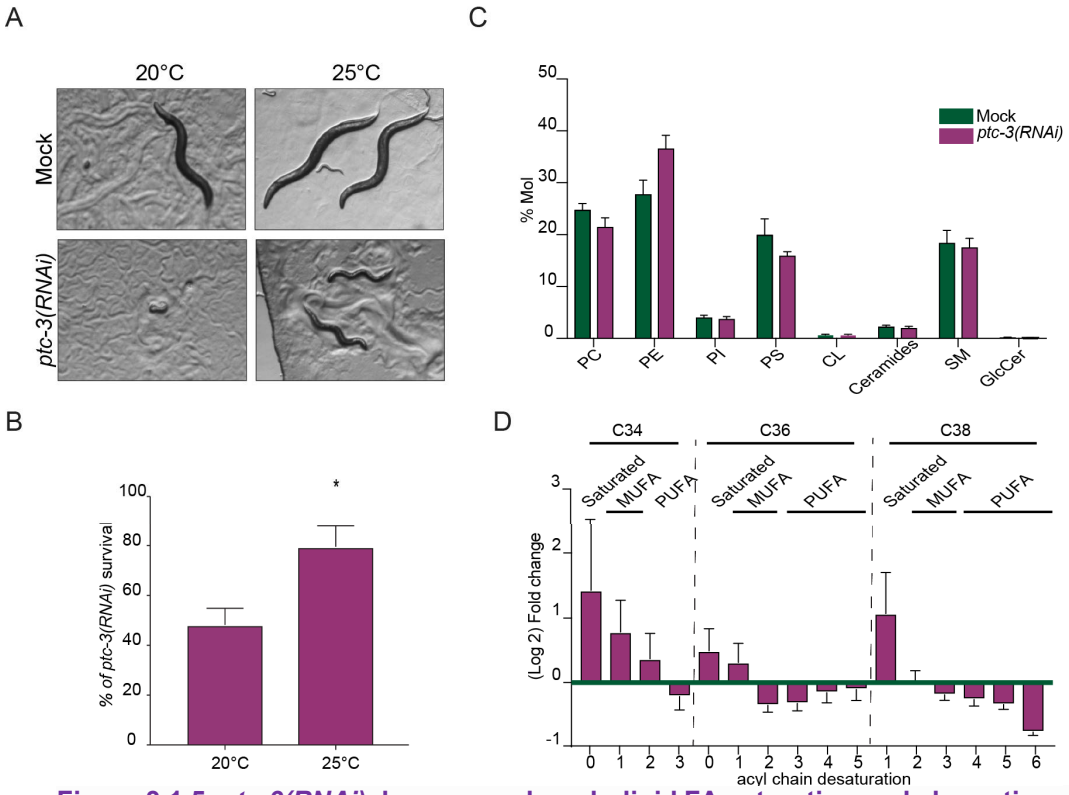

Figure 3.1.5. *ptc-3(RNAi)* decreases phospholipid FA saturation and elongation. (**A**) Increasing the growth temperature from 20°C to 25°C improves the development of *ptc-3(RNAi)* animals. Representative bright field pictures of worms on growth plates. (**B**) Quantification of *ptc-3(RNAi)* survivors at both temperatures. Error bars are SEM. *p<0.05. (**C**) Lipidomics on mock or RNAi treated worms. *ptc-3(RNAi)* worms showed no difference in lipid head group distribution. Error bars are SEM. (**D**) Lipidomics revealed differences in lipid acyl chain composition upon *ptc-3(RNAi)*. There is a shift from PUFAs to saturated FA and MUFAs. Error bars are SEM.

Another factor, which determines the stiffness or fluidity of membranes is the saturation of the acyl chains of lipids. Saturated acyl chains are considered to be relatively straight, allowing a high packing rate of lipids accompanied with the generation of an ordered phase and a reduction in fluidity. In contrast, desaturated fatty acids correlate with less dense packing, higher membrane fluidity, and lower bending rigidity. Therefore, we performed lipidomics and determined the level of phospholipid acyl chain saturation upon *ptc-3(RNAi)*. We did not observe any major difference in the headgroup composition of the most important lipid species (Fig. 3.1.5C). In contrast, we detected a reduction in polyunsaturated fatty acids (PUFAs) in *ptc-3(RNAi)* worms as there was a marked decrease

in acyl chain length and desaturation (Fig. 3.1.5D). This reduction in PUFAs is not due to a general reduction in lipids upon *ptc-3(RNAi)* compared to mock treatment, but rather reflects a shift from PUFAs to more saturated, shorter FAs. This shift towards more saturated FAs supports our hypothesis that the cholesterol accumulation contributes, directly or indirectly, to the morphological changes of the ER membrane.

3.1.3.7 NHR-49 and FAT-7 overexpression rescue *ptc-3(RNAi)* animals

The reduction in PUFAs could potentially be due to inhibition or lower expression of fatty acid desaturases and elongases. A potential candidate to check this hypothesis is the desaturase FAT-7, which appeared to be down-regulated during heat adaptation to counteract the increase in membrane fluidity at high temperature [147]. Overexpression of FAT-7 in the intestine resulted in better survival of *ptc-3(RNAi)* animals (Fig. 3.1.6A and B). The rescued animals were darker than their counterparts (Fig. 3.1.6A), suggesting that they were able to store fat. FAT-7 expression is regulated by the PPARα homolog NHR-49 [148,149]. Similar to what we had observed for FAT-7 overexpression, increasing intestinal NHR-49 levels improved survival of *ptc-3(RNAi)* animals (Fig. 3.1.6A and B). Rescue of survival due to NHR-49 overexpression was accompanied by restoration of fat storage (Fig. 3.1.6A-D), suggesting that NHR-49 is a major downstream effector of PTC-3. NHR-49 partners with NHR-80, a homolog of mammalian HNF4, to regulate fatty acid desaturation [148]. However, overexpression of NHR-80 did not rescue the *ptc-3(RNAi)* phenotype (Fig. 3.1.6A and B). Our data are consistent with the notion that NHR-49 and FAT-7 are modulators of membrane bending rigidity.

3.1.3.8 Loss of NHR-181 rescues the high cholesterol induced phenotypes in *ptc-3(RNAi)* animals

Nuclear hormone receptors often act context-dependent. Therefore, we wondered whether other NHRs or the loss thereof may contribute to the *ptc-3(RNAi)* phenotype. NHR-8, the *C. elegans* ortholog of vertebrate liver X and vitamin D receptors, was also shown to influence cholesterol levels and fat content [111,150]. Since *nhr-8(RNAi)* animals contained more fat [111], we speculated whether loss of NHR-8 could rescue the *ptc-3(RNAi)* phenotype. However, we could not detect any rescue (Fig. 3.1.S5A). This result may not have been so unexpected since *nhr-8* mutants contain less unsaturated fatty acids [111]. Overexpression of NHR-8 still did not alleviate *ptc-3(RNAi)* defects (Fig. 3.1.S5B), indicating that NHR-8 and PTC-3 act independently.

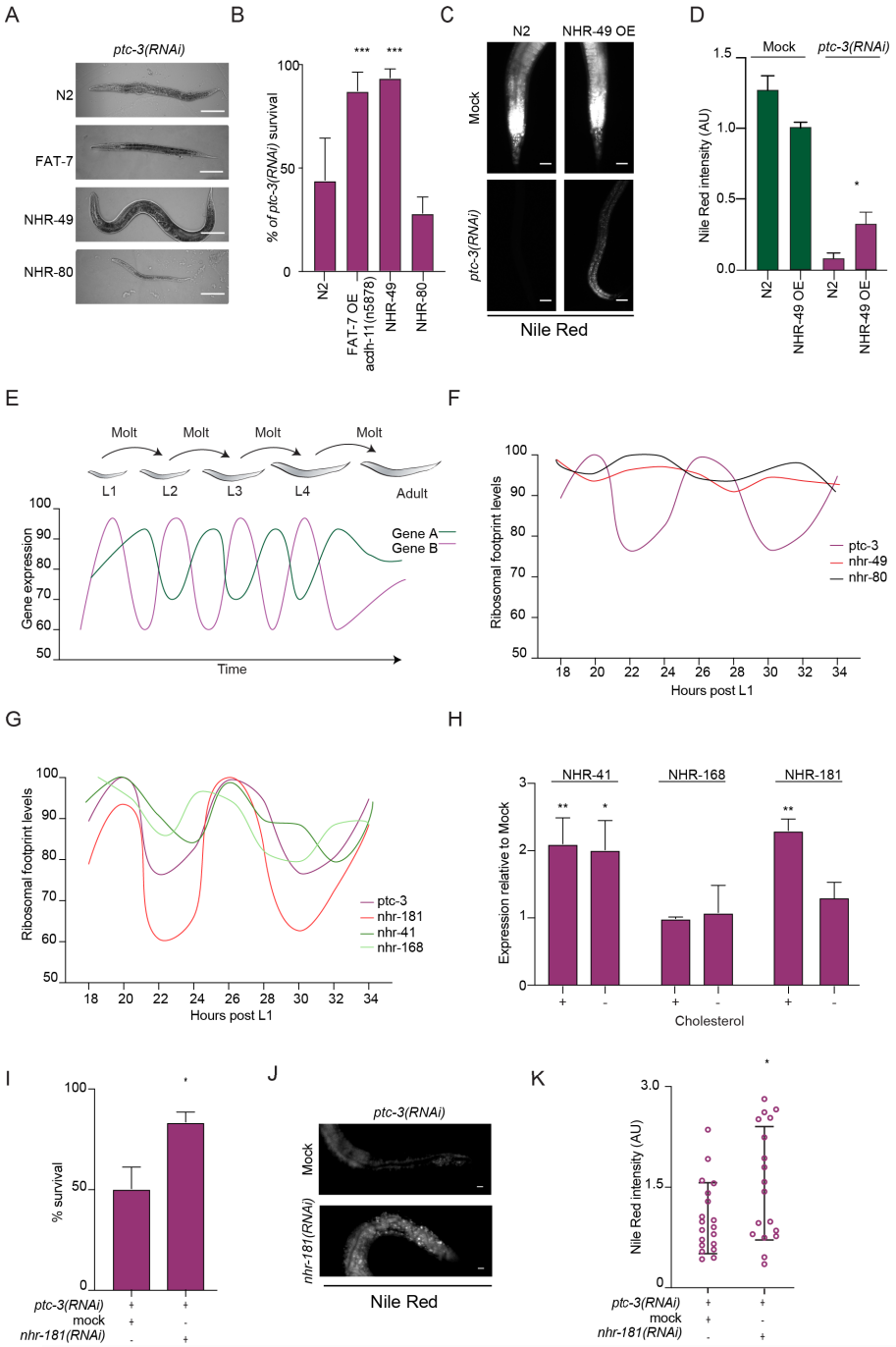

Figure 3.1.6. PTC-3 influences NHR function in a cholesterol-dependent manner. (**A**) Overexpression of NHR-49 or FAT-7 partially rescues *ptc-3(RNAi)* defects. Representative DIC images of worms. Scale bars 100 µm. (**B**) Quantification of survival rate upon overexpression of FAT-7, NHR-49 or NHR-80 in *ptc-3(RNAi)* animals. Error bars are SD. *** p<0.0001. (**C**) Over expression of NHR-49 partially restores fat accumulation in *ptc-3(RNAi)* animals. Nile Red staining. Scale bars 20 µm. (**D**) Quantification of data shown in (C). (**E**) Schematic representation of ribosomal footprints of mRNA during *C. elegans* larval development. Oscillatory changes in mRNA levels during developmental time. The timing, amplitude and whether a gene is oscillating is gene specific. (**F**) PTC-3, but not NHR-49 or NHR-80, expression oscillates during development. Data plotted from [79]. (**G**) Ribosomal footprint oscillations of NHR-181, NHR-168 and NHR-41 are similar to PTC-3 (data from [79]). (**H**) NHR-181 expression is modulated dependent on cholesterol levels. qRT-PCR analysis of NHR-41, NHR-168 and NHR-181 in the presence or absence of cholesterol in the growth medium. Error bars are SEM. ** p<0.001 * p<0.05. (**I**) Genetic interaction between PTC-3 and NHR-181. Knockdown of NHR-181 rescues *ptc-3(RNAi)* lethality. (J) *nhr-181(RNAi)* partially restores fat accumulation in *ptc-3(RNAi)* animals. Nile Red staining. Scale bars 20 µm. (**K**) Quantification of data shown in (J).

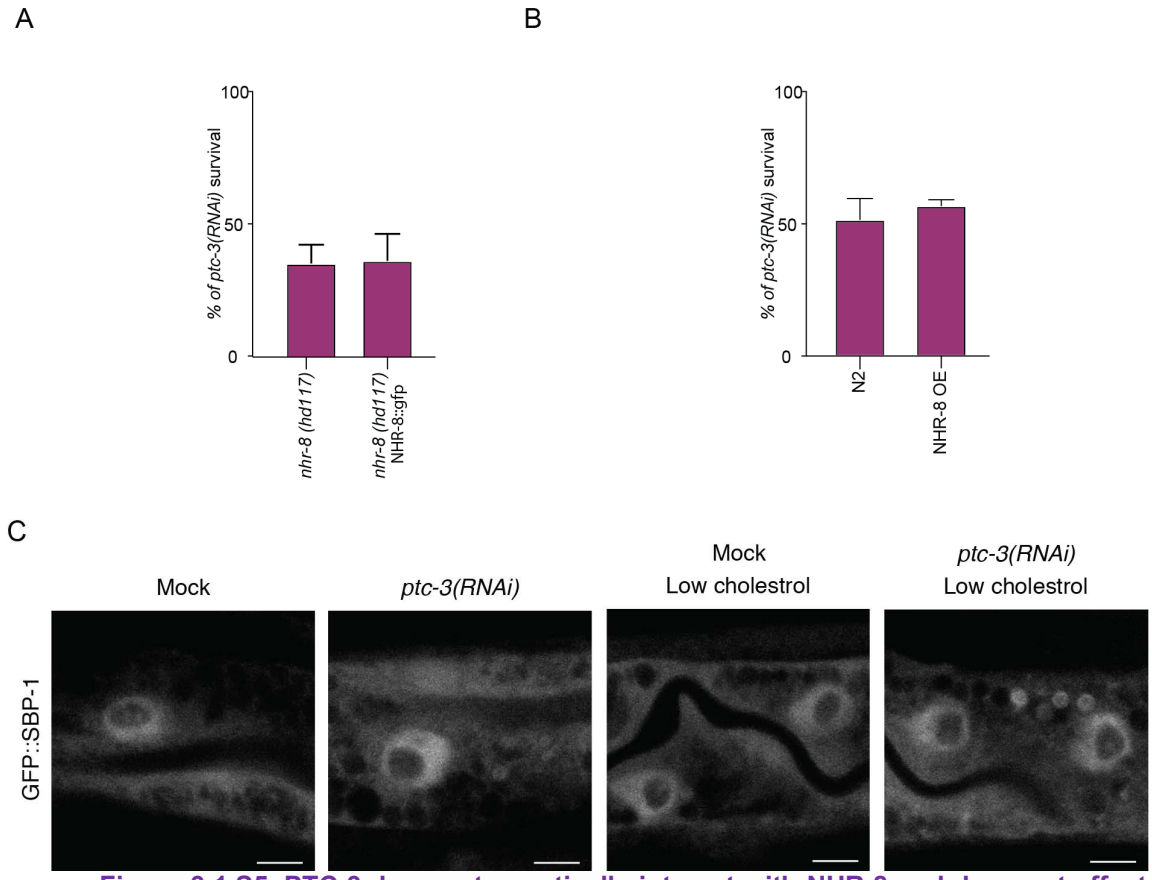

Figure 3.1.S5. PTC-3 does not genetically interact with NHR-8 and does not affect SBP-1 localization. *nhr-8(hd117)* animals were treated with *ptc-3(RNAi)* and survival was compared with *nhr-8(hd117)* NHR-8::GFP expressing animals. (**B**) NHR-8 over-expressing animals were treated with *ptc-3(RNAi)* and survival was scored. (**C**) SBP-1::GFP localization was determined under different RNAi and cholesterol conditions.

C. elegans expresses 278 nuclear hormone receptors. To identify possible NHRs important in a PTC-3-dependent pathway, we turned to genome-wide expression data during development. *C. elegans* goes through 4 larval stages before reaching adulthood (Fig. 3.1.6E). Each transition from one larval stage to the next is accompanied by the synthesis of a new, larger cuticula, in a process referred to as molting. Genome-wide RNAseq and Riboseq throughout *C. elegans* development revealed an oscillatory behavior of gene expression for many genes [79] (Fig. 3.1.6E). Given the general role of PTC-3 in development and the observed cuticle defects upon *ptc-3(RNAi)*, it was not surprising to find that PTC-3 expression also oscillated (Fig. 3.1.6F). However, NHR-49 expression remained constant during development (Fig. 3.1.6F). We then asked which other NHRs would oscillate in a similar manner as PTC-3. Three NHRs emerged as possible candidates: NHR-41, NHR-168, and NHR-181 (Fig. 3.1.6G). We hypothesized that the expression levels of the NHRs should be responsive to cholesterol levels. Of the three, only expression levels of the HNF4 homolog NHR-181 were upregulated in high cholesterol i.e. *ptc-3(RNAi)*, and reduced under low cholesterol conditions (Fig. 3.1.6 H). More importantly, knockdown

of *NHR-181* rescued the *ptc-3(RNAi)* induced lethality to a similar extent than overexpression of NHR-49, irrespective of the cholesterol present in the medium (Fig. 3.1.6 B and I). Moreover, fat content was restored to a similar extent (Fig. 3.1.6 J and K, compare J and C). Taken together, our data imply that NHR-49 positively and NHR-181 negatively regulate membrane bending properties and fat storage in response to high cholesterol levels.

3.1.4 Discussion

We explored the role of the *C. elegans* PTCH homolog, PTC-3, in the absence of the classical functional hedgehog signaling pathway. The function of PTCH proteins is conserved from *C. elegans* to man because similar to what has been proposed for mammalian PTCH [77,90,93], PTC-3 is a cholesterol transporter, which exports cholesterol out of the cell. PTC-3 appears to be the major cholesterol transporter in the apical plasma membrane in the *C. elegans* intestine, since knockdown of PTC-3 resulted in strong intracellular cholesterol accumulation, most notably in the apical plasma membrane.

As a consequence of the cholesterol accumulation, the balance of tubular and sheet-like ER was strongly skewed towards sheet structures (Fig. 3.1.7). Moreover, lipid droplet synthesis, which originates at the ER, was greatly reduced. We propose that the ER membranes in *ptc-3(RNAi)* animals have an increased bending rigidity, which does not allow bulging out of lipid droplets. Whether triglycerides still accumulate within the lipid bilayer remains unclear because their detection in the ER membrane was not possible. However, we observed an increase in saturated and mono-unsaturated fatty acid acyl chains (MUFAs) at the expense of polyunsaturated fatty acids (PUFAs) upon knockdown of PTC-3. This imbalance towards shorter and saturated acyl chains should also increase lipid packing and increase membrane bending rigidity. This effect would then be intensified by the accumulation of cholesterol in intracellular membranes, which would furthermore promote membrane stiffness.

While the increase of membrane bending rigidity is probably sufficient to inhibit lipid droplet formation, vesicle formation at the ER and the Golgi apparatus may not be as strongly affected by cholesterol accumulation and the increase in MUFAs because we still observed stacked Golgi apparatus by electron microscopy (Fig 3.1.S6). The difference between lipid droplet formation and vesicle budding is that the COPII coat can bend the entire lipid bilayer [151], while the triglycerides must deform the membrane and push the lipid bilayer apart, a process, which might be less energetically favorable. The COPII coat can thus probably exert the force necessary to bend the ER membranes in the mutant.

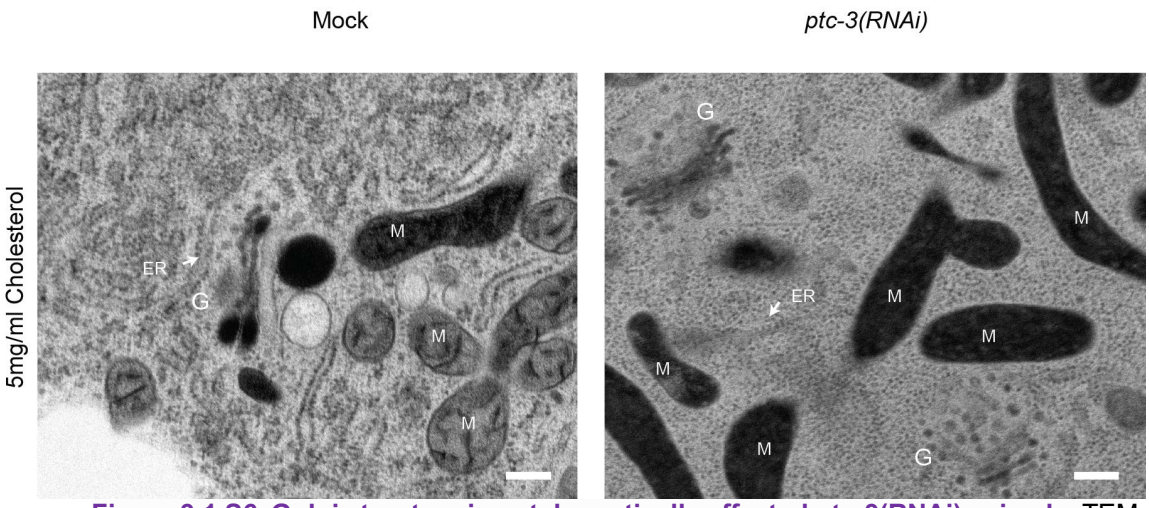

Figure 3.1.S6. Golgi structure is not dramatically affected ptc-3(RNAi) animals. TEM images showing Golgi structure in Mock and *ptc-3(RNAi)* treated animals. No mayor disruption of the Golgi apparatus was observed. ER: Endoplasmic reticulum, M: mitochondria, G: Golgi.

However, the cholesterol accumulation may not only have a structural role in stiffening of membranes, together with MUFAs and saturated fatty acid acyl chains. It was shown previously that cholesterol can act as a hormone in *C. elegans* [122,152,153]. In support of this notion, we observed cuticular defects with intestine-specific knockdown on PTC-3, indicating that there are cell non-autonomous effects of *ptc-3(RNAi)*. Given that PTC-3 is a cholesterol transporter, we speculate that the increased cholesterol levels are the causative of the cuticle defects. Moreover, cholesterol may also change the transcriptional program and reduce the expression of genes required for FA desaturation and elongation. In fact, overexpression of the PPARα homolog NHR-49 rescued the *ptc-3(RNAi)*-induced fat storage and developmental arrest phenotype. In mammalian cells, PPARα requires PUFAs for activation [147,154]. We hypothesize that reduced PUFA levels downregulate NHR-49 activity, which could be compensated by the overexpression of NHR-49. Alternatively, but not mutually exclusive, the interaction between NHR-49 and NHR-80, which are jointly controlling FA elongation and desaturation [148], would be disrupted by high cholesterol levels, and NHR-49 would instead team up with NHR-181. This complex could then negatively regulate FAT and ELO gene expression when cholesterol levels increase in the cell. A circumstantial argument that puts weight on this latter possibility is that both NHR-80 and NHR-181 are homologs of mammalian HNF4 proteins. Thus, it is tempting to speculate that the exchange of one HNF4 like molecule for another would shift the activity of NHR-49 from promoting elongation and desaturation to repressing these processes. Interestingly, a C-terminal truncation in Ptch1 in adult mice led to a reduction of white fat tissue and PPARγ levels, suggesting that the SMO-independent pathway we uncovered might be conserved in mammals [155].

NHR-49 and NHR-181 appear to be specific downstream effectors of PTC-3 activity levels, as downregulating NHR-8 did not improve PTC-3-dependent phenotypes. Likewise, SREB, which is a major responder to alteration in cellular cholesterol levels and which has been shown to regulate the expression of fatty acid elongases and desaturases in mammalian cells [115]. However, knockdown of PTC-3 did not affect the nuclear localization of the *C. elegans* SREB homolog SBP-1 (Fig. 3.1.S5C). However, NHR-49 activity clearly is affected by increased cholesterol levels since overexpression of its target and activator FAT-7 [147] partially rescued *ptc-3(RNAi)* phenotypes.

In sum, we used *C. elegans* to reveal potential ancestral functions of PTCH family proteins because it lacks smoothened and other canonical hedgehog signaling pathway components, which have been lost during evolution [71,75]. In fact, it has been proposed that PTCH and related proteins such NPC1 and dispatched evolved separately from smoothened [58]. PTCH belongs to the family of RND transporters, which are already present in bacteria. For most bacterial RNDs, the substrates are unknown. However, the family most related to PTCH transports hopanoids, which are structural and functional analogs of sterols [58]. Next to PTC-3, *C. elegans* encodes another PTCH protein PTC-1 and 18 PTCH-related proteins (PTRs), presumably all RND transporters. It is tempting to speculate that these PTCs and PTRs are transporting small molecules, presumably sterols, and thereby contributing to cellular homeostasis and potential intra- and intercellular communication.

Finally, our data strongly implicate cellular cholesterol levels, membrane composition, and nuclear hormone receptors such as PPARα and HNF4 in non-canonical Hh signaling pathways. They also provide a framework on how to distinguish between SMO-dependent and -independent functions in mammals. Our results might be in particularly important for the understanding of diseases such as multiple myeloma in which canonical and non-canonical Hh signaling have been implicated [156,157].

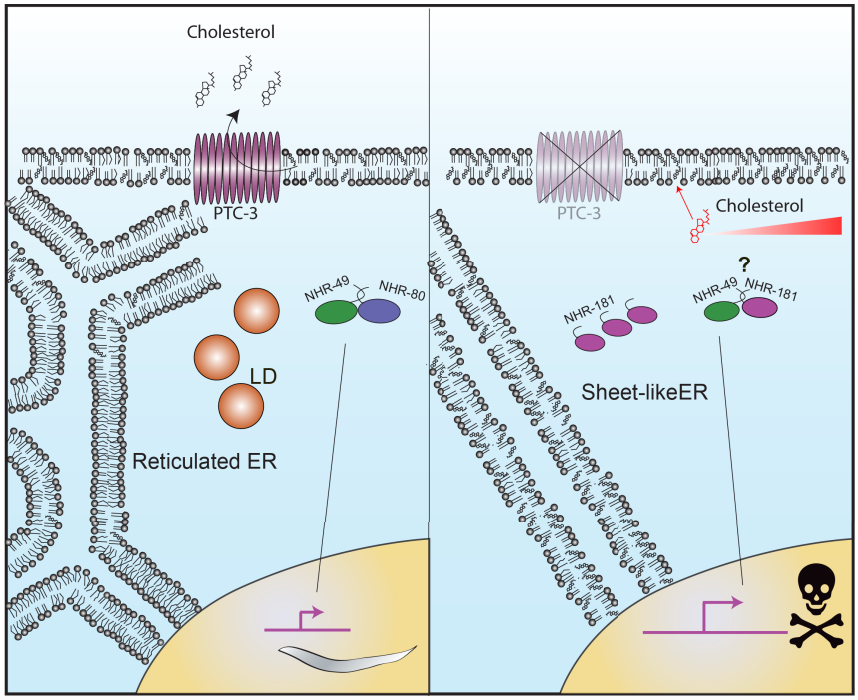

Figure 3.1.7. Model of how PTC-3 and the loss thereof affects ER structure and LD formation. PTC-3 controls intracellular cholesterol levels directly by promoting its efflux. In the absence of PTC-3, cells accumulate cholesterol, which in turn directly influence membrane properties. In addition, cholesterol directly or indirectly affects NHRs, which subsequently leads to a reduction of acyl chain length and desaturation. This second effect enhances the changes in membrane properties and leads to changes in ER morphology and LD formation.

3.1.5 Materials and methods

3.1.5.1 General methods and strains

C. elegans was cultured and maintained as described previously[120] at 20°C unless it was specified different. RNAi was carried out using sequenced and confirmed clones from the Ahringer library, as mock nontargeting dsRNA from the Ahringer library clone Y95B8A_84.g was used [158]. For low cholesterol conditions cholesterol was omitted and agar replaced by agarose. RNAi feeding experiments were performed for 3 days starting from L1 larvae. When adult *ptc-3(RNAi)* were needed worms were grown with RNAi mock bacteria until L2 stage and then transferred to *ptc-3(RNAi)* plates for 2 days. For developmental and survival assays eggs from 1-day adult worms were hatched in M9 buffer (3 g KH_2PO_4, 6 g Na_2HPO_4, 5 g NaCl, 1 ml 1 M $MgSO_4$, H_2O to 1 l; sterilized by autoclaving) overnight without bleaching. L1s were transferred to RNAi plates and grown at 20°C. Survival and developmental stage were assessed after 72 hr. For double RNAi experiments *ptc-3(RNAi)* was diluted 1:1 with the second RNAi or mock expressing bacteria. *nhr-49(nr2041) [ges-1p::3xHA::nhr-49(cDNA)::unc-54 3'UTR + myo-3p::mCherry::unc-54 3'UTR]* and for gut specific RNAi *kbIs7 [nhx-2p::rde-1 + rol-6(su1006*)] was used , *sbp-1(ep79)*

[sbp-1::GFP::SBP-1; rol-6(su1006)], were obtained from the Caenorhabditis Genetics Center (CGC). *nhr-8(hd117)* mutant and nhr-8::GFP over expressing strains were described previously [111]. For the cholesterol sensor strains generation the PFO-derived D4 domain mutants YDA (D434W Y415A A463W) and YQDA (D434W Y415A A463W Q433W) fused to a mCherry N-terminal tag were cloned using the NEBuilder HiFi DNA Assembly Cloning Kit (NEB #E5520) and introduced into pBlueScriptII with a VHA-6 promoter and tub terminator using the primers pvha6_fwd gacggtatcgataagcttgatatcggtatactatttattactcgatacttttg, pvha6_rev cacgcttgccatttttatgggttttggtagg, for the promoter amplification, for the sensor amplification D4H_fwd aaacccataaaaaatggcaagcgtgagcaag, D4H_rev ttttgcatttatcttaattgtaagtaatactagatccagggtataaag were used, and tubter_fwd acttacaattaagataaatgcaaaatcctttcaag, tubter_rev actagtggatcccccgggctgcaggtgagacttttttcttggc for tubulin terminator. The plasmid was microinjected at a concentration of 50 ng/µl into both arms of the syncytial gonads of N2 worms. SUR-5::GFP at 10 ng/µl concentration was co-injected as transformation marker and 40 ng/µl of lambda DNA as carrier was used. Animals containing the cholesterol sensors were grown at 25°C and fed with OP50 RNAi-competent bacteria [159]. The *ptc-3::gfp* reporter pCH115.1 was constructed by inserting a gfp cassette into the same site within the ptc-3 locus as described in [18] in the fosmid WRM064cC06, following the recombineering

protocol described in [160]. The gfp cassette was PCR-amplified by using pBALU1 vector and primers CH428 gaaaaagagatttggcctactgcagtcgaggaaacccacaaatggcgactatgagtaaaggagaagaacttttca and CH429 gccgaaaaactcgaacttacatttgaaacattgctcggcacactttgacttttgtatagttcatccatgcca, and the *galK* module was excised after its insertion to the fosmid. As co-injection marker pMF435: Ppgp-1::mCherry::unc-54 3'UTR was used [161].

3.1.5.2 Microscopy

Live worms were immobilized with 50 mM levamisole in M9 and mounted on a slide with 2% agarose. The worms were imaged with a Zeiss Axioplan 2 microscope equipped with a Zeiss Axio Cam MRm camera (Carl Zeiss, Aalen Oberkochen, Germany) and the objectives EC Plan-Neofluar 10x/0.3, EC Plan-Neofluar 20x/0.50, EC Plan-Neofluar 40/1.30. All images were adjusted to the same parameters with OMERO.web 5.3.4-ice36-b69. Images of D4H cholesterol sensors, Filipin III staining and TRAM::GFP were obtained on a Zeiss LSM 880 microscope with Airyscan with Plan-Apochromat 63x/1.4 Oil DIC M2. The fast mode was used, and images were processed using the Zen Black software.

3.1.5.3 Coherent Anti-Stokes Raman Spectroscopy

Worms were mounted on a slide with 2% agarose with 20 mM levamisol. A Leica TCS SP8 system with a CARS laser picoEmerald. The lasers were beam to 816.4 nm while keeping the Stokes beam constant at 1,064.6 nm. The scan speed was set to 400 Hz. A z-stack per worm was imaged along the intestine and 19 animals from 3 experiments were collected per condition. The number of lipid droplets in each stack was assessed with the Fiji plug-in Lipid Droplet Counter. The data was analyzed with a one tail ANOVA followed by Dunnett's multiple comparisons test in Prism 7.

3.1.5.4 TEM and FIB SEM

For transmission electron microscopy (TEM) and focused-ion beam scanning electron microscopy (FIB-SEM), worms were frozen as follows. *C. elegans* animals were picked with a worm pick from agar plate and transferred to a droplet of M9 medium on a 100 µm cavity of a 3 mm aluminium specimen carrier (Engineering office M. Wohlwend GmbH, Sennwald, Switzerland). 5 - 10 worms were added to the droplet and the excess M9 medium was sucked off with dental filter tips. A flat aluminium specimen carrier was dipped in 1-hexadecene and added on top. Immediately, the specimen carrier sandwich was transferred to the middle plate of an HPM 100 high-pressure freezer (Leica

Microsystems, Vienna, Austria) and frozen immediately without using ethanol as synchronizing medium.

Freeze-substitution was carried out in water-free acetone containing 1% OsO_4 for 8 hr at -90°C, 7 hr at -60°C, 5 hr at -30°C, 1 hr at 0°C, with transition gradients of 30°C/hr, followed by 30 min incubation at RT. Samples were rinsed twice with acetone water-free, block-stained with 1% uranyl acetate in acetone (stock solution: 20% in MeOH) for 1 hr at 4°C, rinsed twice with water-free acetone and embedded in Epon/Araldite (Merck, Darmstadt, Germany): 66% in acetone overnight, 100% for 1 hr at RT and polymerized at 60°C for 20 hr. Ultrathin sections (50 nm) were post-stained with Reynolds lead citrate and imaged in a Talos 120 transmission electron microscope at 120 kV acceleration voltage equipped with a bottom mounted Ceta camera using the Maps software (Thermo Fisher Scientific, Eindhoven, The Netherlands).

For Focused ion beam scanning electron tomography, a trimmed Epon/Araldite block containing a single *C. elegans* was mounted on a regular SEM stub using conductive carbon and coated with 10 nm of carbon by electron beam evaporation to render the sample conductive. Ion milling and image acquisition was performed simultaneously in an Auriga 40 Crossbeam system (Zeiss, Oberkochen, Germany) using the FIBICS Nanopatterning engine (Fibics Inc., Ottawa, Canada). A large trench was milled at a current of 16 nA and 30 kV, followed by fine milling at 240 pA and 30 kV during image acquisition with an advance of 5 nm per image. Prior to starting the fine milling and imaging, a protective Platinum layer of approximately 300 nm was applied on top of the surface of the area of interest using the single gas injection system at the FIB-SEM. SEM images were acquired at 1.9 kV (30 µm aperture) using an in-lens energy selective backscattered electron detector (ESB) with a grid voltage of 550 V, and a dwell time of 1 µs and a line averaging of 130 lines. The pixel size was set to 5 nm and tilt-corrected to obtain isotropic voxels. The final image stack was registered and cropped to the area of interest using the Fiji image-processing package [https://imagej.net/TrakEM2]. FIB-SEM images were processed with iLastik[162] and pixel classification was done. The classifier was trained to separate different object classes, ER, cytoplasm and other organelles. The training was done individually for each dataset. A 3D reconstruction was later handled with IMARIS 9.2.

3.1.5.5 Lipidomic analysis

Worms were cultured in liquid media as described previously [163]. Feeding bacteria were prepared by growing RNAi bacteria to an OD_{600} of 0.6 in LB-Amp medium and then inducing dsRNA expression with 1 mM IPTG for 24 hr. Bacteria were harvested, resuspended to OD_{600} 400. Synchronized populations of worms were grown from L1 larvae to L2 stage in mock bacteria and then transferred into RNAi bacteria until they reach early

adulthood. Young adults were collected and washed once in ddH_2O. 8,000 young adults were used for glycerophospholipid and sphingolipid analysis while sterol analysis was done from 40,000 young adults. Pellets were frozen and stored at -80°C until extraction. Lysis was performed on a Cryolysis machine (Precellys 24, lysis & homogenization machine (Bertin Technologies)) at 4°C using 100 µl 1.4 mm zirconium oxide beads in 800 µl MS-H_2O with three cycles of 45 sec bursts at 6,200 rpm followed by 45 sec interruptions. Lysates were eluted into glass tubes with lipid standards (glycerophospholipid and sphingolipid standards: di-lauryl phosphatidylcholine, di-lauryl phosphatidylethanolamine, di-lauryl phosphatidylinositol, di-lauryl phosphatidylserine, tetra-lauryl cardiolipin, C17 ceramide, C12 sphingomyelin, C8 glucosylceramide, all from Avanti Polar Lipids; sterol standard: ergosterol from Fluka) and beads were washed and eluted again with 200 µl MS-H_2O. Lipids were extracted with chloroform and methanol according to Bligh and Dyer [164] following a published protocol [165]. Briefly, 3.6 ml organic solvent ($CHCl_3$/MeOH=1:2, v:v) were added to the 1 ml aqueous lysate, mixed and centrifuged to clear extract from worm debris. Extracts were transferred to new glass tubes and phase separation was induced by addition of 0.5 mL MS-H_2O and 0.5 ml $CHCl_3$. Samples were centrifuged, and the organic phase was collected. For sterol analysis total lipid extract was dried directly in a centrivap. To separate sterols from other lipids solid phase extraction on a Chromabond® SiOH column (Macherey-Nagel, Germany) was performed. Columns were washed two times with 1 ml $CHCl_3$. Total lipid extract from 40,000 worms was resuspended in 250 µl $CHCl_3$ by vortexing and sonication. The extract was then applied to the column and eluted with two times 650 µl $CHCl_3$. The flow-through and $CHCl_3$ elutions were combined, dried and used for sterol analysis by GC-MS. In the case of glycerophospholipid and sphingolipid analysis, total lipid extract was split in two and dried. One aliquot was used without further treatments for glycerophospholipid analysis and inorganic phosphate determination while the other underwent methylamine treatment and desalting via butanol extraction [166].

Glycerophospholipid and sphingolipid analysis was performed following a worm adapted version of a previously published method [167]. LC-MS or HPLC grade solvents were used and the samples were pipetted in a 96 well plate (final volume = 100 µl). Positive mode solvent: $CHCl_3$/MeOH/H_2O (2:7:1 v/v) + 5mM NH_4Ac. Negative mode solvent: $CHCl_3$/MeOH (1:2 v/v) + 5mM NH_4Ac. The glycerophospholipid and sphingolipid aliquots were resuspended in 250 µl $CHCl_3$/MeOH (1:1 v/v) and sonicated for 5 min. The glycerophospholipids were diluted 1:10 in negative and positive mode solvents and the sphingolipids were diluted 1:5 in positive mode solvent and infused onto the mass spectrometer. Tandem mass spectrometry for the identification and quantification of glycerophospholipid and sphingolipid molecular species was performed using multiple reaction monitoring (MRM) with a TSQ Vantage Triple Stage Quadrupole Mass

Spectrometer (Thermo Fisher Scientific, Bremen, Germany) equipped with a robotic nanoflow ion source, Nanomate HD (Advion Biosciences, Ithaca, NY). The collision energy was optimized for each lipid class. Each biological replicate was read in two technical replicates each comprising three measurements for each transition. Lipid concentrations were calculated relative to the corresponding internal standards and then normalized to the total phosphate content of each total lipid extract. Sterol analysis was done as previously described [166].

3.1.5.6 Nile Red Staining

Nile Red staining was performed as described previously[168]. Worms were washed with 1 ml M9 into a 1.5 ml siliconized microfuge tube. Worms were allowed to sink by gravity on ice and were washed with M9. Approximately 30 µl of M9 and worms at the bottom of the tube were left. 0.2 ml of 40% isopropanol was added and incubated for 3 min for fixation. The fixative was removed and 150 µl of Nile Red solution (6 µl of Nile Red 0.5 mg/ml in acetone per 1 ml of 40% isopropanol) was added to the worms for 30 min at 20°C with gentle rocking in the dark. Worms were washed once with 1 ml M9 buffer and mounted on a 2% agarose pad for microscopy. Intensity analysis was performed using Fiji with at least 11 worms per condition from 3 different experiments. The data was analyzed with a one tail ANOVA followed by Dunnett's multiple comparisons test in Prism 7.

3.1.5.7 TopFluor cholesterol staining

The experiment was performed as described previously as [89]. PTC-3 CDS was amplified with the primers ptc-3TEF_F 5'-actagtggatcccccgggctgcaggATGAAGGTGCATTCGGAACAAC-3' ptc-3TEF_R 5'-gacggtatcgataagcttgatatcgTTACTTGTGCGCTGGCGATG-3' from cDNA and cloned into the yeast plasmid p426TEF. A point mutation (D697A) was introduced with the Q5® Site-Directed Mutagenesis Kit (E0554S NEB). Yeasts were cultured to an OD_{600} of 4, washed with cold water and resuspend to 10 OD_{600} in 50 mM HEPES buffer pH 7.0. Yeasts were incubated protected from light with 5 µM TopFluor® Cholesterol (810255, Avanti Polar Lipids) for 2 hr at 20°C. They were washed once with cold ddH_2O and resuspend with HEPES buffer, after 20 min the yeast were spun down, and the supernatant was measured with filters 485ex 520em on a plate reader (DTX880, Multimode Detector, Beckman Coulter). The efflux was normalized to the initial fluorescence of the yeast. Worms were washed off a plate with M9 buffer and put on a shaker in M9 buffer with 5 mM TopFluor® Cholesterol for 1 hr at 20°C. Worms were washed with M9 buffer once to remove the excess of Topfluor® Cholesterol and chase in M9 buffer was performed for 1 hr before imaging.

3.1.5.8 Immunofluorescence and PTC-3 antibody.

Immunofluorescence of *C. elegans* was performed as described previously [169], with slight modifications: Worms were blocked with PTB (1% BSA, 1x PBS, 0.1 % Tween20, 0.05 % NaN_3,1 mM EDTA) and secondary antibody was diluted in PTB. Peptide antibodies against *C. elegans* PTC-3 were generated in rabbits by Eurogentec using peptides SASHSSDDESSPAHK and EVRRGPELPKENGLG. Serum was used in a 1:100 dilution and Alexa Fluor 488-goat anti-rabbit IgG (H+L) (Invitrogen; A-11034) 1:5,000. Worms were washed 2x in M9 and mounted with fluorescence protecting media (ProLong™ Glass Antifade Mountant Invitrogen P36984). Worms were imaged on a Zeiss LSM 880 microscope as described in the Microscopy section.

3.1.5.9 Filipin staining

Worms were fixed in glyoxal solution (2.835 ml ddH_2O, 0.789 ml EtOH, 0.313 ml glyoxal (40% stock solution from Sigma-Aldrich, #128465) 0.03 ml glacial acetic acid. pH 4.5) for 30 min on ice, and for another 30 min at RT, followed by 30 min of quenching in 100 mM NH_4Cl at RT and O/N post quenching at 4°C [170]. Worms were washed 2x 30 min with M9 and left in 50 µl of M9 in which 50 µl of Filipin III ready-made solution (Sigma-Aldrich, SAE0087) was added for 1 hr in the dark at RT. Worms were washed 2x in M9 and mounted with fluorescence protecting media (ProLong™ Glass Antifade Mountant Invitrogen P36984). Worms were imaged on a Zeiss LSM 880 microscope as described above.

3.1.5.10 Western Blot

Worm Lysate from synchronous L3 worm cultures was prepared in Laemmli buffer with 6 M urea with glass beads in a FastPrep machine (MP Biomedicals, Irvine, CA) for 2x 30 sec. Samples were run on a 7.5% SDS-PAGE before transfer onto nitrocellulose membranes (Amersham Protran; 10600003). Membranes were blocked in TBS containing 5% milk for 1 hr at RT. First antibody incubation was done O/N at 4°C and the secondary HRP-coupled antibodies goat anti-Mouse IgG (H+L) (ThermoFisher scientific; 31430; 1:10,000) or polyclonal HRP-conjugated goat-anti-rabbit IgG (ThermoFisher scientific; 31460; 1:10,000) for 1 hr at RT. The blots were developed using WesternBright ECL HRP substrate (K-12045 Advansta) in a Fusion FX7 (Vilber Lourmat) image acquisition system.

3.1.5.11 qRT-PCR

RNA for qRT-PCR was extracted with TRIzol according to the manufacturer's instructions from synchronous worms 26 hr after L1. The RNA was DNase digested and

reverse transcribed using Maxima H Minus First Strand cDNA Synthesis Kit, with dsDNase (ThermoFischer Scientific). The resulting cDNA was diluted 1:10 for further analysis. The StepOne RT-PCR system combined with StepOne Software (Applied Biotechnologies) was used for analysis. The presented values are based on three biological replicates. Expression levels were normalized to cdc-42 Primer sequences: nhr41_F 5'-ACGTCGAGTCGTCCACATTT-3', nhr41_R 5'-TCAGATCTCCCGAGCTCAAT-3', nhr181_F 5'-TGCGGAACAAAAAGCAGAGC-3', nhr181_R 5'-ATCTTTGTAGGTTACGTGACCC-3', cdc42_F 5'-CCTCTATCGTATCCACAG-3', cdc42_R 5'-GGTCTTTGAGCAATGATG-3', nhr168_F 5'- GGGAAACTGGCACCAATGAAG-3', nhr168_R 5'- GTTGCGAGAGGTCAGGCACCG-3'. The data was analyzed with a two-way ANOVA followed by uncorrected Fisher's LSD test in Prism 7.

3.1.6 Acknowledgements

We thank J. Fürst, J. Stevens, J. Solinger, A. Stetak (Division of Molecular Neuroscience, University of Basel), I. Katic (FMI, Basel), the IMCF-Biozentrum and Microscopy Center of the University of Zürich for the technical support, and Y. Hauser (FMI, Basel) for helpful discussions. We thank J. Brewer and V. Solovyeva (University of Southern Denmark) for the help with the CARS experiments. S. Mango, T. Bürglin and M. Labouesse are acknowledged for critical reading of the manuscript. We thank A. Antebi for sharing strains. Some strains were provided by the CGC, which is funded by NIH Office of Research Infrastructure Programs (P40 OD010440). The project was supported by the Swiss National Science Foundation (CRSII3_141956) (AS), JSPS KAKENHI Grant Number 18K06246 (MF) and the University of Basel.

3.2 The role of the PTCHD homolog PTR-4 in epidermal function

The following chapter was in preparation for publication at the time of the submission of this thesis.

The role of the PTCHD homolog PTR-4 in epidermal function

Carla E. Cadena del Castillo[1], Jennifer D. Cohen[2], J. Thomas Hannich[3], Andres Kaech[4], Meera Sundaram[2], Howard Riezman[3] and Anne Spang[1]

[1]Biozentrum, University of Basel, Switzerland, [2]Department of Genetics, University of Pennsylvania Perelman School of Medicine, Philadelphia, Pennsylvania.[3] Department of Biochemistry and NCCR Chemical Biology, University of Geneva, Switzerland, [4]Center for Microscopy and Image Analysis, University of Zürich, Switzerland,

Corresponding Author:
Anne Spang
Biozentrum
University of Basel
Klingelbergstrasse 70
CH-4056 Basel
Switzerland
Email: anne.spang@unibas.ch
Phone: +41 61 207 2380

Author contributions

AS and CECC designed the experiments. CECC performed the majority of the experiments. TH and HR performed the lipidomic analysis. AK generated the TEM data. JDC and MS created PTR-4::sfGFP and *ptr-4(cs279)* strains. AS, CECC, TH and HR analyzed the data.

3.2.1 Abstract

Hh signaling is essential during animal development. Accordingly, perturbations in the Hh signaling are one cause of a variety of developmental defects. The function of the Hh receptor PTCH as a cholesterol transporter is needed to achieve healthy development. Whether Patched related proteins (PTRs) play a similar role, remains unclear. Here we show that the essential *C. elegans'* PTR, PTR-4, is also capable of controlling cholesterol levels. Loss of PTR-4 function leads to cholesterol accumulation in the epidermis and thereby potentially perturbs the secretion of cuticular proteins. We suggest a tight regulation of membrane cholesterol levels during development.

3.2.2 Introduction

The Hh (Hh) pathway is essential during metazoan development. Therefore, perturbations in the Hh signaling are one cause of a variety of developmental defects. The Hh receptor PTCH acts as a cholesterol transporter [77,89,95]. This transporter function is conserved from worms to mammals (Section 3.1, [171]). Whether sterol transporter activity is a common effector between PTCH and other PTCH-like proteins as PTCH domain-containing proteins (PTCHD) and Patch related proteins (PTR) has not yet been addressed. PTCHD and PTR proteins comprise a group of proteins that share a common ancestor with PTCH proteins [58]. These proteins belong to a protein superfamily that conserves archaeal and bacterial resistance-nodulation division transporters (RND) and the lysosomal cholesterol transporter NPC1. RNDs are proton antiporters able to catalyze the transmembrane efflux of substrates from the cells [58]. Hitherto, their possible role as cholesterol regulators remains to be determined.

There are four PTCHD proteins in mammals. PTCHD1 is a protein linked to autism spectrum disorder, but it is not involved in Hh signaling [63–65]. Meanwhile, the role of PTCHD3 and PTCHD4 remains elusive. On the other hand, PTCHD2/DISP3 is needed for neuronal differentiation and seems to play a role in cholesterol homeostasis[172–174], suggesting a conserved role in sterol regulation. *C. elegans* encodes 25 PTR proteins. Most of them have been described to play a role in molting [72]; however, the precise mechanism of most of PTRs is unknown. Most of PTRs have conserved motives in the transmembrane domains 4 and 10 [18], which have been described to be necessary for PTCH cholesterol transport function[77]. Accordingly, a role of PTRs in sterol regulation could be expected. Furthermore, some studies showed that PTR proteins are connected to cholesterol regulation [96,97]. For instance, the phenotypes displayed by the loss of PTRs suggest a link between PTRs and cholesterol [72]. In particular, molting, which on top of being impaired by altering constituents of the cuticle, can be affected in worms that grow without cholesterol or are knockdown of PTRs (PTR-1, PTR-2, PTR-3, PTR-4, PTR-5, PTR-6, PTR-8, PTR-9, PTR-10, PTR-12, PTR-13, PTR-14, PTR-16, PTR-17, PTR-18, PTR-20, PTR-21, PTR-22, and PTR-23)[72,122,133,134]. Molting is the process in charge of the replacement of the old cuticle with a new one. The cuticle is the exoskeleton of *C. elegans*, which protects the worm from the environment. As a consequence, its integrity is crucial for worm survival. The cuticle needs to be replaced four times during development to fit the growing larva. As expected, molting is essential for healthy growth and development.

Nevertheless, it is intriguing that nematodes need more than 25 different PTR while mammals only 4. One possibility is that worm's PTRs have a highly delimited expression and regulation, and in some cases, possibly specificity for particular sterol derivates, which could allow the worm to regulate cholesterol and other sterols locally and temporally. PTR-

2 and PTR-4 are essential proteins. Therefore, they are non-redundant; this supports the hypothesis of tight temporal regulation in addition to the possible specificity for particular sterols. In the present work, we characterized the role of the essential PTCHD homolog PTR-4. We could confirm that PTR-4 can regulate cholesterol levels, and its expression and localization vary through larval development. We demonstrate that while specific functions of the worm PTCH homolog PTC-3 as fatty acid regulation (Section 3.1, [171]) were not widely affected by the lack of PTR-4 during larval development. The absence of PTR-4 results in cuticle defects, and as a consequence, worms display locomotive problems.

3.2.3 Results

3.2.3.1 PTC and PTR proteins, differences and similarities

To gain a better understanding of the possible function of PTR proteins, we questioned about the molecular function of PTRs. As a first step, we focused on the essential PTR homolog PTR-4 and inquired whether the PTR-4 tridimensional structure is similar to either PTCH or PTCHD proteins. Structure prediction using Phyre2 [84] revealed that both PTCHD1 and PTR-4 have a similar structure to the mammalian PTCH1 (Fig. 3.2.1A, B, and C). Interestingly, PTCHD1 and PTR-4 have the highest similarity to PTCH1 in the transporter regions; this is similar to the predicted structure of the worms PTCH homolog PTC-3 (Fig. 3.2.1D). Subsequently, we examined the conservation in PTCHDs and PTRs of the specific residues from PTCH1 involved in cholesterol transport. After the protein alignment [175], we observed that in PTCHD1, 3, and 4, the described key residues in the transmembrane domains 4 and 10 are not conserved, while the essential worm proteins PTR-4 and PTR-2 did conserve them (Fig. 3.2.1E). These results suggested that it is very likely that PTR proteins have conserved cholesterol transporter function. In contrast, PTCHD1 protein may be acting throughout a different mechanism. On that account, it would be expected that PTRs and PTCHD proteins perform different roles in the cell.

3.2.3.2 PTR-4 modulates cholesterol levels

Given the structural conservation, we hypothesized that at least a subset of PTR proteins are transporters and might transport cholesterol similarly to PTCH and NPC1. To test this, we analyzed cholesterol levels in the hypomorphic mutant *ptr-4(cs279)*. This mutant has an insertion in the 3' UTR, likely reducing the amount of PTR-4 protein (personal communication Meera Sundaram). In this mutant, the fluorescent Topfluor Cholesterol accumulated in the epidermal area (Fig. 3.2.2A). Similarly, Filipin III was enriched in the *ptr-4(cs279)* strain (Fig. 3.2.2A). To corroborate these findings, we analyzed the endogenous cholesterol levels in the knockdown of PTR-4 protein by mass spectrometry. Comparably to what we have observed previously in a knockdown of *C. elegans'* PTCH homolog PTC-3, *ptr-4(RNAi)* animals showed an increase of cholesterol like *ptc-3 (RNAi)* worms (Fig. 3.2.2B), suggesting a conserved role of PTR-4 in cholesterol transport or alternative in its mobilization and conversion into 7- dehydrocholesterol. Our results suggest a conserved role for PTR-4 in the modulation of cholesterol levels.

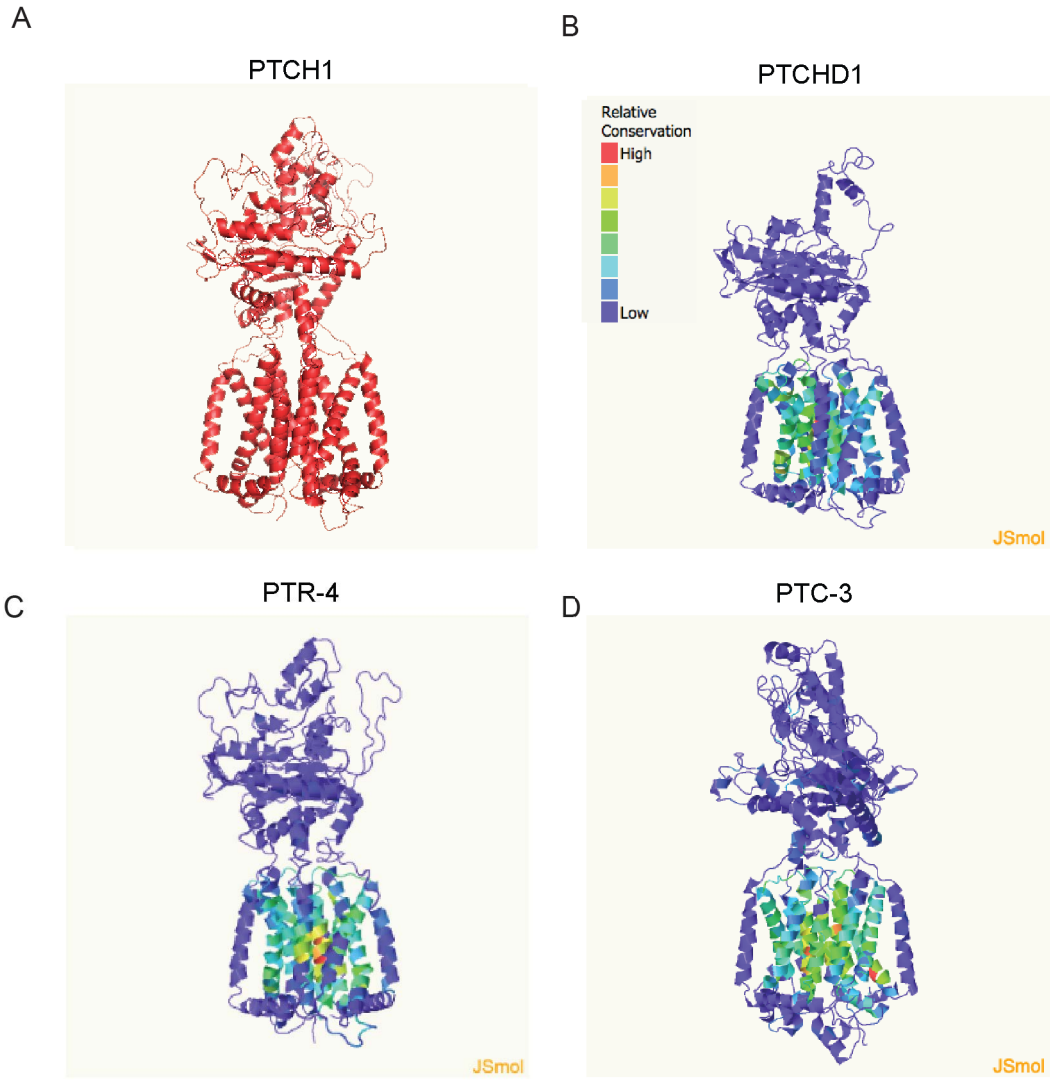

E

	TM4 GxxxD/E	TM10 GxxxD/E
PTC1_HUMAN	PFLALGVGVDDVFLLAH	VGIGVEFTVHVALAFLT
PTC1_CAEEL	PFLTLGIGVDNMFMLLH	VGIGVEFTVHVVVSFLT
PTC3_CAEEL	PFLSLGLGIDDMFLLLH	VGIGVEFTAHVELAFLT
PTHD1_HUMAN	PFVMLGHGLYGTFEMLS	INYTIDNCAPMLSTFVL
PTHD2_HUMAN	AFVIVGIGVDDVFVFIN	VGSSVDYCVHLVEGYLL
PTHD3_HUMAN	PFLILGVGVDDMFIMIS	----------
PTHD4_HUMAN	PFFAMGHGTKGVFELLS	LNFAIDHCAPLLFTFVL
PTR2_CAEEL	PFLVLAVGVDNMFLMVA	IGFSVDYSAHIAYGYVV
PTR4_CAEEL	PFLVLAVGVDDDFLMMA	IGLAVDYSVHICYRYHR

Figure 3.2.1. Structural resemblance of PTCH and PTCHD proteins. **(A)**. Structure of PTCH1 protein [90]. Structural comparison between PTCHD1 (**B**), PTR-4 (**C**), and PTC-3 (**D**) with PTCH1 shows higher conservation in the transmembrane domains, structural analysis was done with Phyre2 [84]. **(E)**. Alignment of the GxxxD motif in the human proteins PTCH1, PTCHD1, and PTCHD2/DISP3 with *C. elegans* proteins PTC-1, PTC-3, PTR-2, and PTR-4. This motif is linked with the permease transporter domains located in TM4 and TM10. PTC1 and 3 have completely conserved the key residues; PTR proteins suffer minor changes with a G/A substitution; PTCHD proteins 1, 3, and 4 did not conserve the domains. The alignment was performed with Clustal Omega [175].

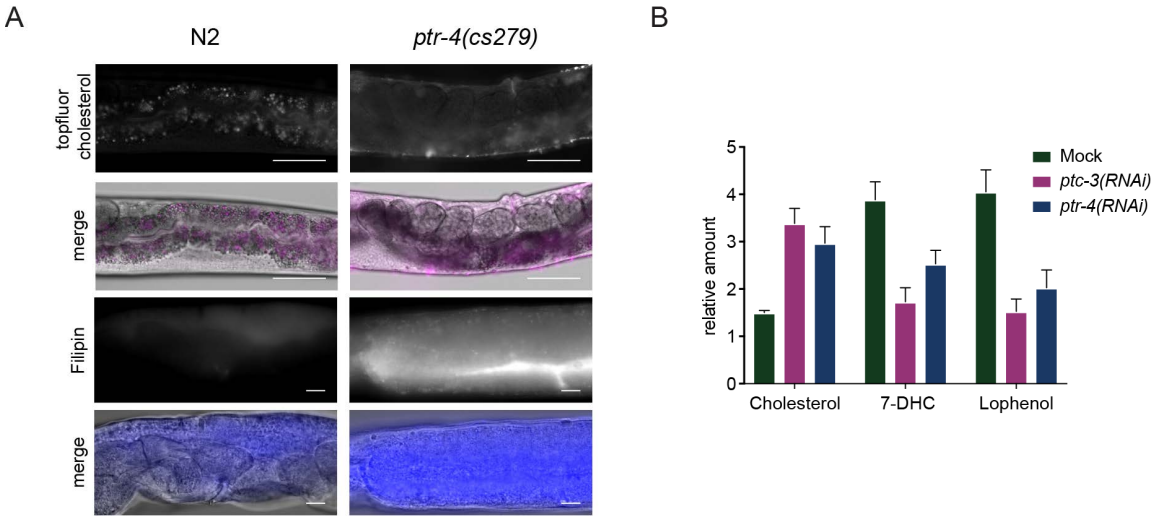

Figure 3.2.2. Cholesterol accumulates in PTR-4 deficient animals. (A). *ptr-4(cs279)* worms showed cholesterol accumulation. N2 or *ptr-4(cs279)* worms were incubated with 2.5 mM TopFluor-cholesterol for 1 hr. After 1 hr chase, animals were imaged. Scale bar 50 μm. Alternative N2 and *ptr-4(cs279)* adult animals were stained with FilipinIII. Staining can be observed in *ptr-4(cs279)* animals. Scale bar 10 μm. **(B)**. Quantification of sterols by MS showing cholesterol accumulation and low 7-DHC and Lophenol upon *ptc-3(RNAi)* and *ptr-4(RNAi)*. *ptc-3(RNAi)* data is the same as depicted in Fig. 3.1.5.

3.2.3.3 PTR-4 and PTC-3 play differential roles in worm physiology

As a consequence of the cholesterol accumulation in *ptc-3(RNAi)* animals, fatty acid acyl chain saturation and length were reduced [171]. Therefore, we asked whether the knockdown of PTR-4 would have a similar effect. To answer this question, we tested by mass spectrometry whether acyl-chain elongation and desaturation were impaired in *ptr-4(RNAi)* treated animals. No effect on phospholipid distribution was observed by the lipidomic analysis in PTR-4 knockdown (Fig. 3.2.3A). Additionally, the acyl chain length was unchanged in comparison to the control, but the saturation levels were affected similarly as in *ptc-3(RNAi)* but to a lesser extent (Fig. 3.2.3B section 3.1.3.6).

Next, we examined whether PTC-3 and PTR-4 could have a genetic interaction. L1 nematodes were grown on *ptc-3(RNAi)*, *ptr-4(RNAi)*, or both combined, and we assessed the effect of the double knockdown in developmental arrest. Unexpectedly, the double knockdown had a moderate but consistent improvement in larval development, increasing the percentage of worms able to develop from an eight percent to 25.7%. Our results suggest that PTC-3 and PTR-4 have different roles in *C. elegans* development. Still, it is elusive why we observed synthetic rescue of *ptc-3(RNAi)* by *ptr-4(RNAi).* We propose that they could transfer cholesterol from two different cell types or compartments, generating an evener distribution of cholesterol among different membranes upon the double KD. As a consequence, this would induce a milder developmental phenotype. Nevertheless, our results suggest that PTC-3 and PTR-4 have non-redundant and rather opposite functions.

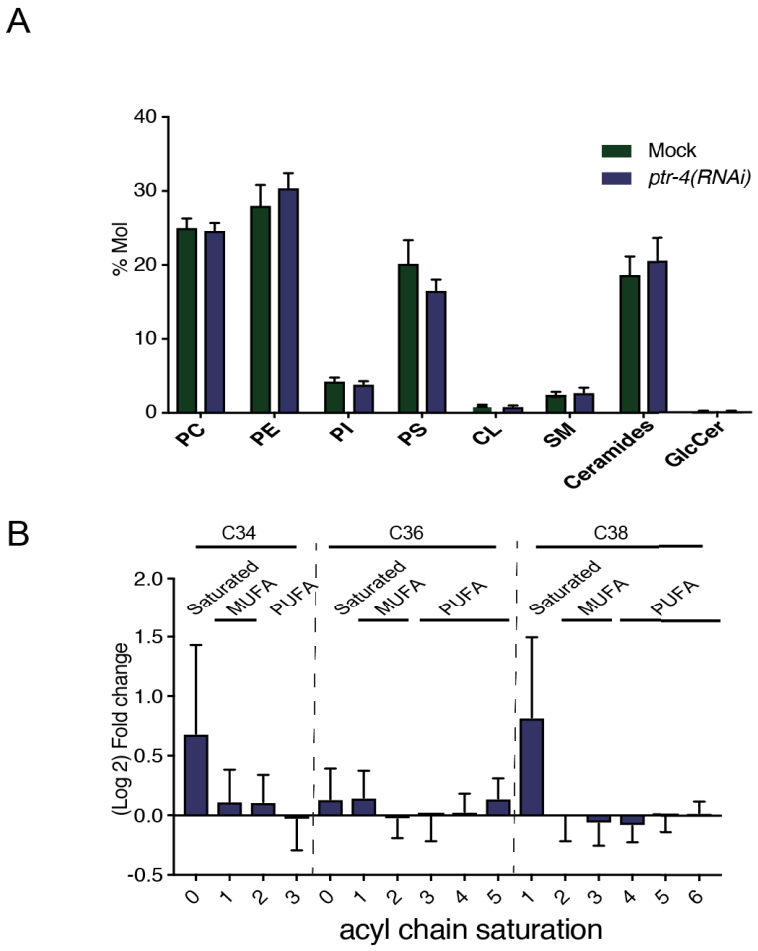

Figure 3.2.3. PTR-4 knockdown affects FAs saturation. (**A**) Lipidomics on mock or *ptr-4(RNAi)* treated worms. *ptr-4(RNAi)* worms showed no significant difference in lipid head group distribution. Error bars are SEM. (**B**) Lipidomics revealed a milder difference in lipid acyl chain composition upon *ptr-4(RNAi)* with accumulation of unsaturated acyl chains. PC phosphatidyl choline, PE phosphatidyl ethanolamine, PI phosphatidyl inositol, PS phosphatidyl serine, CL cardiolipin, SM Sphingomyelin, Glc Cer glucosyl ceramide. Error bars are SEM.

3.2.3.4 Role of PTR-4 in cuticle function

To better understand the function of PTR-4, we revisited the described PTR-4 phenotypes. One of the most striking phenotypes of both the PTR-4 hypomorph strain *ptr-4(cs279)* and *ptr-4(RNAi)* treated animals is a locomotion defect in adult worms (Fig. 3.2.4A). This phenotype was also confirmed by a swimming test in *ptr-4(RNAi)* worms (Fig. 3.2.4B). In *C. elegans*, locomotion requires the alternation of the contraction of body wall muscles that are connected to the cuticle[132]. Osmolarity regulation and turgor pressure are essential to maintain the turgor pressure of the nematode and consequently to achieve movement. Both hypo- and hyperosmotic conditions lead to abnormal internal pressure, which promotes the failure of the worm's hydrostatic skeleton leading to paralysis [176]. Since

cuticle integrity is a critical factor in osmolarity control, the locomotive phenotype in the PTR-4 hypomorph (Fig. 3.2.4A and B) could be related defects in the cuticle structure and integrity. Therefore, we analyzed the cuticle structure. While in N2 worms, the cuticle shows the characteristic patterned structure with circumferential ridges (annuli) divided by the alae (Fig. 3.2.4C and D) the cuticles of *ptr-4(cs279)* worms showed no visible annuli and the alae was interrupted. Epidermal imaging revealed autofluorescent structures between the epidermis and the cuticle in *ptr-4(cs279)* animals (Fig. 3.2.4E). To address the nature of these aggregates, we performed electron microscopy in *ptr-4(RNAi)* worms. We observed cuticular abnormalities in RNAi-treated animals (Fig. 3.2.4F), such as vesicles accumulating in the cuticle (Fig. 3.2.4 E and F). Next, we tested the cuticle permeability by placing N2, and *ptr-4(cs279)* worms in a solution containing the cuticle impermeable dye DAPI. After 15 minutes, *ptr-4(cs279)* animals showed staining in the epidermis while N2 animals remained unstained (Fig. 3.2.4H and I), implying that the permeability barrier in the cuticle is defective in the absence of PTR-4. Therefore, we wondered whether the cuticular defects are related to the production of the cuticle during larval development. PTR-4 has been reported to oscillate throughout larval development. Under more precise scrutiny of the PTR-4 oscillatory pattern, it can be observed that the higher ribosomal footprint levels of PTR-4 occur few hours after molting (Fig. 3.2.4G) [79], suggesting that its expression is linked to the production of the new cuticle. This information, together with the suggested expression, indicate that the defects may be related to a defective epidermal function.

3.2.3.5 PTR-4 epidermal expression

In the nematode, the epidermis is necessary for the storage of nutrients and the deposition of stage-specific cuticles. Characteristic features of impaired epidermal development or function are defects in body morphogenesis, muscle development, and cuticle structure. Mutants affecting epidermal functions lead to arrested animals and adults with dumpy phenotype and locomotive problems, similar to the phenotype observed in the *ptr-4(cs279)* strain and *ptr-4(RNAi)* treated nematodes. Expression data shows most of the PTR-4 expression in the epidermis followed by glial cells (Fig. 3.2.5A) [81]. To characterize in detail PTR-4 expression. We used an endogenously tagged PTR-4::sfGFP strain. The tagged strain developed normally and showed no phenotypes, suggesting PTR-4 is functional. Since the defect in locomotion upon the PTR-4 knockdown occurs after the last molting, we analyzed the expression of PTR-4 in the L4 stage. As expected from the transcriptomic data, there is a strong PTR-4::sfGFP signal in the epidermis. As well, we could detect expression in the L4 developing vulva (p5 and p7 cells), and rectal cells (Fig. 3.2.5B). The epidermal expression supports the idea that PTR-4 could be affecting the production of the new cuticle.

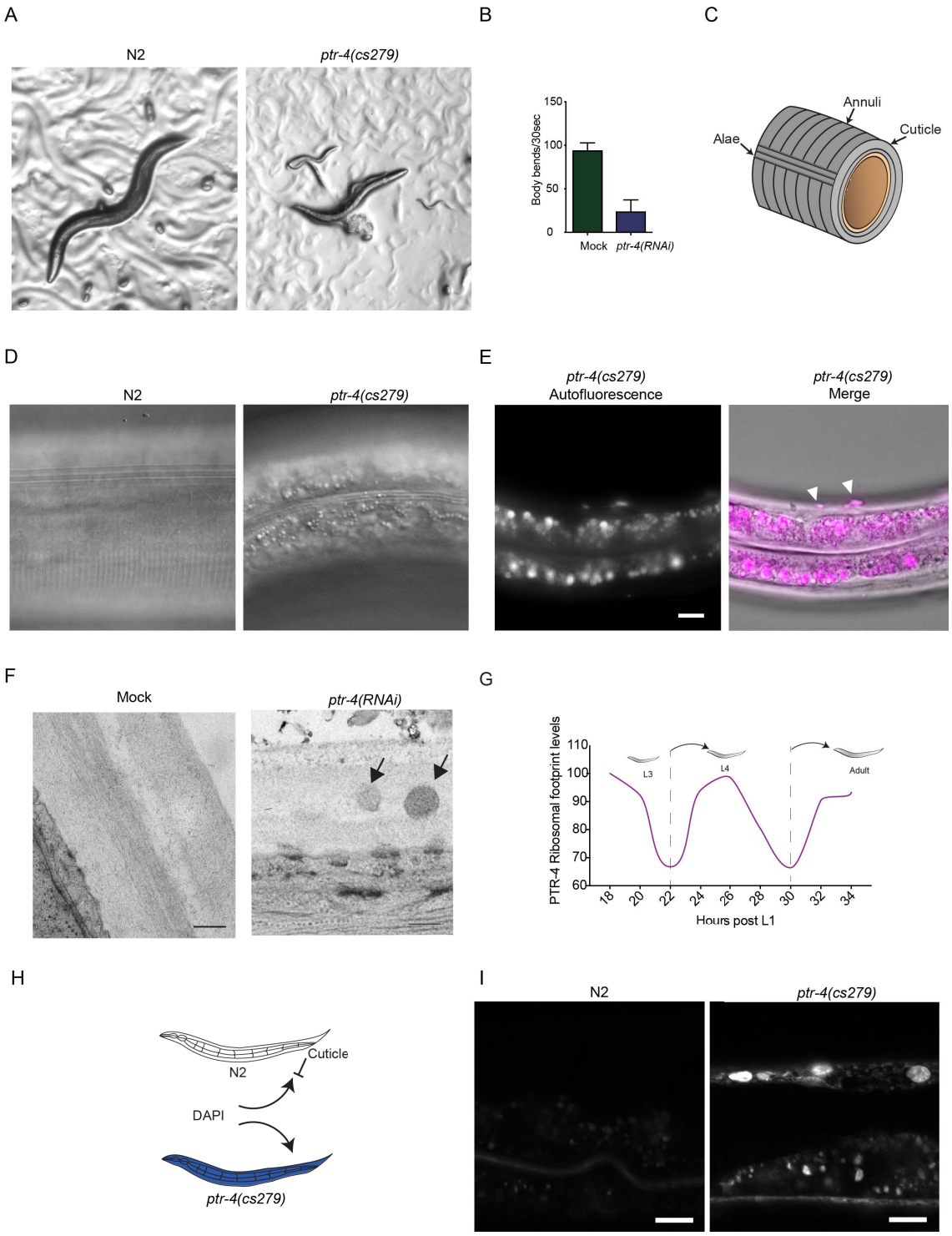

Figure 3.2.4. PTR-4 lost induces cuticular defects. (A) *ptr-4(cs279)* animals have a dumpy appearance and a locomotive phenotype. (**B**) N2 and *ptr-4(RNAi)* worms were placed in M9 media and were allowed to swim. Body bend analysis in a 30 seconds test showed reduced motility upon *ptr-4(RNAi)*. (**C**) Organization and structure of the cuticle. (**D**) DIC images of N2 and *ptr-4(cs279)* worms. The cuticle in *ptr-4(cs279)* worms showed a defective structure. (**E**) Autofluorescence in *ptr-4(cs279)* animals, high autofluorescence is observed in the intestine and in protrusions from the cuticle. (**F**). TEM images showing cuticle structure in Mock and *ptr-4(RNAi)* treated animals. In ptr-4 knockdown, some vesicular-like structures were observed embedded in the cuticle. (**G**). Detailed PTR-4 ribosomal footprints oscillations of from a published dataset [79]. (**H**) Permeability test using the impermeable dye DAPI. In animals with an intact cuticle DAPI, is not able to infiltrate and stain cell nuclei. (**I**) Representative DAPI images of N2 or *ptr-4(cs279)* upon DAPI incubation. Scale bars 10 µm.

3.2.3.6 PTR-4 time-dependent expression

The notion that PTR-4 could regulate the formation of the cuticle made us wonder about PTR-4 expression pattern during the development. As PTR-4 mRNA levels vary throughout larval development, we wondered whether protein levels echoed the mRNA oscillations. L4 worms were staged accordingly to the vulva development, as previously described by [177] (Fig. 3.2.6A). We observed that while the protein is not present in early L4 worms after the mid-L4 stage, it can be observed at the plasma membrane, and once the worms reach the late-L4 stage, the PTR-4 cannot be detected anymore (Fig. 3.2.6B). This pattern is observed in the epidermis, vulva, and rectum, which correspond to the three main tissues where PTR-4 expression is detected. Still, the exact role of this specific pattern is not known.

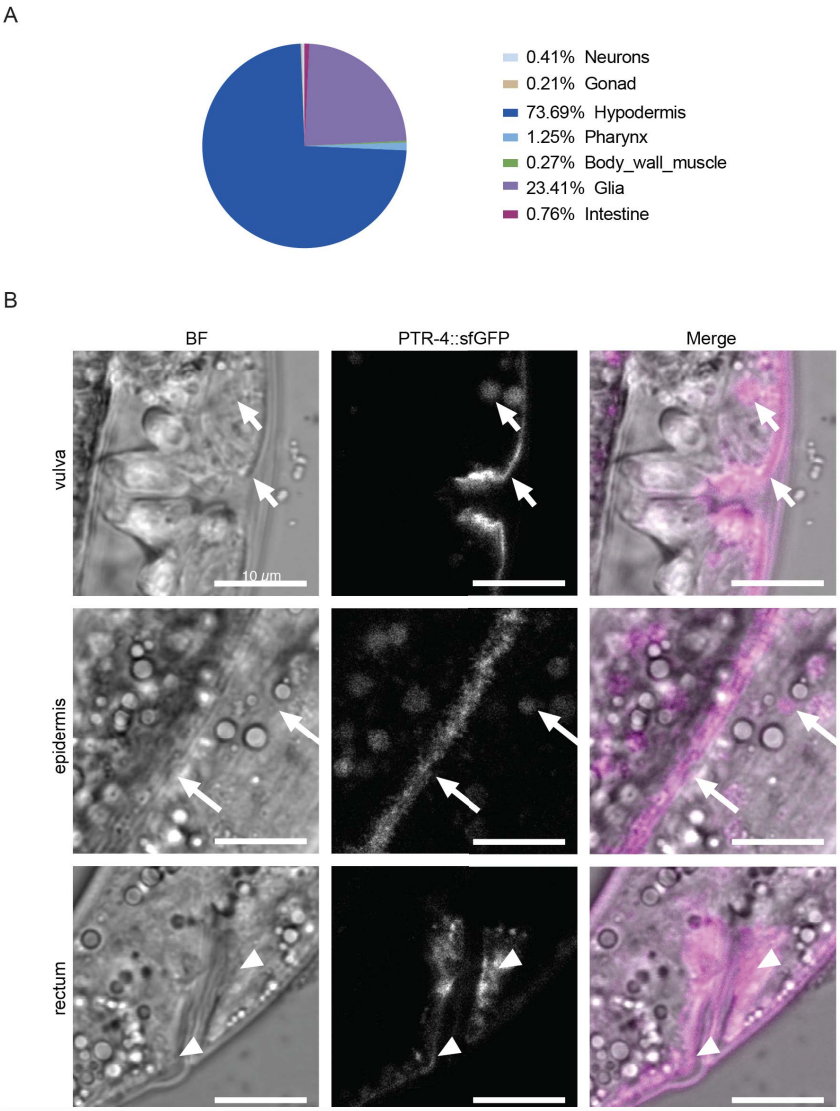

Figure 3.2.5. PTR-4 in vivo localization. (**A**) Detailed expression pattern for PTR-4 from data in (Fig 3.2.1B). PTR-4 is expressed mainly in the epidermis followed by glial expression. (**B**). PTR-4 epidermal localization was analyzed with PTR-4::sfGFP-tagged strain. Bright-field and confocal images of late L4 animals expressing PTR-4::sfGFP. Arrows pointing the precise PTR-4 localization, both plasma membrane and internal localization, can be observed. Scale bars 10 µm

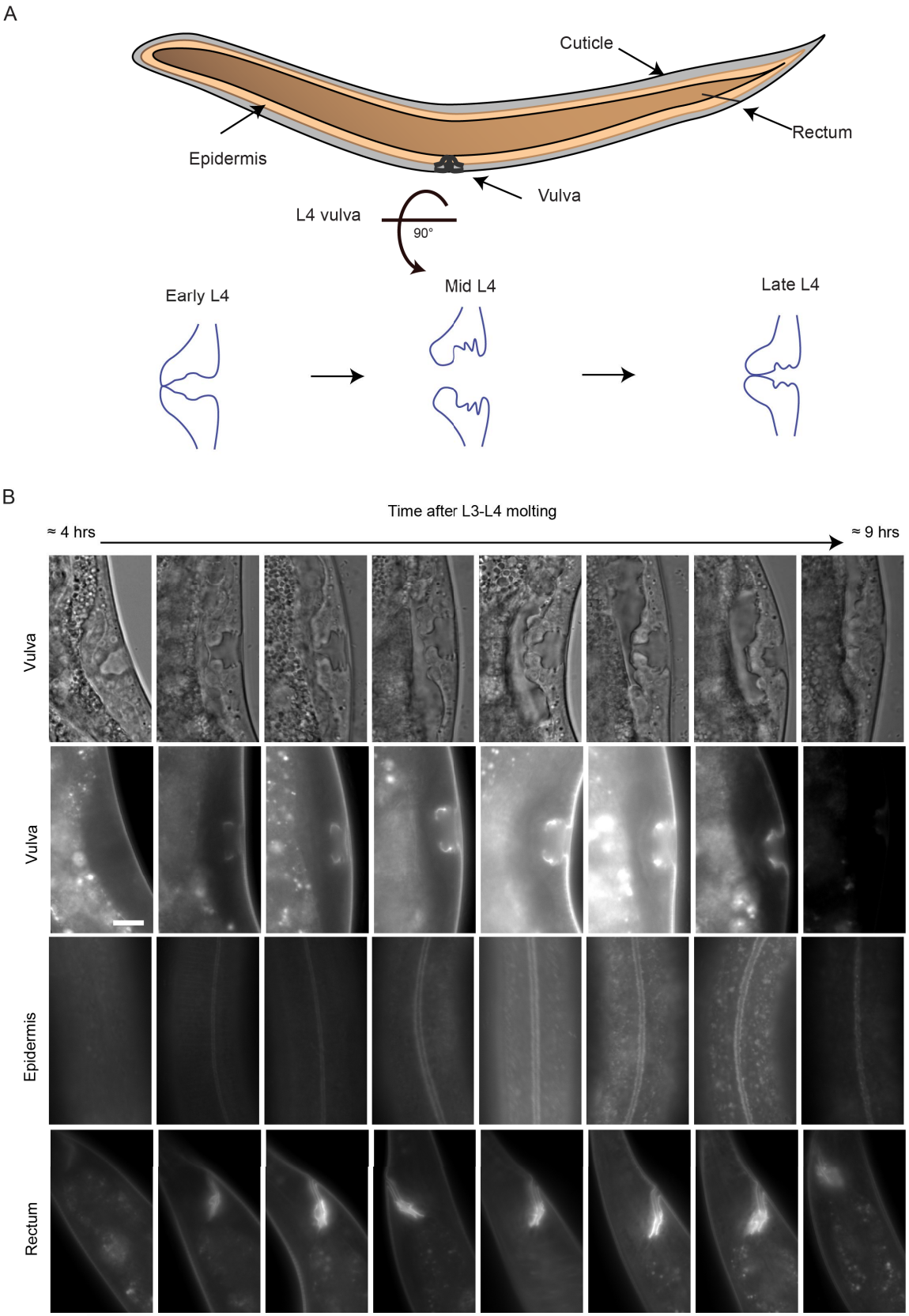

Figure 3.2.6. PTR-4 *in vivo* localization during the L4 larval stage. (**A**) Schematic representation of morphological changes during L4 vulva development. (**B**) PTR-4::sfGFP localization in L4 sub-staged larva. PTR-4::sfGFP expression in the epidermis, rectum, and vulva was confirmed to change during development, while in early L4 there is no PTR-4::sfGFP signal, in mid L4 it can be observed at the membrane, in late L4 animals it localizes to internal structures and prior to molting the signal disappears. Scale bar 10 µm.

3.2.3.7 PTR-4 time-dependent localization

As shown above, PTR-4 was present in the epidermal, vulva, and rectal cells. In mid-L4 animals, PTR-4 localizes to the plasma membrane while at later stages, PTR4 appears in circular compartments (Fig. 3.2.6B). To better understand the nature of these structures, we made use of super-resolution imaging. As before, we observed that in the mid-L4 stage, PTR-4 was localized exclusively to the plasma membrane in the epidermal cells (hyp7). In later stages, PTR-4 was present in plasma membrane invaginations (Fig. 3.2.7A). By the end of the L4 stage, PTR-4 was no longer resident at the plasma membrane, but moved to internal compartments, potentially endosomes (Fig. 3.2.7A and B). Thus, PTR-4 localization seems to be controlled through L4 larval development.

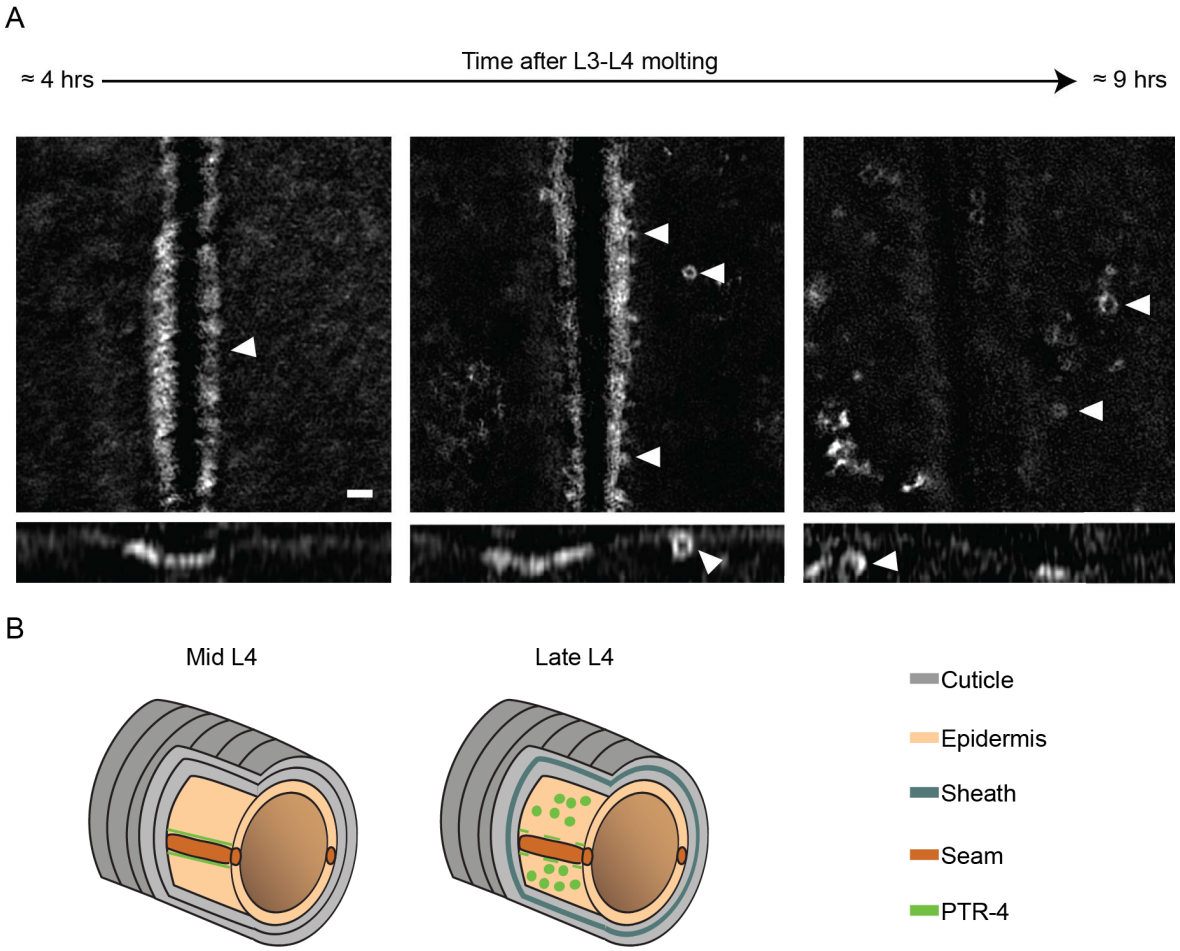

Figure 3.2.7. PTR-4 *in vivo* dynamic localization during the L4 larval stage. (**A**) Structural illumination (SIM) images of PTR-4::sfGFP. In mid-L4 worms, PTR-4::sfGFP was at the plasma membrane, as the development proceeds, PTR-4::sfGFP gathers in membrane invaginations. At late L4 stages, PTR-4::sfGFP localizes exclusively in intracellular compartments. Scale bar 1 µm. (**B**) Schematic representation of (A).

3.2.4 Discussion and outlook

The molecular role of PTCH proteins has been associated with the regulation of membrane cholesterol (section 3.2 and [87,89,90,95,171]). Therefore, it is feasible that other proteins sharing structural similarities with PTCH as PTRs conserve this function. In *C. elegans*, the study of this group of proteins remained widely elusive despite some homologs play a crucial role in worm development [72]. Our results advocate that PTR-4 has a cholesterol regulation function. However, more experiments are still needed to determine the functionality of the putative transporter domain. We cannot exclude the possibility that PTR-4 is sensing cholesterol and regulating a cholesterol transporter. Hence, *in vitro* experiments in a heterologous system, such as yeast, are necessary to establish PTR-4 as a cholesterol transporter.

Provided that *C. elegans* is a cholesterol auxotroph, it is likely that in nature, worms face low cholesterol levels. Consequently, the worms have probably developed means to transport the available cholesterol to the cellular compartments and tissues that require it. Cholesterol requirements may vary during development. Therefore, a possible scenario is that PTR proteins are in charge of such a process. However, it is not clear if they do this by direct transport of cholesterol or by the sensing of it and further regulation of its transport.

PTRs are similar to bacterial resistance-nodulation division transporters (RND). Since RNDs can pump a variety of small molecules [76], we must consider that some PTRs might be regulating other compounds, possibly even another sterol. Still, more research is needed to clarify this concern. We postulate that the sterol regulation mechanism is not exclusive of PTCH proteins, but also it is a role of other similar proteins. For instance, the overexpression of the mammalian related protein PTCHD2 promotes cholesterol accumulation in the ER [174]. As well, in *C. elegans*, there is evidence supporting this premise, PTR-6 mutation induces changes in membrane permeability that can be counteracted by the depletion of mboa-1(SOAT1 homolog), which catalyzes the formation of cholesterol esters[97].

Furthermore, our results suggest that PTR-4 primarily functions in the epidermal cells (hyp7). As we observe that the PTR-4 levels oscillate during larval development, it is possible that cholesterol levels at the epidermal plasma membrane and extracellular matrix (ECM) oscillate during development too (Fig. 3.2.9). As a result, in the absence of PTR-4 cholesterol levels in the epidermis may increase. Hence, it is likely that in the ECM, cholesterol might decrease, triggering a cholesterol imbalance that has consequences in cuticle formation and stability. This effect could be related to an impaired function of the epidermis or an altered ECM (Fig. 3.2.9).

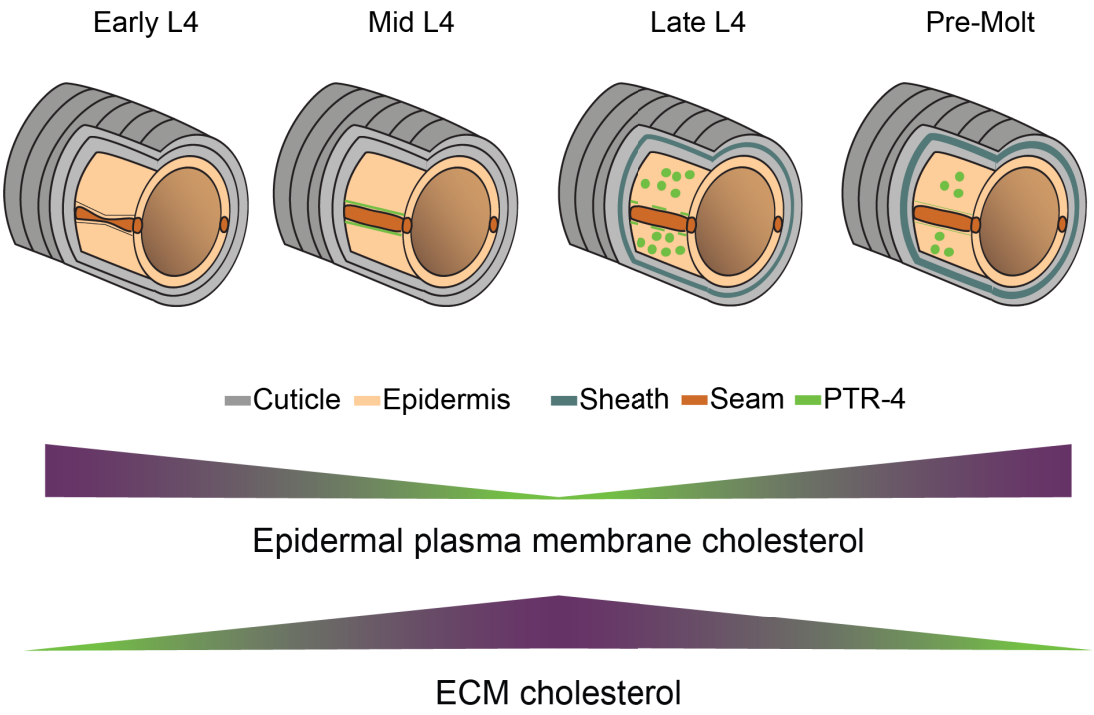

Figure 3.2.9. PTR-4 and epidermal function. (**A**) PTR-4 levels oscillate during larval development, likely generating changing cholesterol levels during the development. In the absence of PTR-4, cholesterol levels in the epidermis increase. As a consequence, they might decrease in the ECM, therefore causing an imbalance that could have negative consequences in the ECM functions that could affect the cuticular structure.

Recent studies have shown that PTR-4 is required to localize the zona pellucida (ZP)-domain protein LET-653 at the apical extracellular matrix (J. D. Cohen unpublished data). This requirement suggests a role of PTR-4 in the ECM structure. A possible link between PTR-4 function and ECM stability could be cholesterol. The cholesterol levels affected by the PTR-4 function might be sensed by a group of proteins known as lipocalins. Lipocalins are known for having a role in transporting sterols, phospholipids, and sphingolipids[178–180]. Lipocalins are found in the ECM and are required for ECM organization [181]. Remarkably, in a similar way as PTR-4, components of the ECM, such as LET-653, oscillate through development[79,182] supporting a possible link between PTR-4 and ECM function.

3.2.5 Materials and Methods

3.2.5.1 General *C. elegans* methods and strains

C. elegans nematodes were cultured and maintained as described previously[120] and in chapter 3.1.5.1 Endogenously tagged sfGFP::PTR-4 strains and a hypomorphic allele induced by an insertion in PTR-4 3´UTR produced by the Sundaram lab were used.

3.2.5.2 Swimming test

Young adults were placed on M9 buffer for 5 sec. The body bends were counted for 30 sec. At least eight worms of each condition were analyzed per experiment, and the experiment was performed three times. The results are presented as the average of tail movements per 30 sec. The data were analyzed with a one-tail ANOVA followed by Dunnett's multiple comparisons test in Prism 7.

3.2.5.3 Cuticle barrier assays

DAPI staining was performed accordingly to Moribe et al. [183], with minor modifications. For staining, we used 10 µg/µl of DAPI in M9. Animals were scored by fluorescence microscopy for DAPI staining in nuclei.

3.2.5.4 Lipidomic analysis

The lipidomic analysis was done as described in chapter 3.1.5.5

3.2.5.5 Top Fluor cholesterol staining

Worms were processed as described in chapter 3.1.5.7

3.2.5.6 Microscopy

Live worms and images were treated as described in chapter 3.1.5.2. Structure illumination microscopy was done with DeltaVision OMX Optical Microscope (version 4), Software: DeltaVision OMX softWoRx. Oil 1.518

3.2.5.7 Filipin staining

Worms were treated and imaged as described in chapter 3.1.5.9.

3.2.5.8 TEM

Transmission electron microscopy was done as described in chapter 3.1.5.4.

4. Future directions and preliminary results

In this thesis, we have shown that PTC-3 modulates cholesterol levels and FA acyl chain composition. We hypothesize that these membrane properties are changing in response to PTC-3. Since the regulation of membrane properties has a broad impact on general cell physiology and signaling, we reason that this regulation could be a mechanism by which other proteins might be affected by PTC-3. Therefore, as an additional branch of this project, we addressed the potential role of PTC-3 in endocytosis as a consequence of the regulation of membrane properties.

For this, we established the following objectives:

- Analyze the potential genetic interaction between PTC-3 and endocytic regulators.
- Examine the effect of PTC-3 in the endosomal pathway organization.
- Inspect the effect of FA acyl chain length manipulation in the endosomal pathway organization.

4.1 Potential roles of cholesterol plasma membrane levels in intracellular traffic

4.1.1 Introduction

Endocytosis refers to the uptake of material into a cell by an invagination of the plasma membrane culminating in a membrane-bounded vesicle[184]. It controls the distribution of membrane-bound components and the internalization of extracellular components such as proteins and lipids. Newly generated endocytic carriers fuse to form early endosomes, from which cargoes can be sorted for transport to the trans-Golgi network, recycling, or degradation [184,185]. The membrane identity of these compartments is mostly determined by Rab GTPases [186]. For instance, the small GTPase RAB-5 labels and determines the specific membrane environment of early endosomes, and during endosomal maturation, it is exchanged to RAB-7 by the RAB-GEF SAND-1/MON-1-CCZ-1 complex [186,187]. Endocytosis is an essential process, and its deregulation leads to developmental problems and diseases such as cancer [184].

Unpublished work from our lab suggested that PTC-3 could have a role in endosomal regulation. An RNAi screen identifying genetic interactors of SAND-1 showed that *sand-1* deletion partially rescues the lethality of PTC-3 depletion (Solinger, unpublished data). Additional work suggested that *ptc-3(RNAi)* rescued the SAND-1 block in endosome maturation (Ingemann unpublished data). However, the precise role of PTC-3 in the regulation of the endosomal pathway remains elusive. In *Drosophila,* PTC prevents the movement of SMO from intracellular vesicles to the plasma membrane. As well, it has been proposed that PTC promotes the delivery of SMO to lysosomes [188]. Furthermore, in *Drosophila*, the endosomal-lysosomal pathway regulates axon pruning, and PTC can downregulate this pathway in a SMO independent manner [189]. These data suggest that endocytosis and protein localization regulation by PTCH is likely to be a direct effect of PTCH, supporting the notion that PTCH proteins might be involved in intracellular trafficking.

The mechanism by which PTCH proteins affect traffic is still elusive. It has been shown that PTC associates with Caveolin-1 [190], a protein involved in the generation of cholesterol-rich protrusion in the plasma membrane (caveolae), which could function as initiation points of endocytosis [191–193]. Whether this association provides PTCH a mean to regulate endocytosis, or whether it is related to PTCH regulation, is currently unknown. In the present thesis, we showed (Section 3.1) that PTC-3 can affect the composition of membranes. Therefore, we postulate that a possible mechanism of PTC as an endocytic regulator is by altering plasma membrane composition. In this section, we aimed to address this possibility.

4.1.2 Results

4.1.2.1 Genetic interaction between SAND-1 PTC-3

As a first step to analyze the role of PTC-3 in the endosomal pathway, we decided to confirm the genetic interaction of SAND-1 and PTC-3 (Solinger unpublished data). Indeed, the SAND-1 deletion mutant *sand-1(ok1963)* was able to partially rescue *ptc-3(RNAi)* (Fig. 4.1.1). Therefore, we hypothesized that in *C. elegans*, PTC-3 function and the endosomal pathway are associated.

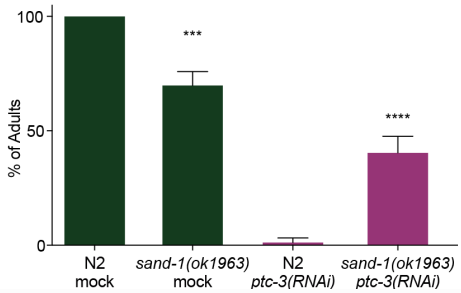

Figure 4.1.1. Loss of SAND-1 provokes synthetic rescue of ptc-3(RNAi) induced lethality. Genetic interaction between SAND-1 and PTC-3 is observed upon *ptc-3(RNAi)* treatment on the *sand-1(ok1963)* mutant. The graph displays the percentage of adults over alive animals *** p <0.0001 n >80 worms in 3 independent experiments.

4.1.2.2 Effect of PTC-3 in the endosomal pathway

To elucidate whether *ptc-3* genetic interaction with *sand-1* can be related to an effect of PTC-3 in the endosomal system, we decided to determine the consequence of *ptc-3* knockdown on early and late endosomes. Previous reports have shown that in the adult worm gut, the endocytic compartments have a defined distribution making this tissue a good endocytic model [194]. In the gut cells, early endosomes marked with RAB-5 are near to the apical membrane, followed by late endosomes enriched with RAB-7 (Fig. 4.1.2A)[194]. We analyzed the distribution of early endosomes labeled by GFP::RAB-5 and late endosomes by mCherry::RAB-7. Both early and late endosomes were affected in the *ptc-3(RNAi)*. In mock-treated animals, RAB-5 positive early endosomes are found near the gut lumen, whereas in *ptc-3(RNAi)* treated animals, there appeared to be an increase in RAB-5 positive compartments and they localized towards the cell center. The late endosomal compartment labeled with mCherry::RAB-7 was expanded and showed partial colocalization with the early marker GFP::RAB-5 (Fig. 4.1.2B). Even though we could observe in the EM analysis enlargement of some round compartments (Fig. 4.1.2C), whether these enlarged compartments correspond to RAB-7 positive endosomes or another compartment remains unclear. Further analysis by correlative light electron microscopy (CLEM) is needed to be able to answer definitely this open question.

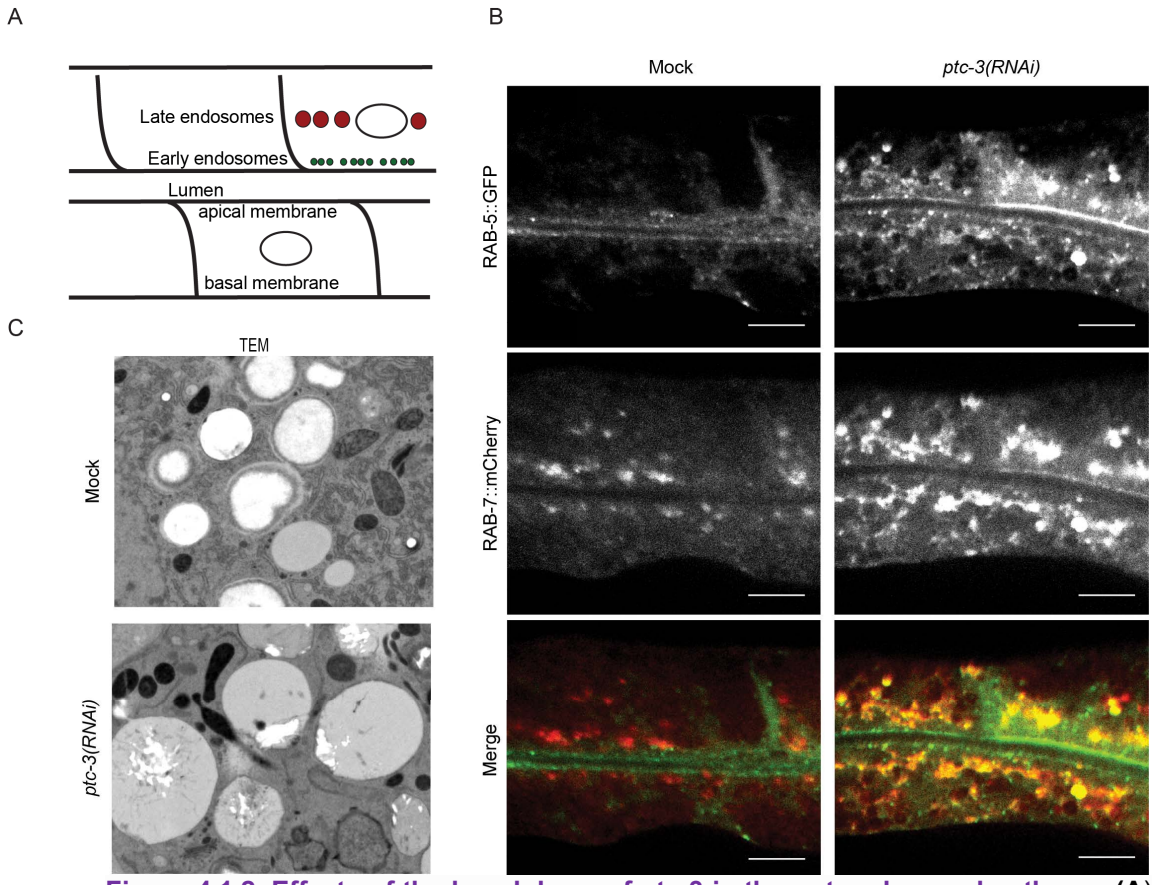

Figure 4.1.2. Effects of the knockdown of ptc-3 in the gut endosomal pathway. (**A**) RAB-5 positive early endosomes are concentrated near the gut lumen, followed by late endosomes label with RAB-7 (adapted from [194]). (**B**) Knockdown of *ptc-3* in *C. elegans* expressing GFP::RAB-5 and mCherry::RAB-7 in the intestine. Early endosomes labeled with GFP::RAB-5 are concentrated near the gut lumen in the mock, while in *ptc-3(RNAi)* treated animals, they also accumulate in the cell center. Late endosomes, labeled with mCherry::RAB-7, are altered in *ptc-3(RNAi)*, showing accumulation and partial colocalization with GFP::RAB-5. Scale bar 10μm. (**C**) TEM images showing unidentified enlarge round-shaped structures upon *ptc-3(RNAi)* in the *C. elegans* gut.

4.1.2.3 Effect of PTC-3 in the recycling

One explanation for the expansion of the endocytic compartments upon *ptc-3(RNAi)* could be that recycling to the plasma membrane is defective and cargoes would accumulate in early and late endosomes. To test this hypothesis, we determined the effect of *ptc-3(RNAi)* on recycling endosomes, which can be labeled by either RAB-11 or RAB-10. RAB-10 is present in basolateral recycling endosomes, and RAB-11 is responsible for apical recycling in the worm gut [195,196]. In mock-treated worms, RAB-11 positive recycling endosomes localize near the apical membrane. This localization was not altered after the knockdown (Fig. 4.1.3), indicating that recycling to the PM is not impaired. Still, it was possible that the basolateral recycling was affected. Therefore, we tested the effect of PTC-3 depletion on the basolateral recycling marker RFP::RAB-10, which localizes in the middle part of the cell in mock-treated animals. *ptc-3(RNAi)* does not affect RAB-10 distribution

(Fig. 4.1.3). These data indicate that PTC-3 might be affecting the endosomal pathway without disturbing recycling. Thus, it is likely that the PTC-3 function affects endosomal maturation.

We propose that the effects on traffic could be a consequence of the alteration in the properties of membranes. However, more work is needed to address which is the precise distribution of cholesterol in different intracellular membranes, and which role is it playing in the regulation of diverse cellular processes such as traffic and signaling.

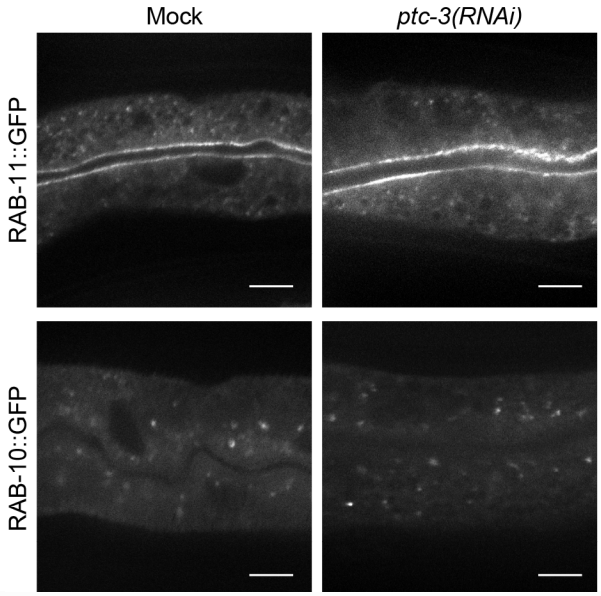

Figure 4.1.3. *ptc-3(RNAi)* induces no effect on recycling in the intestine. *ptc-3(RNAi)* in animals expressing GFP::RAB-11 or RFP::RAB-10 in the worm gut. RAB-11 positive endosomes localize near the apical membrane. GFP::RAB-11 and RFP::RAB-10 are not altered under RNAi conditions. Scale bars 10 μm

4.1.2.4 Effect of fatty acid acyl chain length manipulation in the endosomal pathway.

Given the effect of PTC-3 on fatty acid acyl chain length and desaturation, we hypothesize that part of the changes that we observe in the PTC-3 knockdown might be related to the changes in membrane properties. We reasoned that by affecting FA saturation levels, we might be able to mimic the effects of *ptc-3(RNAi)* on early and late endosomes. Fatty acid elongases and desaturases regulate FA acyl chain length and saturation. Thus, we performed knockdowns of the nematode homologs of the stearoyl-CoA desaturase (fat-5 and 7) or fatty acid elongases (elo-4). Under those conditions, the RAB-5 compartment showed no overlap with RAB-7 (Fig. 4.1.4) Nevertheless, we could observe that in all cases, RAB- 7 localization is altered, showing a similar phenotype as in *ptc-3(RNAi)* (Fig. 4.1.4). Consequently, the effects observed in the RAB-7 positive endosomes might be related to the alterations of FA properties, but cholesterol accumulation might be playing a central role in the RAB-5 phenotype. Hitherto, the specific cholesterol amounts and FA length and

saturation levels in each endosomal compartment are not known, and their potential role of them remains to be studied.

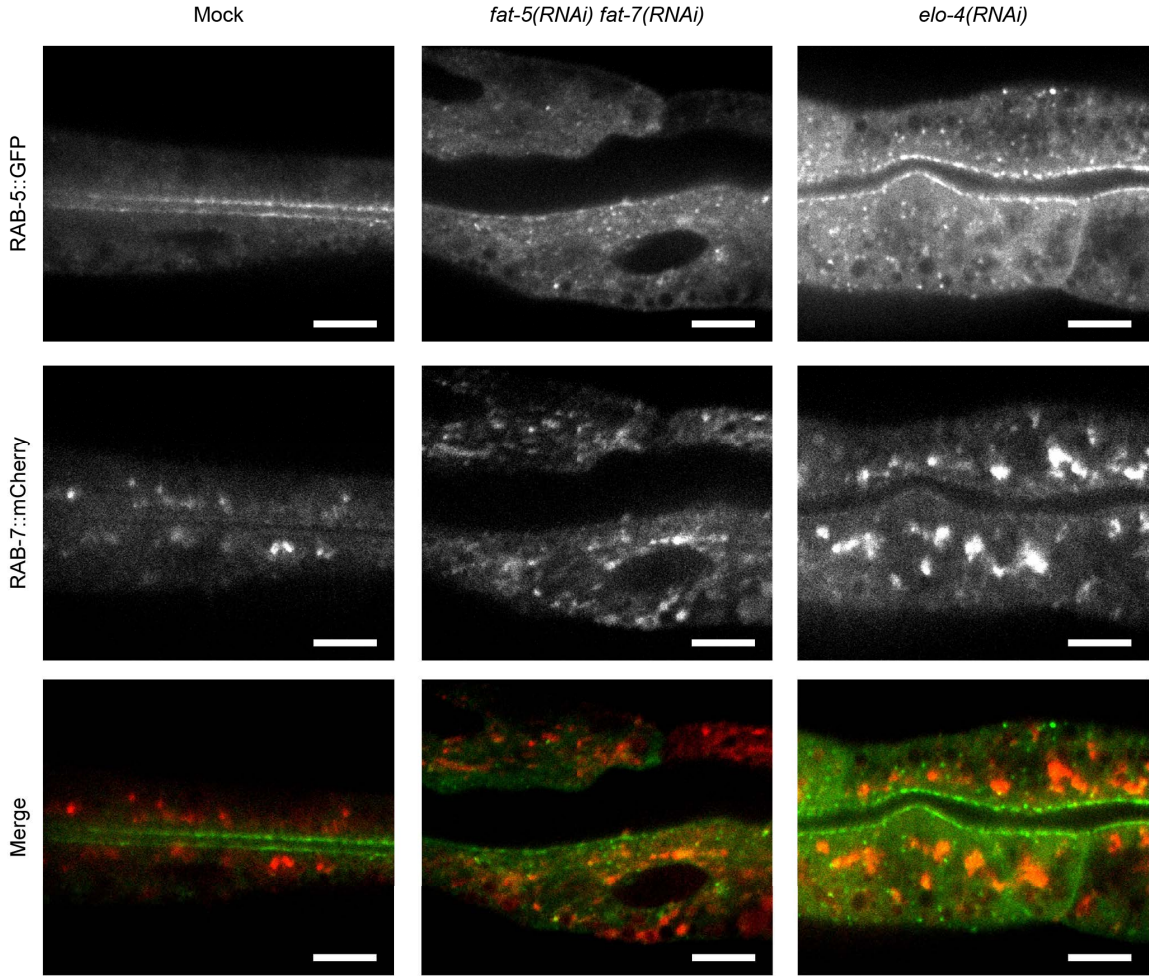

Figure 4. 4. Fatty acid acyl chain composition affects late endosomes localization. fat-5*(RNAi)fat-7(RNAi)* or *elo-4(RNAi)* in animals expressing GFP::RAB-5 and mCherry::RAB-7 in the intestine. Early endosomes labeled with GFP::RAB-5 occasionally relocate to the middle cell region. Late endosomes labeled with mCherry::RAB-7 showed an accumulation and sporadic colocalization with GFP::RAB-5 upon the RNAi treatments mimicking partially the effect of PTC-3 depletion. Scale bars 10 μm

4.1.3 Discussion and outlook

Our results, together with the first analysis of the worm PTC homologs [73], support the idea that the PTC proteins function as regulators of intracellular trafficking. The data on *ptc-3(RNAi)* effects in the endocytic pathway not only provides the basis for the hypothesis that the regulation of traffic is a conserved function of PTCH proteins but also adds the notion that this effect is due to the cholesterol content regulation. Still, the specific function of the PTC proteins in intracellular trafficking is not known. It is tempting to speculate that the genetic interaction between SAND-1 and PTC-3 is related to the regulation of the kinetics of the internalization and further degradation of specific cargoes such as receptors of other signaling pathways (e.g., WNT, EGF). Additional research is fundamental to address their particular roles by studying if they have an impact on specific cargoes. It would be of relevance to learn if PTC-3 is localized to caveolae as the fly homolog PTC1 [190] and whether this localization is cholesterol-dependent.

Since a way to regulate signaling is by the internalization of receptors, and there is considerable evidence of crosstalk mechanisms between the Hh, WNT, and EGF pathways during development [106,197]. The receptor Frizzled (WNT receptor) and EGFR constitute appealing cargoes to analyze. For example, in the absence of the EGF, a considerable proportion of EGFR is located at caveolae and non-caveolae rafts. Upon binding EGF, the EGFRs leave the rafts and initiate a MAP kinase-signaling cascade and are subsequently endocytosed. Interestingly, EGFR endocytosis constitutes an attenuation mechanism and also triggers specific activation of signaling (reviewed in [198]). Additionally, the Wnt signaling pathway is regulated at multiple levels through endocytic processes (reviewed in [199]). Due to the high importance of these pathways in normal development, it is critical to analyze the exact impact of PTCH function in the regulation of these pathways in a mechanism that is related to cholesterol and endocytic modulation.

4.1.4 Materials and Methods

4.1.4.1 General *C. elegans* methods and strains

C. elegans nematodes were cultured and maintained as described previously[120] and as described in chapter 3.1.5.1. For the analysis of the effects on endocytosis, the following *C. elegans* strains and transgenes were used: N2, *sand-1(ok1963)*IV, pwIs429[vha-6::mCherry-rab-7], pwIs72[vha6p::GFP::rab-5 + unc-119(+)], unc-119(ed3) III; pwIs69[vha6p::GFP::rab-11 + unc-119(+)], unc-119(ed3)III; pwIs206[vha6p::GFP::rab-10 + Cb unc-119(+)].

4.1.4.2 Microscopy

Live worms were immobilized with 50 mM levamisole in M9 and mounted on a slide with 2% agarose. The analysis of the endocytic compartments was performed with a spinning-disk confocal system Andor Revolution (Andor Technologies, Belfast, Northern Ireland) mounted onto an IX-81 inverted microscope (Olympus, Center Valley, PA) equipped with an iXonEM+ electron-multiplying charge-coupled device camera (Andor Technologies). Specimens were imaged using a 63X/1.42 numerical aperture oil objective. Each pixel represents 0.107 µm. Excitation is achieved using solid-state 488- and 560-nm lasers. The exposure time was 100 ms. Images were all processed with OMERO in the same way for corresponding experiments.

5. General discussion and outlook

This thesis addressed the molecular mechanism and biological relevance of an essential and non-canonical Hh signaling pathway. The study of the Hh non-canonical pathway has been difficult due to the essential role of the different pathway components in development. To uncover the mechanism by which PTCH inhibits SMO took almost 50 years of research, and just now, we can start exploring whether this is a shared mechanism to target other membrane proteins and processes. For instance, it was not until 2018 that PTCH's cholesterol-dependent mechanism could be irrefutably proven *in vitro* [90]. One reason for the slow study of PTCH function is that the receptor PTCH is a large multipass transmembrane transporter-like protein that is highly insoluble, and it was not until significant advances in Cryo-EM were made that its structure could be resolved in 2018 [85,87,88]. Nevertheless, significant advances have been made, the implications of PTCH mediated membrane cholesterol modulation, additionally to SMO regulation, are mysterious. Furthermore, the effect of PTCH's cholesterol regulation in non-canonical pathways is not known.

There is substantial evidence that PTCH and Hh proteins can have an impact on cell physiology, diseases, and development independently of the canonical Hh pathway [41,52,53,55,57,200]. Importantly, it is already demonstrated that in the case of SMO, the consequences of PTCH action can be reflected in a long-distance range. Moreover, the PTCH effect can be detected in a non-cell autonomous manner [59]. Therefore, it is plausible that there are other targets of PTCH, which have escaped discovery, because, as SMO, they may lack physical interaction with PTCH making their identification difficult.

The study of SMO-independent effects has long been under-investigated due to the lack of a proper system to study it. Furthermore, PTCH function as a cholesterol modulator *in vivo* has merely been addressed in the situation of individual cells, but not in the context of a whole organism. This has generated a lack of knowledge in the context of a complex system where cells need to communicate and respond accordingly to specific developmental requirements. As a consequence, there was the need to establish a system in which the intrinsic function of PTCH proteins as cholesterol regulators is conserved, but the action of SMO is dispensable. *C. elegans* is just the perfect system for these type o studies.

5.1 *C. elegans* as a model organism to study PTCH functions independently of SMO.

The worm lacks a canonical Hh-SMO pathway, but the action of the PTCH homologs is essential for worm survival and development. It has been proposed that the SMO signaling axis of the Hh pathway was originally part of a sterol homeostasis pathway [58]. Therefore, there is the possibility that PTCH has initially regulated other cellular functions, yet, this has not been addressed before [75]. To deeply analyze this possibility, we used the nematode *C. elegans* in which the Hedgehog pathway is not fully conserved. However, the action of the PTCH homologs is crucial for worm development and survival [72]. For that reason, it is expected that nematodes have SMO independent targets. Here, we evaluated the role of the essential PTCH homologs PTC-3, as well as the PTCH related protein PTR-4, as a way to learn more about the PTCH functions independently of SMO. We studied two crucial aspects of PTCH mediated cholesterol regulation. First, the consequences of cholesterol regulation by PTCH during development and second, PTCH role in a SMO independent manner in an intact organism. Our results not only support the finding that PTCH proteins' main action involves its ability to transport sterols [77,85,89,91,201]. Additionally, they strongly advocate that regulation of membrane cholesterol is a conserved action mechanism in PTCH proteins. To our knowledge, our data demonstrate for the first time that a PTCH protein functions as a cholesterol modulator in the context of a whole animal.

The use of the nematode as a model organism to study the role of cholesterol accumulation provided us with several advantages. For instance, we could affect the levels of PTC-3 and PTR-4 during development without ultimately impairing growth thanks to the RNAi feeding scheme. This timed RNAi manipulation allowed us to find phenotypes that arise during the late developmental stages. The use of *C. elegans* in forthcoming studies of PTCH would allow researchers to combine general techniques as lipidomics with tissue-specific knockdown and cholesterol detection. In the future, these techniques can help not just to determine the role of different PTCH proteins in the cells but also to look for other targets, as well, to assess more precisely the cholesterol regulation dependent on PTCH proteins and their influence during development in different tissues and cellular structures. Furthermore, with this thesis, we demonstrated that the nematode is an excellent model to study the function of PTCH in cell physiology and animal development.

5.2 PTCH homologs in *C. elegans* and its conserved function.

Since the molecular function of PTCH proteins has been linked to membrane cholesterol regulation, the phenotypes observed in the PTC and PTR homologs mutants

and knockdown in *C. elegans* are likely cholesterol-dependent [77,87–89]. Our data suggest that PTR-4 has cholesterol regulatory capabilities strongly suggesting that, indeed, the role of PTR proteins as cholesterol regulators is conserved (Section 3.2.3.2).

In *C. elegans*, cholesterol is a crucial molecule for the regulation of larval development. Subsequently, the worm must have evolved a way to regulate cholesterol levels in specific tissues and organelles. In contrast to mammals, nematodes are unable to synthesize cholesterol [116]. Therefore, modulation of cholesterol transport and localization controls cholesterol levels, both at the level of tissues and subcellular compartments. In *C. elegans*, PTC and PTR proteins have been expanded and are not redundant [72]. We hypothesize that the individual function of these proteins has not changed, but rather the numerous homologs of PTCH proteins and their fine-tuned expression pattern during development enable the worms to finely regulate levels of cholesterol and perhaps other derived sterols locally and temporally.

5.3 Role of PTC-3 regulating the membrane structure and its possible impact on cell signaling and physiology

The lack of PTCH proteins or its inhibition originates an accumulation of cholesterol at the plasma membrane, which could alter its physicochemical properties. Worms cannot store cholesterol in intestinal lipid droplets [97,202–204]. Therefore, the excess of cholesterol originated by the *ptc-3(RNAi)* cannot be esterified and stored. As a consequence, it accumulates in the membranes and alters their structure to a great extent (Section 3.1.3.5 and 3.1.3.6).

A major question of the effect we observed upon *ptc-3(RNAi)* in the ER structure is that we find PTC-3 located in the apical membrane and not in the ER membrane (Section 3.1.3.1 and 3.1.3.5), as well, we mainly detect cholesterol accumulation at the apical membrane (Section 3.1.3.2). Therefore, the direct involvement of PTC-3 in the regulation of the ER structure might be seen as an inconsistency. It is important to remember that cholesterol can travel from the plasma membrane to the ER and from the ER to other organelles by non-vesicular transport [205–207]. Therefore, even if we observed PTC-3 mainly at the apical plasma membrane, the effect on ER morphology could be a direct consequence of cholesterol accumulation in the ER membrane, because the whole-cell cholesterol levels are likely affected. The fluidity and flexibility of cellular membranes may be altered upon *ptc-3(RNAi),* which could contribute to the broad range of phenotypes observed in the RNAi worms (Section 3.1.3.2). Additionally, the effects observed in the endosomal pathway may be related to this cholesterol imbalance. This may cause altered membrane properties in early endosomes (Section 4.1.2.4). The positive effect in worm

development at higher temperature (25°C) in the *ptc-3(RNAi)* animals supports these hypotheses.

5.4 Role of PTC-3 regulating metabolism

Deregulation of lipid and cholesterol homeostasis has major importance on development and disease for all eukaryotes [111]. Cholesterol is used by cells not only with structural means but also is essential for signaling, namely, to regulate fatty acid metabolism and hormone signaling [112,113,208,209]. In this thesis, we found that the deregulation of cholesterol homeostasis as a consequence of *ptc-3(RNAi)* affects FA metabolism (Section 3.1.3.6). The role of PTCH proteins in the regulation of general lipid metabolism has been previously suggested in mammals, *Drosophila*, and *C. elegans* [78,140,155,210]. The orthologs of SMO, FUS, SUFU, and COS were not conserved in *C. elegans* during evolution [49,71]. Consequently, we believe that the FA regulation mediated by the PTCH could be an ancestral function of the Hh pathway. Thus, we propose that PTCH proteins could generally regulate FA metabolism in a cholesterol-dependent manner, but in a SMO-independent mechanism.

Sterols have been associated with the regulation of FA metabolism alongside with NHRs in both mammals and nematodes[108,109,111]. In vertebrates, NHRs act as lipid sensors to regulate fatty acid and cholesterol metabolism [128]. It is important to note that in the worm, NHRs underwent a vast expansion; consequently, it is not unexpected to find a connection between the worm NHR's expansion and the unique and robust regulation of energy metabolism and metabolic adaptation required by *C. elegans* during development. As mentioned earlier, the function of many NHR family members remains elusive. Levels of lipid storage correlate to levels of different NHRs. NHR-8 and NHR-49 have been shown to have a positive impact on lipid desaturation and accumulation, while DAF-12 and NHR-25 diminish lipid storage [109,111,148,211]. There are fifteen NHRs with clear homologs in other species, while from an ancestral HNF4, the other 279 receptors arose [128,212]. The role of some of them, such as NHR-23, NHR-25, NHR-41, and NHR-67, is related to the control of molting while the function of many others remains elusive. Furthermore, NHR-181 has been described to interact physically with NHR-49 [129,130]. We hypothesized that in *ptc-3(RNAi)* animals NHR-181 could be contending with NHR-80 for NHR-49 interaction (Section 3.1.3.8). Potentially, the modification in FA length and saturation levels could directly affect NHR-181 and NHR-49 since both are homologs of PPARα, which has been described to bind saturated and cis-monounsaturated C14-18 fatty acids constitutively [213].

Additionally, NHR-49 can upregulate genes related to beta-oxidation, fatty acid desaturation, lipid transport, and synthesis of monomethyl branched fatty acids, presumably

in a mechanism dependently on its interaction partner [110,148,149,214,215]. Alternative, NHR-181 could be competing with NHR-49 for the unsaturated FA impairing its activation. A third possibility is that NHR functionality and levels are part of a regulatory process that is altered by the direct binding of cholesterol. More experiments are needed to elucidate the real scenario and the precise mechanism by which *ptc-3(RNAi)* mediated cholesterol accumulation alters NHR signaling.

Another process that could be modulated by PTC-3 is the entry to the dauer stage. As expected, energy metabolism exhibits different patterns between reproductively growing larvae and diapaused animals. During reproductive growth, larvae display aerobic metabolism, and it converts dietary nutrients into acetyl-CoA, which enters the TCA cycle and continues to oxidative phosphorylation. The nuclear hormone receptor DAF-12 besides having a role in the decision between growth and dauer stage, is a central regulator of energy metabolism, capable of the induction of aerobic fat utilization[127], providing another possible link between cholesterol signaling imbalanced as a consequence of PTC-3 knockdown and FA metabolism (Section 3.1.3.6). Interestingly, without PUFAs, worms become more sensitive to low cholesterol levels arresting at higher rates [216]. Still, it is not clear how PUFAs and cholesterol levels synergize during worm development to regulate signaling. Importantly we have uncovered that PTC-3 action is necessary for proper PUFA levels (Section 3.1.3.6). Though, it remains to be addressed whether PTC-3 is directly coupled to the regulation of such a process.

5.5 Cholesterol analysis *in vivo*

During this project, we faced the challenge of studying the levels of cholesterol *in situ*. The analysis of cholesterol distribution and transport *in vivo* has been difficult due to the shortage of technical means to study it. One approach is to visualize cholesterol through the use of fluorescent analogs. Nevertheless, a challenge is the lack of analogs with both suitable brightness and physical-chemical properties similar to the ones of cholesterol. The detection problems prompted the need to develop new tools. Consequently, cholesterol sensors based on fragments of cholesterol-binding toxins were developed. For example, Perfringolysin O (PFO) is a protein secreted by the Gram-positive anaerobe *Clostridium perfringens* that binds to cholesterol [143]. The domain 4 (D4) of PFO is enough to bind cholesterol without the cytotoxicity of the toxin. It is a 13 kDa protein which associates with cholesterol in membranes through four connecting loops. The expression of the D4, in combination with fluorescent proteins such as mCherry, allows cholesterol detection in living cells. Wild type versions of the D4 need at least 30 mol % of cholesterol for binding to membranes, which for several systems is beyond the average concentration. To solve

that problem, mutations aiming to decrease the threshold for cholesterol-binding to the D4 have been developed [143,144].

To study *in vivo* cholesterol accumulation upon PTC-3 depletion. We have taken advantage of the high-affinity mutant versions of the D4 fused to mCherry to implement the use of genetically encoded tissue-specific cholesterol sensors in living nematodes (Section 3.1.3.2). This combination of a D4 that is fluorescently-tag and more sensitive allowed us to study the localization *in vivo* of cholesterol in one specific tissue. Furthermore, these sensors could be used with other tissue-specific promoters and fluorescently tag proteins. This system could be expanded to other tissues and developmental stages, allowing for the first time to monitor cholesterol localization and enrichments during the development of a multicellular organism.

5.6 From linear pathways to real complex networks: *C. elegans* as an model to address the crosstalk between PTCH and other developmental signaling cascades

During development, there is extensive crosstalk between multiple developmental signaling pathways, which indicates that signaling is more a complex network of interactions than the classical linear depiction of individual pathways. There is evidence of the existence of crosstalk between the Hh, WNT, and EGF pathways at different levels. Imbalance of their regulation plays a role in developmental and cancer-associated processes. For example, in mammals, alterations in membrane cholesterol levels can have an impact on a vast number of cellular processes like development and cancer via activation of the WNT and EGF pathway [106,197]. Consequently, membrane cholesterol regulation by PTCH proteins is a crucial crosstalk mechanism that remains widely unexplored [217–219]. For instance, a way to regulate receptor activity is through the internalization of them. Consequently, it would be of great importance to analyze the impact of PTCH cholesterol modulation in the localization of receptors of the central developmental pathways as Frizzled for the Wnt pathway, Notch, and EGFR. It is important to notice that in most animals, currently, it is not possible to affect PTCH cholesterol regulation without affecting SMO regulation. Importantly, while the nematode lacks the Hh canonical pathway, it has a conserved WNT signaling pathway. Therefore, the worm is the perfect model to overcome that problem. We believe that this work has contributed to establish *C. elegans* as a crucial organism to disentangle such complex crosstalk.

6. Abbreviation Index

7-dehydrocholesterol	7-DHC
Coherent anti-Stokes Raman Scattering Microscopy	CARS
Costal 2	Cos2
Cubitus interruptus	Ci
Dafachronic acid	DA
Dehydroergosterol	DHE
Desert hedgehog	DHH
Domain 4 of PFO	D4
Double-stranded RNA	dsRNA
Endoplasmic reticulum	ER
Extracellular matrix	ECM
Fatty acids	FA
Focused ion beam scanning electron microscopy	FIB-SEM
Fused	Fu
G-protein coupled receptor	GPCR
Groundhog	GRD
Groundhog-like	GRL
Hedgehog	Hh
Indian hedgehog	IHH
Interference RNA	RNAi
Low-density lipoproteins	LDL
Lysosome-related organelles	LROs
Mono-unsaturated fatty acid acyl chains	MUFAs
Niemann-Pick type C 1	NPC1
Nuclear hormone receptors	NHRs
PTCH domain-containing proteins	PTCHD
Patched-related proteins	PTR
Perfringolysin O	PFO
Poly unsaturated fatty acids	PUFAs
PTCH proteins	PTC
Quahog	QUA
Resistance-nodulation division transporters	RND
Smoothened	SMO
Sonic hedgehog	SHH
Sterol O-acyltransferase 1	SOAT1

Sterol regulatory element-binding proteins	SREBPs
Sterol-sensing domain	SSD
Suppressor of Fused	SuFu
Ultraviolet	UV
Warthog	WRT
Zona pellucida	ZP

7. Figure Index

8. References

1. De Kruif, P. *Microbe hunters*. (Harcourt Brace, 1996).
2. Gilbert, S. F. *The Questions of Developmental Biology*. *Developmental Biology* (Sinauer Associates, 2005).
3. Willis, Robert, 1799-1878. *The works of William Harvey*. (London : Printed for the Sydenham Society, 1847).
4. Gilbert, S. F. Comparative Embryology. in *Developmental Biology.* (Sunderland (MA): Sinauer Associates, 2000).
5. Schmitt, S. From eggs to fossils: epigenesis and transformation of species in Pander's biology. *Int. J. Dev. Biol.* **49**, 1–8 (2005).
6. Alberts, B. *et al.* Universal Mechanisms of Animal Development. in *Molecular Biology of the Cell* (Garland Science, 2002).
7. Observables upon a monstrous head. *Philos. Trans. R. Soc. London* **1**, 85–86 (1665).
8. Chiang, C. *et al.* Cyclopia and defective axial patterning in mice lacking Sonic hedgehog gene function. *Nature* **383**, 407–413 (1996).
9. Ingham, P. W., Nakano, Y. & Seger, C. Mechanisms and functions of Hedgehog signalling across the metazoa. *Nat. Rev. Genet.* **12**, 393–406 (2011).
10. Ellis, H. M. & Horvitz, H. R. Genetic control of programmed cell death in the nematode C. elegans. *Cell* **44**, 817–829 (1986).
11. Fire, A. *et al.* Potent and specific genetic interference by double-stranded RNA in caenorhabditis elegans. *Nature* **391**, 806–811 (1998).
12. Goldstein, B. Sydney Brenner on the Genetics of Caenorhabditis elegans. *Genetics* **204**, 1–2 (2016).
13. C. elegans Sequencing Consortium. Genome sequence of the nematode C. elegans: a platform for investigating biology. *Science* **282**, 2012–8 (1998).
14. Frézal, L. & Félix, M.-A. C. elegans outside the Petri dish. *Elife* **4**, (2015).
15. Stinchcomb, D. T., Shaw, J. E., Carr, S. H. & Hirsh, D. Extrachromosomal DNA transformation of Caenorhabditis elegans. *Mol. Cell. Biol.* **5**, 3484–3496 (1985).
16. Evans, T. Transformation and microinjection. *WormBook* (2006). doi:10.1895/wormbook.1.108.1
17. Wang, J. & Barr, M. M. RNA Interference in Caenorhabditis elegans. *Methods Enzymol.* **392**, 36–55 (2005).
18. Soloviev, A., Gallagher, J., Marnef, A. & Kuwabara, P. E. C. elegans patched-3 is an

essential gene implicated in osmoregulation and requiring an intact permease transporter domain. *Dev. Biol.* **351**, 242–253 (2011).

19. Corsi, A. K., Wightman, B. & Chalfie, M. Caenorhabditis elegans. (2015). doi:10.1895/wormbook.1.177.1
20. Ingham, P. W. & McMahon, A. P. Hedgehog signaling in animal development: Paradigms and principles. *Genes and Development* **15**, 3059–3087 (2001).
21. Ruiz *et al.* Hedgehog-GLI signaling and the growth of the brain. *Nat Rev Neurosci* **3**, 24–33 (2002).
22. Nüsslein-Volhard, C. & Wieschaus, E. Mutations affecting segment number and polarity in Drosophila. *Nature* **287**, 795–801 (1980).
23. Machold, R. & Fishell, G. Hedgehog patterns midbrain ARChitecture. *Trends Neurosci.* **25**, 10–1 (2002).
24. Agarwala, S., Sanders, T. A. & Ragsdale, C. W. Sonic hedgehog control of size and shape in midbrain pattern formation. *Science (80-.).* **291**, 2147–2150 (2001).
25. Jia, J. & Jiang, J. Decoding the Hedgehog signal in animal development. *Cell. Mol. Life Sci.* **63**, 1249–65 (2006).
26. Ashe, H. L. & Briscoe, J. The interpretation of morphogen gradients. *Development* **133**, 385–394 (2006).
27. Ingham, P. W. & McMahon, A. P. Hedgehog signaling in animal development: paradigms and principles. *Genes Dev* **15**, 3059–3087 (2001).
28. Ma, Y. *et al.* The relationship between early embryo development and tumourigenesis. *J. Cell. Mol. Med.* **14**, 2697–2701 (2010).
29. Madison, B. B., McKenna, L. B., Dolson, D., Epstein, D. J. & Kaestner, K. H. FoxF1 and FoxL1 Link Hedgehog Signaling and the Control of Epithelial Proliferation in the Developing Stomach and Intestine. *J. Biol. Chem.* **284**, 5936–5944 (2009).
30. Nielsen, C. M., Williams, J., van den Brink, G. R., Lauwers, G. Y. & Roberts, D. J. Hh pathway expression in human gut tissues and in inflammatory gut diseases. *Lab. Invest.* **84**, 1631–1642 (2004).
31. Hahn, H. *et al.* A mammalian patched homolog is expressed in target tissues of sonic hedgehog and maps to a region associated with developmental abnormalities. *J. Biol. Chem.* **271**, 12125–8 (1996).
32. Hahn, H. *et al.* Mutations of the human homolog of Drosophila patched in the nevoid basal cell carcinoma syndrome. *Cell* **85**, 841–51 (1996).
33. Ruiz i Altaba, A. & i Altaba, A. Gli proteins and Hedgehog signaling: development and cancer. *Trends Genet* **15**, 418–425 (1999).
34. Goodrich, L. V & Scott, M. P. Hedgehog and patched in neural development and

disease. *Neuron* **21**, 1243–57 (1998).

35. Boyd, A. L., Salci, K. R., Shapovalova, Z., McIntyre, B. A. S. & Bhatia, M. Nonhematopoietic cells represent a more rational target of in vivo hedgehog signaling affecting normal or acute myeloid leukemia progenitors. *Exp. Hematol.* **41**, 858-869.e4 (2013).
36. Zhao, C. *et al.* Hedgehog signalling is essential for maintenance of cancer stem cells in myeloid leukaemia. *Nature* **458**, 776–779 (2009).
37. Park, K.-S. *et al.* A crucial requirement for Hedgehog signaling in small cell lung cancer. *Nat. Med.* **17**, 1504–8 (2011).
38. Bar, E. E. *et al.* Cyclopamine-Mediated Hedgehog Pathway Inhibition Depletes Stem-Like Cancer Cells in Glioblastoma. *Stem Cells* **25**, 2524–2533 (2007).
39. Pelczar, P. *et al.* Inactivation of Patched1 in Mice Leads to Development of Gastrointestinal Stromal-Like Tumors That Express Pdgfrα but Not Kit. *Gastroenterology* **144**, 134-144.e6 (2013).
40. Jia, Y., Wang, Y. & Xie, J. The Hedgehog pathway: role in cell differentiation, polarity and proliferation. *Arch. Toxicol.* **89**, 179–91 (2015).
41. Hasanovic, A. & Mus-Veteau, I. Targeting the Multidrug Transporter Ptch1 Potentiates Chemotherapy Efficiency. *Cells* **7**, 107 (2018).
42. Berlin, J. *et al.* A randomized phase II trial of vismodegib versus placebo with FOLFOX or FOLFIRI and bevacizumab in patients with previously untreated metastatic colorectal cancer. *Clin. Cancer Res.* **19**, 258–67 (2013).
43. Catenacci, D. V. T. *et al.* Randomized Phase Ib/II Study of Gemcitabine Plus Placebo or Vismodegib, a Hedgehog Pathway Inhibitor, in Patients With Metastatic Pancreatic Cancer. *J. Clin. Oncol.* **33**, 4284–92 (2015).
44. Briscoe, J. & Thérond, P. P. The mechanisms of Hedgehog signalling and its roles in development and disease. *Nat. Rev. Mol. Cell Biol.* **14**, 416–429 (2013).
45. Palm, W. *et al.* Secretion and Signaling Activities of Lipoprotein-Associated Hedgehog and Non-Sterol-Modified Hedgehog in Flies and Mammals. *PLoS Biol.* **11**, e1001505 (2013).
46. Khaliullina, H. *et al.* Patched regulates Smoothened trafficking using lipoprotein-derived lipids. *Development* **136**, 4111–4121 (2009).
47. Panáková, D., Sprong, H., Marois, E., Thiele, C. & Eaton, S. Lipoprotein particles are required for Hedgehog and Wingless signalling. *Nature* **435**, 58–65 (2005).
48. Von Ohlen, T., Lessing, D., Nusse, R. & Hooper, J. E. Hedgehog signaling regulates transcription through cubitus interruptus, a sequence-specific DNA binding protein. *Proc. Natl. Acad. Sci. U. S. A.* **94**, 2404–9 (1997).

49. Bürglin, T. R. & Kuwabara, P. E. Homologs of the Hh signalling network in C. elegans. *WormBook* 1–14 (2006).
50. Simpson, F., Kerr, M. C. & Wicking, C. Trafficking, development and hedgehog. *Mech. Dev.* **126**, 279–288 (2009).
51. Cayuso, J., Ulloa, F., Cox, B., Briscoe, J. & Marti, E. The Sonic hedgehog pathway independently controls the patterning, proliferation and survival of neuroepithelial cells by regulating Gli activity. *Development* **133**, 517–528 (2006).
52. Gu, D. & Xie, J. Non-Canonical Hh Signaling in Cancer-Current Understanding and Future Directions. *Cancers (Basel).* **7**, 1684–98 (2015).
53. Brennan, D., Chen, X., Cheng, L., Mahoney, M. & Riobo, N. A. Noncanonical Hedgehog signaling. *Vitam. Horm.* **88**, 55–72 (2012).
54. Szczepny, A. *et al.* The role of canonical and non-canonical Hedgehog signaling in tumor progression in a mouse model of small cell lung cancer. *Oncogene* **36**, 5544–5550 (2017).
55. Jenkins, D. Hedgehog signalling: emerging evidence for non-canonical pathways. **21**, 1023–1034 (2009).
56. Chang, H., Li, Q., Moraes, R. C., Lewis, M. T. & Hamel, P. A. Activation of Erk by sonic hedgehog independent of canonical hedgehog signalling. *Int. J. Biochem. Cell Biol.* **42**, 1462–1471 (2010).
57. Regan, J. L. *et al.* Non-Canonical Hedgehog Signaling Is a Positive Regulator of the WNT Pathway and Is Required for the Survival of Colon Cancer Stem Cells. *Cell Rep.* **21**, 2813–2828 (2017).
58. Hausmann, G., von Mering, C. & Basler, K. The Hedgehog Signaling Pathway: Where Did It Come From? *PLoS Biol.* **7**, e1000146 (2009).
59. Roberts, B., Casillas, C., Alfaro, A. C., Jägers, C. & Roelink, H. Patched1 and Patched2 inhibit Smoothened non-cell autonomously. *Elife* **5**, (2016).
60. Fleet, A. J. & Hamel, P. A. Protein-specific activities of the transmembrane modules of Ptch1 and Ptch2 are determined by their adjacent protein domains. *J. Biol. Chem.* jbc.RA118.004478 (2018). doi:10.1074/jbc.RA118.004478
61. Hu, M. C. C. *et al.* GLI3-dependent transcriptional repression of Gli1, Gli2 and kidney patterning genes disrupts renal morphogenesis. *Development* **133**, 569–578 (2006).
62. Lipinski, R. J., Gipp, J. J., Zhang, J., Doles, J. D. & Bushman, W. Unique and complimentary activities of the Gli transcription factors in Hedgehog signaling. *Exp. Cell Res.* **312**, 1925–1938 (2006).
63. Ung, D. C. *et al.* Ptchd1 deficiency induces excitatory synaptic and cognitive dysfunctions in mouse. *Mol. Psychiatry* **23**, 1356–1367 (2018).

64. Torrico, B. *et al.* Contribution of common and rare variants of the PTCHD1 gene to autism spectrum disorders and intellectual disability. *Eur. J. Hum. Genet.* **23**, 1694–1701 (2015).
65. Chaudhry, A. *et al.* Phenotypic spectrum associated with *PTCHD1* deletions and truncating mutations includes intellectual disability and autism spectrum disorder. *Clin. Genet.* **88**, 224–233 (2015).
66. Huerta-Cepas, J., Bueno, A., Dopazo, J. & Gabaldón, T. PhylomeDB: a database for genome-wide collections of gene phylogenies. *Nucleic Acids Res.* **36**, D491-6 (2008).
67. Huerta-Cepas, J., Capella-Gutiérrez, S., Pryszcz, L. P., Marcet-Houben, M. & Gabaldón, T. PhylomeDB v4: zooming into the plurality of evolutionary histories of a genome. *Nucleic Acids Res.* **42**, D897-902 (2014).
68. Li, H. *et al.* TreeFam: a curated database of phylogenetic trees of animal gene families. *Nucleic Acids Res.* **34**, D572-80 (2006).
69. Ruan, J. *et al.* TreeFam: 2008 Update. *Nucleic Acids Res.* **36**, D735-40 (2008).
70. Huerta-Cepas, J., Capella-Gutiérrez, S., Pryszcz, L. P., Marcet-Houben, M. & Gabaldón, T. PhylomeDB v4: zooming into the plurality of evolutionary histories of a genome. *Nucleic Acids Res.* **42**, D897–D902 (2014).
71. Bürglin, T. R. Evolution of hedgehog and hedgehog-related genes, their origin from Hog proteins in ancestral eukaryotes and discovery of a novel Hint motif. *BMC Genomics* **9**, 127 (2008).
72. Zugasti, O., Rajan, J. & Kuwabara, P. E. The function and expansion of the Patched- and Hedgehog-related homologs in C. elegans. *Genome Res.* **15**, 1402–1410 (2005).
73. Kolotuev, I., Apaydin, A. & Labouesse, M. Secretion of Hedgehog-related peptides and WNT during Caenorhabditis elegans development. *Traffic* **10**, 803–810 (2009).
74. Aspöck, G., Kagoshima, H., Niklaus, G. & Bürglin, T. R. Caenorhabditis elegans has scores of hedgehog-related genes: sequence and expression analysis. *Genome Res.* **9**, 909–23 (1999).
75. Bürglin, T. R. The Hedgehog protein family. *Genome Biol.* **9**, 241 (2008).
76. Tseng, T. T. *et al.* The RND permease superfamily: an ancient, ubiquitous and diverse family that includes human disease and development proteins. *J. Mol. Microbiol. Biotechnol.* **1**, 107–25 (1999).
77. Myers, B. R., Neahring, L., Zhang, Y., Roberts, K. J. & Beachy, P. A. Rapid, direct activity assays for Smoothened reveal Hedgehog pathway regulation by membrane cholesterol and extracellular sodium. *Proc. Natl. Acad. Sci. U. S. A.* **114**, E11141--

E11150 (2017).

78. Lin, C.-C. J. J. & Wang, M. C. Microbial metabolites regulate host lipid metabolism through NR5A-Hedgehog signalling. *Nat. Cell Biol.* **19**, 550–557 (2017).
79. Hendriks, G.-J. J., Gaidatzis, D., Aeschimann, F. & Großhans, H. Extensive oscillatory gene expression during C. elegans larval development. *Mol. Cell* **53**, 380–392 (2014).
80. Chisholm, A. D. & Hsiao, T. I. The Caenorhabditis elegans epidermis as a model skin. I: Development, patterning, and growth. *Wiley Interdiscip. Rev. Dev. Biol.* **1**, 861–878 (2012).
81. Cao, J. *et al.* Comprehensive single-cell transcriptional profiling of a multicellular organism. *Science (80-.).* **357**, 661–667 (2017).
82. Kuwabara, P. E., Lee, M. H., Schedl, T. & Jefferis, G. S. X. E. A C. elegans patched gene, ptc-1, functions in germ-line cytokinesis. *Genes Dev.* **14**, 1933–1944 (2000).
83. Rohlfing, A.-K., Miteva, Y., Moronetti, L., He, L. & Lamitina, T. The Caenorhabditis elegans Mucin-Like Protein OSM-8 Negatively Regulates Osmosensitive Physiology Via the Transmembrane Protein PTR-23. *PLoS Genet.* **7**, e1001267 (2011).
84. Kelley, L. A., Mezulis, S., Yates, C. M., Wass, M. N. & Sternberg, M. J. E. The Phyre2 web portal for protein modeling, prediction and analysis. *Nat. Protoc.* **10**, 845–858 (2015).
85. Gong, X. *et al.* Structural basis for the recognition of Sonic Hedgehog by human Patched1. *Science* **361**, eaas8935+ (2018).
86. Schrodinger LLC. The PyMOL Molecular Graphics System, Version 1.8. (2015).
87. Qi, X., Schmiege, P., Coutavas, E. & Li, X. Two Patched molecules engage distinct sites on Hedgehog yielding a signaling-competent complex. *Science (80-.).* eaas8843+ (2018). doi:10.1126/science.aas8843
88. Qi, X., Schmiege, P., Coutavas, E., Wang, J. & Li, X. Structures of human Patched and its complex with native palmitoylated sonic hedgehog. *Nature* **560**, 128–132 (2018).
89. Bidet, M. *et al.* The hedgehog receptor patched is involved in cholesterol transport. *PLoS One* **6**, e23834+ (2011).
90. Zhang, Y. *et al.* Structural Basis for Cholesterol Transport-like Activity of the Hedgehog Receptor Patched. *Cell* **175**, 1352-1364.e14 (2018).
91. Huang, P. *et al.* Cellular Cholesterol Directly Activates Smoothened in Hedgehog Signaling. *Cell* **166**, (2016).
92. Luchetti, G. *et al.* Cholesterol activates the G-protein coupled receptor Smoothened to promote Hedgehog signaling. *Elife* **5**, (2016).

93. Taipale, J., Cooper, M. K., Maiti, T. & Beachy, P. A. Patched acts catalytically to suppress the activity of Smoothened. *Nature* **418**, 892–897 (2002).
94. Bangs, F. & Anderson, K. V. Primary cilia and Mammalian Hedgehog signaling. *Cold Spring Harb. Perspect. Biol.* **9**, (2017).
95. Weiss, L. E., Milenkovic, L., Yoon, J., Stearns, T. & Moerner, W. E. Motional dynamics of single Patched1 molecules in cilia are controlled by Hedgehog and cholesterol. *Proc. Natl. Acad. Sci. U. S. A.* **116**, 5550–5557 (2019).
96. Novillo, A., Won, S.-J., Li, C. & Callard, I. P. Changes in Nuclear Receptor and Vitellogenin Gene Expression in Response to Steroids and Heavy Metal in Caenorhabditis elegans. *Integr. Comp. Biol.* **45**, 61–71 (2005).
97. Choi, M.-K. *et al.* Maintenance of Membrane Integrity and Permeability Depends on a Patched-Related Protein in Caenorhabditis elegans. (2016). doi:10.1534/genetics.115.179705
98. Chitwood, D. J., Lusby, W. R., Lozano, R., Thompson, M. J. & Svoboda, J. A. Sterol metabolism in the nematodeCaenorhabditis elegans. *Lipids* **19**, 500–506 (1984).
99. SHIEH, H. S., HOARD, L. G. & NORDMAN, C. E. Crystal structure of anhydrous cholesterol. *Nature* **267**, 287–289 (1977).
100. Kumari, A. Cholesterol Synthesis. *Sweet Biochem.* 27–31 (2018). doi:10.1016/B978-0-12-814453-4.00007-8
101. Infante, R. E. & Radhakrishnan, A. Continuous transport of a small fraction of plasma membrane cholesterol to endoplasmic reticulum regulates total cellular cholesterol. *Elife* **6**, (2017).
102. Solanko, K. A., Modzel, M., Solanko, L. M. & Wüstner, D. Fluorescent Sterols and Cholesteryl Esters as Probes for Intracellular Cholesterol Transport. *Lipid Insights* **8**, 95–114 (2015).
103. Morales-Lázaro, S. L. & Rosenbaum, T. *Multiple Mechanisms of Regulation of Transient Receptor Potential Ion Channels by Cholesterol*. **80**, 139–161 (Academic Press, 2017).
104. Yao, Z.-G. *et al.* Regional and cell-type specific distribution of HDAC2 in the adult mouse brain. *Brain Struct. Funct.* 1–11 (2012). doi:10.1007/s00429-012-0416-3
105. Goossens, P. *et al.* Membrane Cholesterol Efflux Drives Tumor-Associated Macrophage Reprogramming and Tumor Progression. *Cell Metab.* (2019). doi:10.1016/j.cmet.2019.02.016
106. Sheng, R. *et al.* Cholesterol selectively activates canonical Wnt signalling over non-canonical Wnt signalling. *Nat. Commun.* **5**, 4393 (2014).
107. Brown, M. S. & Goldstein, J. L. The SREBP pathway: regulation of cholesterol

metabolism by proteolysis of a membrane-bound transcription factor. *Cell* **89**, 331–40 (1997).

108. Yang, F. *et al.* An ARC/Mediator subunit required for SREBP control of cholesterol and lipid homeostasis. *Nature* **442**, 700–704 (2006).
109. Mullaney, B. C. *et al.* Regulation of C. elegans fat uptake and storage by acyl-CoA synthase-3 is dependent on NR5A family nuclear hormone receptor nhr-25. *Cell Metab.* **12**, 398–410 (2010).
110. Taubert, S., Van Gilst, M. R., Hansen, M. & Yamamoto, K. R. A Mediator subunit, MDT-15, integrates regulation of fatty acid metabolism by NHR-49-dependent and -independent pathways in C. elegans. *Genes Dev.* **20**, 1137–1149 (2006).
111. Magner, D. B. *et al.* The NHR-8 nuclear receptor regulates cholesterol and bile acid homeostasis in C. elegans. *Cell Metab.* **18**, 212–224 (2013).
112. Sato, R. Sterol metabolism and SREBP activation. *Arch. Biochem. Biophys.* **501**, 177–181 (2010).
113. Shimano, H. Sterol regulatory element-binding proteins (SREBPs): Transcriptional regulators of lipid synthetic genes. *Progress in Lipid Research* **40**, 439–452 (2001).
114. Nomura, T., Horikawa, M., Shimamura, S., Hashimoto, T. & Sakamoto, K. Fat accumulation in Caenorhabditis elegans is mediated by SREBP homolog SBP-1. *Genes Nutr.* **5**, 17–27 (2010).
115. Walker, A. K. *et al.* A conserved SREBP-1/phosphatidylcholine feedback circuit regulates lipogenesis in metazoans. *Cell* **147**, 840–52 (2011).
116. Hieb, W. F. & Rothstein, M. Sterol requirement for reproduction of a free-living nematode. *Science (80-.).* **160**, 778–780 (1968).
117. Merris, M., Kraeft, J., Tint, G. S. & Lenard, J. Long-term effects of sterol depletion in C. elegans: sterol content of synchronized wild-type and mutant populations. *J. Lipid Res.* **45**, 2044–51 (2004).
118. Cheong, M. C. *et al.* A Potential Biochemical Mechanism Underlying the Influence of Sterol Deprivation Stress on *Caenorhabditis elegans* Longevity. *J. Biol. Chem.* **286**, 7248–7256 (2011).
119. Chitwood, D. J. & Lusby, W. R. Metabolism of plant sterols by nematodes. *Lipids* **26**, 619–627 (1991).
120. Brenner, S. The genetics of Caenorhabditis elegans. *Genetics* **77**, 71–94 (1974).
121. Matyash, V. *et al.* Distribution and transport of cholesterol in Caenorhabditis elegans. *Mol. Biol. Cell* **12**, 1725–36 (2001).
122. Matyash, V. *et al.* Sterol-Derived Hormone(s) Controls Entry into Diapause in Caenorhabditis elegans by Consecutive Activation of DAF-12 and DAF-16. *PLoS*

Biol. **2**, e280 (2004).

123. Motola, D. L. *et al.* Identification of Ligands for DAF-12 that Govern Dauer Formation and Reproduction in C. elegans. *Cell* **124**, 1209–1223 (2006).
124. Aguilaniu, H., Fabrizio, P. & Witting, M. The Role of Dafachronic Acid Signaling in Development and Longevity in Caenorhabditis elegans: Digging Deeper Using Cutting-Edge Analytical Chemistry. *Front. Endocrinol. (Lausanne).* **7**, 12 (2016).
125. Mahanti, P. *et al.* Comparative Metabolomics Reveals Endogenous Ligands of DAF-12, a Nuclear Hormone Receptor, Regulating C. elegans Development and Lifespan. *Cell Metab.* **19**, 73–83 (2014).
126. Antebi, A. Steroid Regulation of C. elegans Diapause, Developmental Timing, and Longevity. in *Current topics in developmental biology* **105**, 181–212 (2013).
127. Wang, Z. *et al.* The Nuclear Receptor DAF-12 Regulates Nutrient Metabolism and Reproductive Growth in Nematodes. *PLOS Genet.* **11**, e1005027 (2015).
128. Antebi, A. Nuclear hormone receptors in C. elegans. *WormBook* 1–13 (2006). doi:10.1895/wormbook.1.64.1
129. Simonis, N. *et al.* Empirically controlled mapping of the Caenorhabditis elegans protein-protein interactome network. *Nat. Methods* **6**, 47–54 (2009).
130. Reece-Hoyes, J. S. S. *et al.* Extensive rewiring and complex evolutionary dynamics in a C. elegans multiparameter transcription factor network. *Mol. Cell* **51**, 116–127 (2013).
131. Arda, H. E. *et al.* Functional modularity of nuclear hormone receptors in a Caenorhabditis elegans metabolic gene regulatory network. *Mol. Syst. Biol.* **6**, 367 (2010).
132. Johnstone, A. P. The cuticle. (2007). doi:10.1895/wormbook.1.138.1
133. Yochem, J., Tuck, S., Greenwald, I. & Han, M. A gp330/megalin-related protein is required in the major epidermis of Caenorhabditis elegans for completion of molting. *Development* **126**, 597–606 (1999).
134. Kuervers, L. M., Jones, C. L., O'Neil, N. J. & Baillie, D. L. The sterol modifying enzyme LET-767 is essential for growth, reproduction and development in Caenorhabditis elegans. *Mol. Genet. Genomics* **270**, 121–131 (2003).
135. Lažetić, V. & Fay, D. S. Molting in C. elegans. *Worm* **6**, e1330246 (2017).
136. Hao, L., Johnsen, R., Lauter, G., Baillie, D. & Bürglin, T. R. Comprehensive analysis of gene expression patterns of hedgehog-related genes. *BMC Genomics* **7**, 280 (2006).
137. Hodgkin, J. A. & Brenner, S. Mutations causing transformation of sexual phenotype in the nematode Caenorhabditis elegans. *Genetics* **86**, 275–87 (1977).

138. Mullaney, B. C. & Ashrafi, K. C. elegans fat storage and metabolic regulation. *Biochim. Biophys. Acta* **1791**, 474–478 (2009).
139. Espelt, M. V., Estevez, A. Y., Yin, X. & Strange, K. Oscillatory Ca $^{2+}$ Signaling in the Isolated *Caenorhabditis elegans* Intestine. *J. Gen. Physiol.* **126**, 379–392 (2005).
140. Habacher, C. *et al.* Ribonuclease-Mediated Control of Body Fat. *Dev. Cell* **39**, 359–369 (2016).
141. Hellerer, T. *et al.* Monitoring of lipid storage in Caenorhabditis elegans using coherent anti-Stokes Raman scattering (CARS) microscopy. *Proc. Natl. Acad. Sci. U. S. A.* **104**, 14658–63 (2007).
142. Xu, S. H. & Nes, W. D. Biosynthesis of cholesterol in the yeast mutant erg6. *Biochem. Biophys. Res. Commun.* **155**, 509–17 (1988).
143. Maekawa, M. Domain 4 (D4) of Perfringolysin O to Visualize Cholesterol in Cellular Membranes-The Update. *Sensors (Basel).* **17**, (2017).
144. Liu, S.-L. *et al.* Orthogonal lipid sensors identify transbilayer asymmetry of plasma membrane cholesterol. *Nat. Chem. Biol.* **13**, 268–274 (2017).
145. Marek, M., Vincenzetti, V. & Martin, S. G. Sterol flow between the plasma membrane and the endosome is regulated by the LAM family protein Ltc1. doi:10.1101/720383
146. Poteryaev, D., Squirrell, J. M., Campbell, J. M., White, J. G. & Spang, A. Involvement of the Actin Cytoskeleton and Homotypic Membrane Fusion in ER Dynamics in *Caenorhabditis elegans*. *Mol. Biol. Cell* **16**, 2139–2153 (2005).
147. Ma, D. K. *et al.* Acyl-CoA Dehydrogenase Drives Heat Adaptation by Sequestering Fatty Acids. *Cell* **161**, 1152–1163 (2015).
148. Pathare, P. P., Lin, A., Bornfeldt, K. E., Taubert, S. & Van Gilst, M. R. Coordinate regulation of lipid metabolism by novel nuclear receptor partnerships. *PLOS Genet.* **8**, e1002645+ (2012).
149. Van Gilst, M. R., Hadjivassiliou, H., Jolly, A. & Yamamoto, K. R. Nuclear hormone receptor NHR-49 controls fat consumption and fatty acid composition in C. elegans. *PLoS Biol.* **3**, e53 (2005).
150. Ashrafi, K. *et al.* Genome-wide RNAi analysis of Caenorhabditis elegans fat regulatory genes. *Nature* **421**, 268–272 (2003).
151. Matsuoka, K. *et al.* COPII-coated vesicle formation reconstituted with purified coat proteins and chemically defined liposomes. *Cell* **93**, 263–275 (1998).
152. Hannich, J. T. *et al.* Methylation of the Sterol Nucleus by STRM-1 Regulates Dauer Larva Formation in Caenorhabditis elegans. *Dev. Cell* **16**, 833–843 (2009).
153. Kurzchalia, T. V. & Ward, S. Why do worms need cholesterol? *Nat. Cell Biol.* **5**, 684–688 (2003).

154. Dhe-Paganon, S., Duda, K., Iwamoto, M., Chi, Y.-I. & Shoelson, S. E. Crystal Structure of the HNF4α Ligand Binding Domain in Complex with Endogenous Fatty Acid Ligand. *J. Biol. Chem.* **277**, 37973–37976 (2002).
155. Li, Z. *et al.* Reduced white fat mass in adult mice bearing a truncated Patched 1. *Int. J. Biol. Sci.* **4**, 29–36 (2008).
156. Agarwal, J. R. *et al.* Activation of Liver X Receptors Inhibits Hedgehog Signaling, Clonogenic Growth, and Self-Renewal in Multiple Myeloma. *Mol. Cancer Ther.* **13**, 1873–1881 (2014).
157. Blotta, S. *et al.* Canonical and noncanonical Hedgehog pathway in the pathogenesis of multiple myeloma. *Blood* **120**, 5002–5013 (2012).
158. Kamath, R. S. *et al.* Systematic functional analysis of the Caenorhabditis elegans genome using RNAi. *Nature* **421**, 231–237 (2003).
159. Xiao, R. *et al.* RNAi Interrogation of Dietary Modulation of Development, Metabolism, Behavior, and Aging in C. elegans. *Cell Rep.* **11**, 1123–1133 (2015).
160. Tursun, B., Cochella, L., Carrera, I. & Hobert, O. A Toolkit and Robust Pipeline for the Generation of Fosmid-Based Reporter Genes in C. elegans. *PLoS One* **4**, e4625 (2009).
161. Fukuyama, M., Kontani, K., Katada, T. & Rougvie, A. E. The C. elegans Hypodermis Couples Progenitor Cell Quiescence to the Dietary State. *Curr. Biol.* **25**, 1241–1248 (2015).
162. Sommer, C., Straehle, C., Koethe, U. & Hamprecht, F. A. Ilastik: Interactive learning and segmentation toolkit. in *Biomedical Imaging: From Nano to Macro, 2011 IEEE International Symposium on* 230–233 (2011).
163. Stiernagle, T. Maintenance of C. elegans. *WormBook* (2006). doi:10.1895/wormbook.1.101.1
164. BLIGH, E. G. & DYER, W. J. A rapid method of total lipid extraction and purification. *Can. J. Biochem. Physiol.* **37**, 911–917 (1959).
165. Schwudke, D. *et al.* Top-Down Lipidomic Screens by Multivariate Analysis of High-Resolution Survey Mass Spectra. *Anal. Chem.* **79**, 4083–4093 (2007).
166. Guri, Y. *et al.* mTORC2 Promotes Tumorigenesis via Lipid Synthesis. *Cancer Cell* **32**, 807-823.e12 (2017).
167. da Silveira Dos Santos, A. X. *et al.* Systematic lipidomic analysis of yeast protein kinase and phosphatase mutants reveals novel insights into regulation of lipid homeostasis. *Mol. Biol. Cell* **25**, 3234–46 (2014).
168. Pino, E. C., Webster, C. M., Carr, C. E. & Soukas, A. A. Biochemical and high throughput microscopic assessment of fat mass in Caenorhabditis elegans. *J. Vis.*

Exp. (2013). doi:10.3791/50180

169. Ackema, K. B., Sauder, U., Solinger, J. A. & Spang, A. The ArfGEF GBF-1 Is Required for ER Structure, Secretion and Endocytic Transport in C. elegans. *PLoS One* **8**, e67076 (2013).
170. Richter, K. N. *et al.* Glyoxal as an alternative fixative to formaldehyde in immunostaining and super-resolution microscopy. *EMBO J.* **37**, 139–159 (2018).
171. Cadena del Castillo, C. E. *et al.* Patched regulates lipid homeostasis by controlling cellular cholesterol levels. *bioRxiv* 816256 (2019). doi:10.1101/816256
172. Konířová, J. *et al.* Modulated DISP3/PTCHD2 expression influences neural stem cell fate decisions. *Sci. Rep.* **7**, 41597 (2017).
173. Zíková, M. *et al.* DISP3 promotes proliferation and delays differentiation of neural progenitor cells. *FEBS Lett.* **588**, 4071–4077 (2014).
174. Zikova, M., Corlett, A., Bendova, Z., Pajer, P. & Bartunek, P. DISP3, a Sterol-Sensing Domain-Containing Protein that Links Thyroid Hormone Action and Cholesterol Metabolism. *Mol. Endocrinol.* **23**, 520–528 (2009).
175. Sievers, F. & Higgins, D. G. Clustal Omega for making accurate alignments of many protein sequences. *Protein Sci.* **27**, 135–145 (2018).
176. Moribe, H. *et al.* Tetraspanin protein (TSP-15) is required for epidermal integrity in Caenorhabditis elegans. *J. Cell Sci.* **117**, 5209–20 (2004).
177. Mok, D. Z. L., Sternberg, P. W. & Inoue, T. Morphologically defined sub-stages of C. Elegans vulval development in the fourth larval stage. *BMC Dev. Biol.* **15**, (2015).
178. Flower, D. R. The lipocalin protein family: structure and function. *Biochem. J.* **318 (Pt 1)**, 1–14 (1996).
179. Watanabe, H. *et al.* Lipocalin 2 binds to membrane phosphatidylethanolamine to induce lipid raft movement in a PKA-dependent manner and modulates sperm maturation. *Development* **141**, 2157–64 (2014).
180. di Masi, A., Trezza, V., Leboffe, L. & Ascenzi, P. Human plasma lipocalins and serum albumin: Plasma alternative carriers? *J. Control. Release* **228**, 191–205 (2016).
181. Forman-Rubinsky, R., Cohen, J. D. & Sundaram, M. V. Lipocalins Are Required for Apical Extracellular Matrix Organization and Remodeling in Caenorhabditis elegans. *Genetics* **207**, 625–642 (2017).
182. Gill, H. K. *et al.* Integrity of Narrow Epithelial Tubes in the C. elegans Excretory System Requires a Transient Luminal Matrix. *PLOS Genet.* **12**, e1006205 (2016).
183. Moribe, H. *et al.* No Title. **117**, (2004).
184. Huotari, J. & Helenius, A. Endosome maturation. *EMBO J.* **30**, 3481–3500 (2011).
185. Solinger, J. A. & Spang, A. Tethering complexes in the endocytic pathway: CORVET

and HOPS. *FEBS J.* **280**, 2743–2757 (2013).

186. Poteryaev, D., Datta, S., Ackema, K., Zerial, M. & Spang, A. Identification of the Switch in Early-to-Late Endosome Transition. *Cell* **141**, 497–508 (2010).
187. Poteryaev, D., Fares, H., Bowerman, B. & Spang, A. Caenorhabditis elegans SAND-1 is essential for RAB-7 function in endosomal traffic. *EMBO J.* **26**, 301–312 (2007).
188. Rohatgi, R. & Scott, M. P. Patching the gaps in Hedgehog signalling. *Nat. Cell Biol.* **9**, 1005–1009 (2007).
189. Issman-Zecharya, N. & Schuldiner, O. The PI3K Class III Complex Promotes Axon Pruning by Downregulating a Ptc-Derived Signal via Endosome-Lysosomal Degradation. *Dev. Cell* **31**, 461–473 (2014).
190. Karpen, H. E. *et al.* The sonic hedgehog receptor patched associates with caveolin-1 in cholesterol-rich microdomains of the plasma membrane. *J. Biol. Chem.* **276**, 19503–19511 (2001).
191. Pelkmans, L. & Helenius, A. Endocytosis Via Caveolae. *Traffic* **3**, 311–320 (2002).
192. Root, K. T., Plucinsky, S. M. & Glover, K. J. Recent Progress in the Topology, Structure, and Oligomerization of Caveolin: A Building Block of Caveolae. *Curr. Top. Membr.* **75**, 305–336 (2015).
193. Alberts, B. *et al.* Transport into the cell from the plasma membrane: endocytosis. in *Molecular Biology of the Cell* 695–752 (Garland Science, 2002).
194. Solinger, J. A. & Spang, A. Loss of the Sec1/Munc18-family proteins VPS-33.2 and VPS-33.1 bypasses a block in endosome maturation in Caenorhabditis elegans. *Mol. Biol. Cell* **25**, 3909–3925 (2014).
195. Chen, C. C.-H. *et al.* RAB-10 Is Required for Endocytic Recycling in the *Caenorhabditis elegans* Intestine. *Mol. Biol. Cell* **17**, 1286–1297 (2006).
196. Winter, J. F. *et al.* Caenorhabditis elegans screen reveals role of PAR-5 in RAB-11-recycling endosome positioning and apicobasal cell polarity. *Nat. Cell Biol.* **14**, 666–676 (2012).
197. Ringerike, T., Blystad, F. D., Levy, F. O., Madshus, I. H. & Stang, E. Cholesterol is important in control of EGF receptor kinase activity but EGF receptors are not concentrated in caveolae. *J. Cell Sci.* **115**, 1331–1340 (2002).
198. Tomas, A., Futter, C. E. & Eden, E. R. EGF receptor trafficking: consequences for signaling and cancer. *Trends Cell Biol.* **24**, 26–34 (2014).
199. Brunt, L. & Scholpp, S. The function of endocytosis in Wnt signaling. *Cell. Mol. Life Sci.* **75**, 785–795 (2018).
200. Monkkonen, T., Landua, J. D., Visbal, A. P. & Lewis, M. T. Epithelial and non-epithelial Ptch1 play opposing roles to regulate proliferation and morphogenesis of

the mouse mammary gland. *Development* **144**, 1317–1327 (2017).

201. Lee, H. J. J. *et al.* Assessing cholesterol storage in live cells and C. elegans by stimulated Raman scattering imaging of phenyl-Diyne cholesterol. *Sci. Rep.* **5**, (2015).
202. McKay, S. J. *et al.* Gene expression profiling of cells, tissues, and developmental stages of the nematode C. elegans. *Cold Spring Harb. Symp. Quant. Biol.* **68**, 159–69 (2003).
203. Hunt-Newbury, R. *et al.* High-Throughput In Vivo Analysis of Gene Expression in Caenorhabditis elegans. *PLoS Biol.* **5**, e237 (2007).
204. Vrablik, T. L., Petyuk, V. A., Larson, E. M., Smith, R. D. & Watts, J. L. Lipidomic and proteomic analysis of Caenorhabditis elegans lipid droplets and identification of ACS-4 as a lipid droplet-associated protein. *Biochim. Biophys. Acta* **1851**, 1337–45 (2015).
205. Sandhu, J. *et al.* Aster Proteins Facilitate Nonvesicular Plasma Membrane to ER Cholesterol Transport in Mammalian Cells. *Cell* **175**, 514-529.e20 (2018).
206. Wu, H., Carvalho, P. & Voeltz, G. K. Here, there, and everywhere: The importance of ER membrane contact sites. *Science* **361**, eaan5835 (2018).
207. Phillips, M. J. & Voeltz, G. K. Structure and function of ER membrane contact sites with other organelles. *Nat. Rev. Mol. Cell Biol.* **17**, 69–82 (2016).
208. Colgan, S. M., Al-Hashimi, A. A. & Austin, R. C. Endoplasmic reticulum stress and lipid dysregulation. *Expert Rev. Mol. Med.* **13**, e4 (2011).
209. Wollam, J. & Antebi, A. Sterol Regulation of Metabolism, Homeostasis, and Development. (2011). doi:10.1146/annurev-biochem-081308-165917
210. Suh, J. M. M. *et al.* Hedgehog signaling plays a conserved role in inhibiting fat formation. *Cell Metab.* **3**, 25–34 (2006).
211. Ashrafi, K. Obesity and the regulation of fat metabolism. *WormBook* (2007). doi:10.1895/wormbook.1.130.1
212. Gissendanner, C. R., Crossgrove, K., Kraus, K. A., Maina, C. V & Sluder, A. E. Expression and function of conserved nuclear receptor genes in Caenorhabditis elegans. *Dev. Biol.* **266**, 399–416 (2004).
213. Wisely, G. B. *et al.* Hepatocyte nuclear factor 4 is a transcription factor that constitutively binds fatty acids. *Structure* **10**, 1225–34 (2002).
214. Kniazeva, M., Crawford, Q. T., Seiber, M., Wang, C.-Y. & Han, M. Monomethyl Branched-Chain Fatty Acids Play an Essential Role in Caenorhabditis elegans Development. *PLoS Biol.* **2**, e257 (2004).
215. Obregon, D. *et al.* Soluble amyloid precursor protein-Î± modulates Î²-secretase activity and amyloid-Î² generation. *Nat Commun* **3**, 777+ (2012).

216. Galles, C. *et al.* Endocannabinoids in Caenorhabditis elegans are essential for the mobilization of cholesterol from internal reserves. *Sci. Rep.* **8**, 6398 (2018).
217. Mangelberger, D., Kern, D., Loipetzberger, A., Eberl, M. & Aberger, F. Cooperative Hedgehog-EGFR signaling. *Front. Biosci. (Landmark Ed.* **17**, 90–9 (2012).
218. Götschel, F. *et al.* Synergism between Hedgehog-GLI and EGFR Signaling in Hedgehog-Responsive Human Medulloblastoma Cells Induces Downregulation of Canonical Hedgehog-Target Genes and Stabilized Expression of GLI1. *PLoS One* **8**, e65403 (2013).
219. Mimeault, M. & Batra, S. K. Frequent deregulations in the hedgehog signaling network and cross-talks with the epidermal growth factor receptor pathway involved in cancer progression and targeted therapies. *Pharmacol. Rev.* **62**, 497–524 (2010).